
Fast and Three-rious: Speeding Up Weak Supervision with Triplet Methods

Daniel Y. Fu^{*1} Mayee F. Chen^{*1} Frederic Sala¹ Sarah M. Hooper² Kayvon Fatahalian¹ Christopher Ré¹

Abstract

Weak supervision is a popular method for building machine learning models without relying on ground truth annotations. Instead, it generates probabilistic training labels by estimating the accuracies of multiple noisy labeling sources (e.g., heuristics, crowd workers). Existing approaches use latent variable estimation to model the noisy sources, but these methods can be computationally expensive, scaling superlinearly in the data. In this work, we show that, for a class of latent variable models highly applicable to weak supervision, we can find a *closed-form solution* to model parameters, obviating the need for iterative solutions like stochastic gradient descent (SGD). We use this insight to build FLYINGSQUID, a weak supervision framework that runs *orders of magnitude* faster than previous weak supervision approaches and requires fewer assumptions. In particular, we prove bounds on generalization error without assuming that the latent variable model can exactly parameterize the underlying data distribution. Empirically, we validate FLYINGSQUID on benchmark weak supervision datasets and find that it achieves the same or higher quality compared to previous approaches without the need to tune an SGD procedure, recovers model parameters 170 times faster on average, and enables new video analysis and online learning applications.

1. Introduction

Modern machine learning systems require large amounts of labeled training data to be successful. Weak supervision is a class of popular methods for building models without resorting to manually labeling training data (Dehghani et al., 2017b;a; Jia et al., 2017; Mahajan et al., 2018; Niu et al., 2012); it drives applications used by billions of people every

day, ranging from Gmail (Sheng et al., 2020) to AI products at Apple (Ré et al., 2020) and search products (Bach et al., 2019). These approaches use noisy sources, such as heuristics, crowd workers, external knowledge bases, and user-defined functions (Gupta & Manning, 2014; Ratner et al., 2019; Karger et al., 2011; Dawid & Skene, 1979; Mintz et al., 2009; Zhang et al., 2017; Hearst, 1992) to generate probabilistic training labels without hand-labeling.

The major technical challenge in weak supervision is to efficiently estimate the accuracies of—and potentially the correlations among—the noisy sources without any labeled data (Guan et al., 2018; Takamatsu et al., 2012; Xiao et al., 2015; Ratner et al., 2018). Standard approaches to this problem, from classical crowdsourcing to more recent methods, use latent variable probabilistic graphical models (PGMs) to model the primary sources of signal—the agreements and disagreements between sources, along with known or estimated source independencies (Dawid & Skene, 1979; Karger et al., 2011; Ratner et al., 2016).

However, latent variable estimation is challenging, and the techniques are often sample- and computationally-complex. For example, Bach et al. (2019) required multiple iterations of a Gibbs-based algorithm, and Ratner et al. (2019) required estimating the full inverse covariance matrix among the sources, while Sala et al. (2019) and Zhan et al. (2019) required the use of multiple iterations of stochastic gradient descent (SGD) to learn accuracy parameters. These limitations make it difficult to use weak supervision in applications that require modeling complex temporal or spatial dependencies, such as video and image analysis, or in streaming applications that have strict latency requirements. In contrast, our solution is motivated by a key observation: that by breaking the problem into minimal subproblems—solving parameters for triplets of sources at a time, similar to Joglekar et al. (2013) and Chaganty & Liang (2014)—we can reduce parameter estimation into solving systems of equations that have simple, *closed-form solutions*.

Concretely, we show that, for a class of binary Ising models, we can reduce the problem of accuracy and correlation estimation to solving a set of systems of equations whose size is linear in the number of sources. These systems admit a closed-form solution, so we can estimate the model parameters in time linear in the data with provable bounds,

^{*}Equal contribution ¹Department of Computer Science, Stanford University ²Department of Electrical Engineering, Stanford University. Correspondence to: Daniel Y. Fu <danfu@cs.stanford.edu>.

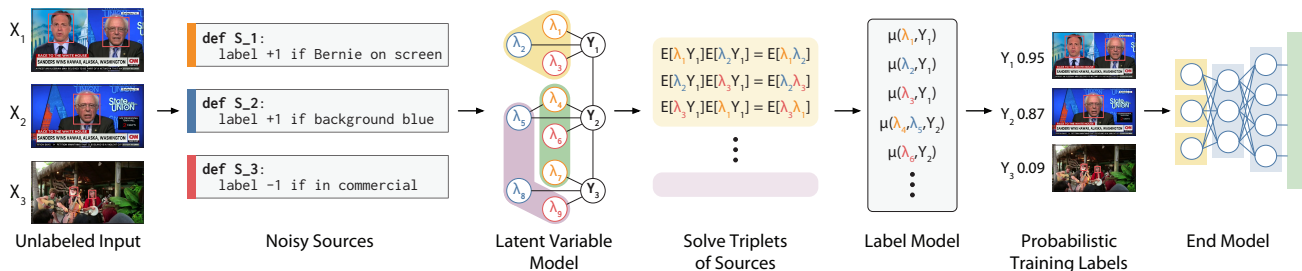


Figure 1. The FLYINGSQUID pipeline. Users provide weak supervision sources, which generate noisy labels for a set of unlabeled data. FLYINGSQUID uses a latent variable model and constructs triplets of sources to turn model parameter estimation into a set of minimal subproblems with closed-form solutions. The label model then generates probabilistic training labels to train a downstream end model.

even though inference is NP-hard in general Ising models (Chandrasekaran et al., 2008; Koller & Friedman, 2009). Critically, the class of Ising models we use captures many weak supervision settings and is larger than that used in previous efforts. We use these insights to build FLYINGSQUID, a new weak supervision framework that learns label source accuracies with a closed-form solution.

We analyze the downstream performance of end models trained with labels generated by FLYINGSQUID, and prove the following results:

- We prove that the generalization error of a model trained with labels generated by FLYINGSQUID scales at the same asymptotic rate as supervised learning.
- We analyze model misspecification using KL divergence, a more fine-grained result than Ratner et al. (2019).
- We show that our parameter estimation approach can be sample optimal up to constant factors via an information-theoretic lower bound on minimax risk.
- We prove a first-of-its-kind result for downstream generalization of a window-based online weak supervision algorithm, accounting for distributional drift.

Next, we empirically validate FLYINGSQUID on three benchmark weak supervision datasets that have been used to evaluate previous state-of-the-art weak supervision frameworks (Ratner et al., 2018), as well as on four video analysis tasks, where labeling training data is particularly expensive and modeling temporal dependencies introduces significant slowdowns in learning graphical model parameters. We find that FLYINGSQUID achieves the same or higher quality as previous approaches while learning parameters orders of magnitude faster. Since FLYINGSQUID runs so fast, we can learn graphical model parameters *in the training loop* of a discriminative end model. This allows us to extend FLYINGSQUID to the online learning setting with a window-based algorithm, where we update model parameters at the same time as we generate labels for an end model. In summary, we observe the following empirical results:

- We replicate evaluations of previous approaches and match or exceed their accuracy (up to 4.9 F1 points).
- On tasks with relatively simple graphical model structures, FLYINGSQUID learns model parameters 170 times faster on average; on video analysis tasks, where there are complex temporal dependencies, FLYINGSQUID learns up to 4,000 times faster.
- We demonstrate that our window-based online weak supervision extension can both update model parameters and train an end model completely online, outperforming a majority vote baseline by up to 15.7 F1 points.

We release FLYINGSQUID as a novel layer integrated into PyTorch.¹ This layer allows weak supervision to be integrated off-the-shelf into any deep learning model, learning the accuracies of noisy labeling sources in the same training loop as the end model. Our layer can be used in any standard training set up, enabling new modes of training from multiple label sources.

2. Weakly Supervised Machine Learning

In this section, we give an overview of weak supervision and our problem setup. In Section 2.1, we give an overview of the inputs to weak supervision from the user’s perspective. In Section 2.2, we describe the formal problem setup. Finally, in Section 2.3, we show how the problem reduces to estimating the parameters of a latent variable PGM.

2.1. Background: Weak Supervision

We first give some background on weak supervision at a high level. In weak supervision, practitioners programmatically generate training labels through the process shown in Figure 1. Users build multiple weak supervision sources that assign noisy labels to data. For example, an analyst trying to detect interviews of Bernie Sanders in a corpus of cable TV news may use off-the-shelf face detection and identity classification networks to detect frames where Sanders is on

¹<https://github.com/HazyResearch/flyingsquid>

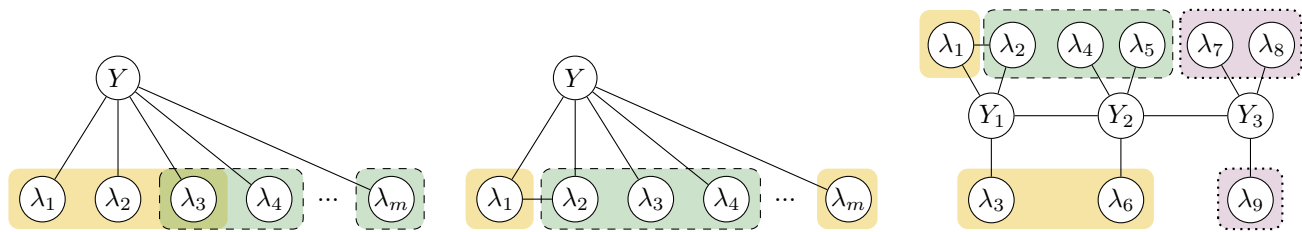


Figure 2. Example of dependency structure graphs and triplets (rectangles). Left: Conditionally independent sources; Middle: With dependencies. Right: Multiple temporally-correlated labels $\{Y_1, Y_2, Y_3\}$ with per-label sources.

screen, or she may write a Python function to search closed captions for instances of the text “Bernie Sanders.” Critically, these weak supervision sources can vote or abstain on individual data points; this lets users express high-precision signals without requiring them to have high recall as well. For example, while the text “Bernie Sanders” in the transcript is a strong signal for an interview, the absence of the text is not a strong signal for the absence of an interview (once he is introduced, his name is not mentioned for most of the interview).

These sources are noisy and may conflict with each other, so a latent variable model, which we refer to as a *label model*, is used to express the accuracies of and correlations between them. Once its parameters are learned, the model is used to aggregate source votes and generate probabilistic training labels, which are in turn used to train a downstream discriminative model (*end model* from here on).

2.2. Problem Setup

Now, we formally define our learning problem. Let $\mathbf{X} = [X_1, X_2, \dots, X_D] \in \mathcal{X}$ be a vector of D related elements (e.g., contiguous frames in a video, or neighboring pixels in an image). Let $\mathbf{Y} = [Y_1, Y_2, \dots, Y_D] \in \mathcal{Y}$ be the vector of *unobserved* true labels for each element (e.g., the per-frame label for event detection in video, or a per-pixel label for a segmentation mask in an image). We refer to each Y_i as a *task*. We have $(\mathbf{X}, \mathbf{Y}) \sim \mathcal{D}$ for some distribution \mathcal{D} . We simplify to binary $Y_i \in \{\pm 1\}$ for ease of exposition (we discuss the multi-class case in Appendix C.2). Let m be the number of sources S_1, \dots, S_m , each assigning a label $\lambda_j \in \{\pm 1\}$ to some single element X_i to vote on its respective Y_i , or abstaining ($\lambda_j = 0$).

The goal is to apply the m weak supervision sources to an unlabeled dataset $\{\mathbf{X}^i\}_{i=1}^n$ with n data points to create an $n \times m$ label matrix L , combine the source votes into element-wise probabilistic training labels, $\{\tilde{\mathbf{Y}}^i\}_{i=1}^n$, and use them to train a discriminative classifier $f_w : \mathcal{X} \rightarrow \mathcal{Y}$, *all without observing any ground truth labels*.

2.3. Label Model

Now, we describe how we use a probabilistic graphical model to generate training data based on labeling function outputs. First, we describe how we use a graph to specify the conditional dependencies between label sources and tasks. Next, we describe how to represent the task labels \mathbf{Y} and source votes $\boldsymbol{\lambda}$ using a binary Ising model from user-provided conditional dependencies between sources and tasks. Then, we discuss how to perform inference using the junction tree formula and introduce the label model parameters our method focuses on estimating.

Conditional Dependencies Let a graph G_{dep} specify conditional dependencies between sources and tasks, using standard technical notions from the PGM literature (Koller & Friedman, 2009; Lauritzen, 1996; Wainwright & Jordan, 2008). In particular, the lack of an edge in G_{dep} between a pair of variables indicates independence conditioned on a *separator set* of variables (Lauritzen, 1996). We assume that G_{dep} is user-provided; it can also be estimated directly from source votes (Ratner et al., 2019). Figure 2 shows three graphs, capturing different relationships between tasks and supervision sources. Figure 2 (left) is a single-task scenario where noisy source errors are conditionally independent; this case covers many benchmark weak supervision datasets. Here, $D = 1$, and there are no dependencies between different elements in the dataset (e.g., randomly sampled comments from YouTube for sentiment analysis). Figure 2 (middle) has dependencies between the errors of two sources (λ_1 and λ_2). Finally, Figure 2 (right) depicts a more complex scenario, where three tasks have dependencies between them. This structure is common in applications with temporal dependencies like video; for example, Y_1, Y_2, Y_3 might be contiguous frames (Sala et al., 2019).

Binary Ising Model We augment the dependency graph G_{dep} to set up a binary Ising model on $G = (V, E)$. Let the vertices $V = \{\mathbf{Y}, \mathbf{v}\}$ contain a set of hidden variables \mathbf{Y} (one for every task Y_i) and observed variables \mathbf{v} , generated by augmenting $\boldsymbol{\lambda}$. We generate \mathbf{v} by letting there be a pair of binary observed variables (v_{2i-1}, v_{2i}) for each label source λ_i , such that (v_{2i-1}, v_{2i}) is equal to $(1, -1)$ when $\lambda_i = 1$,

$(-1, 1)$ when $\lambda_i = -1$, and $(1, 1)$ or $(-1, -1)$ with equal probability when $\lambda_i = 0$. This mapping also produces an augmented label matrix \mathcal{L} from the empirical label matrix L , which contains n samples of source labels.

Next, let the edges E be constructed as follows. Let $Y^{dep}(i)$ denote the task that λ_i labels for all $i \in [1, m]$. Then for all i , there is an edge between each of (v_{2i-1}, v_{2i}) and $Y^{dep}(i)$ representing the accuracy of λ_i as well as an edge between v_{2i-1} and v_{2i} representing the abstain rate of λ_i . If there is an edge between λ_i and λ_j in G_{dep} , then there are four edges between (v_{2i-1}, v_{2i}) and (v_{2j-1}, v_{2j}) . We also define $Y(j)$ as the hidden variable that v_j acts on for all $j \in [1, 2m]$; in particular, $Y(2i-1) = Y^{dep}(i)$.

Inference The Ising model defines a joint distribution $P(\mathbf{Y}, \boldsymbol{\lambda})$ (detailed in Appendix C.1), which we wish to use for inference. We can take advantage of the graphical model properties of G_{dep} for efficient inference. In particular, suppose that G_{dep} is triangulated; if not, edges can always be added to G_{dep} until it is. Then, G_{dep} admits a junction tree representation with maximal cliques $C \in \tilde{\mathcal{C}}_{dep}$ and separator sets $S \in \mathcal{S}_{dep}$. Inference is performed via a standard approach, using the junction tree formula

$$P(\mathbf{Y}, \boldsymbol{\lambda}) = \prod_{C \in \tilde{\mathcal{C}}_{dep}} \mu_C / \prod_{S \in \mathcal{S}_{dep}} \mu_S^{d(S)-1}, \quad (1)$$

where μ_C is the marginal probability of a clique C , μ_S is the marginal probability of a separator set S , and $d(S)$ is the number of maximal cliques S is adjacent to (Lauritzen, 1996; Wainwright & Jordan, 2008). We refer to these marginals as the *label model parameters* $\boldsymbol{\mu}$.

We assume the distribution prior $P(\bar{\mathbf{Y}})$ is user-provided, but it can also be estimated directly by using source votes as in Ratner et al. (2019) or by optimizing a composite likelihood function as in Chaganty & Liang (2014). Some other marginals are directly observable from the votes generated by the sources S_1, \dots, S_m . However, marginals containing elements from both \mathbf{Y} and $\boldsymbol{\lambda}$ are not directly observable, since we do not observe \mathbf{Y} . The challenge is thus recovering this set of marginals $P(Y_i, \dots, Y_j, \lambda_k, \dots, \lambda_l)$.

3. Learning The Label Model

Now that we have defined our label model parameters $\boldsymbol{\mu}$, we need to recover the parameters directly from the label matrix L without observing the true labels \mathbf{Y} . First, we discuss how we recover the mean parameters of our Ising model using Algorithm 1 (Section 3.1). Then, we map the mean parameters to label model parameters (Section 3.2) by computing expectations over cliques of G and applying a linear transform to obtain $\boldsymbol{\mu}$. Finally, we discuss an extension to the online setting (Section 3.3).

Algorithm 1 Triplet Method (before averaging)

Input: Set of variables Ω_G , augmented label matrix \mathcal{L}
 Initialize $A = \emptyset$
while $\exists v_i \in \Omega_G - A$ **do**
 Pick $v_j, v_k : v_i \perp v_j | Y(i), v_i \perp v_k | Y(i), v_j \perp v_k | Y(i)$.
 Estimate $\hat{\mathbb{E}}[v_i v_j] = \frac{1}{n} \sum_t \mathcal{L}_{it} \mathcal{L}_{jt}$, $\hat{\mathbb{E}}[v_i v_k] = \frac{1}{n} \sum_t \mathcal{L}_{it} \mathcal{L}_{kt}$, and $\hat{\mathbb{E}}[v_j v_k] = \frac{1}{n} \sum_t \mathcal{L}_{jt} \mathcal{L}_{kt}$.
 $\hat{a}_i \leftarrow \sqrt{|\hat{\mathbb{E}}[v_i v_j] \cdot \hat{\mathbb{E}}[v_i v_k] / \hat{\mathbb{E}}[v_j v_k]|}$
 $\hat{a}_j \leftarrow \sqrt{|\hat{\mathbb{E}}[v_i v_j] \cdot \hat{\mathbb{E}}[v_j v_k] / \hat{\mathbb{E}}[v_i v_k]|}$
 $\hat{a}_k \leftarrow \sqrt{|\hat{\mathbb{E}}[v_i v_k] \cdot \hat{\mathbb{E}}[v_j v_k] / \hat{\mathbb{E}}[v_i v_j]|}$
 $A \leftarrow A \cup \{v_i, v_j, v_k\}$
end while
return RESOLVESIGNS(\hat{a}_i) $\forall v_i \in V$

Inputs and Outputs As input, we take in a label matrix L that has, on average, better-than-random samples; dependency graph G_{dep} ; and the prior $P(\bar{\mathbf{Y}})$. As output, we want to compute $\boldsymbol{\mu}$, which would enable us to produce probabilistic training data via (1).

3.1. Learning the Mean Parameters

We explain how to compute the mean parameters $\mathbb{E}[Y_i], \mathbb{E}[Y_i Y_j], \mathbb{E}[v_i Y(i)],$ and $\mathbb{E}[v_i v_j]$ of the Ising model. Note that all of these parameters can be directly estimated besides $\mathbb{E}[v_i Y(i)]$. Although we cannot observe $Y(i)$, we can compute $\mathbb{E}[v_i Y(i)]$ using a closed-form method by relying on notions of independence and rates of agreement between groups of three conditionally independent observed variables for the hidden variable $Y(i)$. Set $a_i := \mathbb{E}[v_i Y(i)]$, which can be thought of as the *accuracy* of the observed variable scaled to $[-1, +1]$. The following proposition produces sufficient signal to learn from:

Proposition 1. *If $v_i \perp v_j | Y(i)$, then $v_i Y(i) \perp v_j Y(i)$.*

Our proof is provided in Appendix C.1.1. This follows from a symmetry argument applied to the conditional independence of two variables v_i and v_j given $Y(i)$. Then

$$a_i a_j = \mathbb{E}[v_i Y(i)] \mathbb{E}[v_j Y(i)] = \mathbb{E}[v_i v_j Y(i)^2] = \mathbb{E}[v_i v_j],$$

where we used $Y(i)^2 = 1$. While we cannot observe a_i , the product of $a_i a_j$ is just $\mathbb{E}[v_i v_j]$, the observable rate at which a pair of variables act together. We can then utilize a third variable v_k such that $a_i a_k$ and $a_j a_k$ are also observable, and solve a system of three equations for the accuracies up to sign, e.g., $|a_i|, |a_j|, |a_k|$. We explain how to recover signs with the RESOLVESIGNS function in Appendix C.1.5.

Formally, define $\Omega_G = \{v_i \in V : \exists v_j, v_k \text{ s.t. } v_i \perp v_j | Y(i), v_j \perp v_k | Y(i), v_i \perp v_k | Y(i)\}$ to be the set of variables that can be grouped into triplets in this way. For each

Algorithm 2 Label Model Parameter Recovery

Input: G_{dep} , distribution prior $P(\bar{Y})$, label matrix L .
 Augment G_{dep} and L to generate $G = (V, E)$ with clique-set \mathcal{C} and augmented label matrix \mathcal{L} .
 Obtain set of variables Ω_G with solvable accuracies.
 Compute mean parameters and estimate all $\hat{a}_i = \hat{\mathbb{E}}[v_i Y(i)]$ using Algorithm 1.
for clique $C \in \mathcal{C}$ of observed variables **do**
 Compute $\hat{a}_C = \hat{\mathbb{E}}[\prod_{k \in C} v_k Y(C)]$ by factorizing into observable averages and mean parameters.
 Map \hat{a}_C in G to $\hat{a}_{C_{dep}}$ in G_{dep} .
 Linearly transform $\hat{a}_{C_{dep}}$ to $\hat{\mu}_{C_{dep}}$.
end for
return Label model parameters $\hat{\mu}$

variable $v_i \in \Omega_G$, we can compute the accuracy a_i by solving the system $a_i a_j = \mathbb{E}[v_i v_j]$, $a_i a_k = \mathbb{E}[v_i v_k]$, $a_j a_k = \mathbb{E}[v_j v_k]$. In many practical settings, $\Omega_G = V$, so the *triplet method* of recovery applies to each v_i , motivating Algorithm 1 (some examples of valid triplet groupings shown in Figure 2). Note that variables can appear in multiple triplets, and variables do not necessarily need to vote on the same task $Y(i)$ as long as they are conditionally independent given $Y(i)$. Different triplets give different accuracy values, so we compute accuracy values from all possible triplets and use the mean or median over all triplets. In cases where Ω_G is not equal to V , we supplement the triplet method with other independence properties to recover accuracies on more complex graphs, detailed in Appendix C.2.

3.2. Mapping to the Label Model Parameters

Now we map the mean parameters of our Ising model to label model parameters. We use the mean parameters to compute relevant expectations over the set \mathcal{C} of all cliques in G , map them to expectations over cliques \mathcal{C}_{dep} in G_{dep} , and linearly transform them into label model parameters. Define $Y(C)$ as the hidden variable that the entire clique $C \in \mathcal{C}$ of observed variables acts on. Each expectation over a clique of observed variables C and $Y(C)$, denoted $a_C := \mathbb{E}[\prod_{k \in C} v_k Y(C)]$, can be factorized in terms of the mean parameters and directly observable expectations (Appendix C.1.2). For instance, $v_i v_j \perp\!\!\!\perp Y(i, j)$ for $(v_i, v_j) \in E$, such that $\mathbb{E}[v_i v_j Y(i, j)] = \mathbb{E}[v_i v_j] \cdot \mathbb{E}[Y(i, j)]$.

Next, we convert the expectations over cliques in G back into expectations over cliques in G_{dep} . Denote $a_{C_{dep}} := \mathbb{E}[\prod_{k \in C_{dep}} \lambda_k Y^{dep}(C_{dep})]$ for each source clique $C_{dep} \in \mathcal{C}_{dep}$; then, there exists a $C \in \mathcal{C}$ over $\{v_{2k-1}\}_{k \in C_{dep}}$ such that $a_C = \mathbb{E}[\prod_{k \in C_{dep}} v_{2k-1} Y^{dep}(C_{dep})] = a_{C_{dep}}$ (Appendix C.1.3).

Finally, the label model parameters, which are marginal

distributions over maximal cliques and separator sets, can be expressed as linear combinations of $a_{C_{dep}}$ and probabilities that can be estimated directly from the data. Below is an example of how to recover $\mu_i(a, b) = P(Y^{dep}(i) = a, \lambda_i = b)$ from $\mathbb{E}[\lambda_i Y^{dep}(i)]$:

$$\begin{bmatrix} 1 & 1 & 1 & 1 & 1 & 1 \\ 1 & 0 & 1 & 0 & 1 & 0 \\ 1 & 1 & 0 & 0 & 0 & 0 \\ 1 & 0 & 0 & 0 & 0 & 1 \\ 0 & 0 & 1 & 1 & 0 & 0 \\ 0 & 0 & 1 & 0 & 0 & 0 \end{bmatrix} \begin{bmatrix} \mu_i(1,1) \\ \mu_i(-1,1) \\ \mu_i(1,0) \\ \mu_i(-1,0) \\ \mu_i(1,-1) \\ \mu_i(-1,-1) \end{bmatrix} = \begin{bmatrix} P(Y^{dep}(i)=1) \\ P(\lambda_i=1) \\ P(\lambda_i Y^{dep}(i)=1) \\ P(\lambda_i=0) \\ P(\lambda_i=0, Y^{dep}(i)=1) \end{bmatrix}. \quad (2)$$

$P(\lambda_i Y^{dep}(i) = 1)$ can be written as $\frac{1}{2}(\mathbb{E}[\lambda_i Y^{dep}(i)] - P(\lambda_i = 0) + 1)$ and $P(\lambda_i = 0, Y^{dep}(i) = 1)$ is factorizable due to the construction of G , so all values on the right of (2) are known, and we can solve for μ_i . Extending this example to larger cliques requires computing more a_C values and more directly estimatable probabilities; we detail the general case in Appendix C.1.4.

3.3. Weak Supervision in Online Learning

Now we discuss an extension to online learning. Online learning introduces two challenges: first, samples are introduced one by one, so we can only see each \mathbf{X}^t once before discarding it; second, online learning is subject to *distributional drift*, meaning that the distribution P_t each $(\mathbf{X}^t, \mathbf{Y}^t)$ is sampled from changes over time. Our closed-form approach is fast, both in terms of sample complexity and wall-clock time, and only requires computing the averages of observable summary statistics, so we can learn μ_t online with a rolling window, interleaving label model estimation and end model training. We describe this online variant of our method and how window size can be adjusted to optimize for sampling noise and distributional drift in Appendix C.3.

4. Theoretical Analysis

In this section, we analyze our method for label model parameter recovery and provide bounds on its performance. First, we derive a $\mathcal{O}(1/\sqrt{n})$ bound for the sampling error $\|\hat{\mu} - \mu\|_2$ in Algorithm 2. Next, we show that this sampling error has a tight minimax lower bound for certain graphical models, proving that our method is information-theoretically optimal. Then, we present a generalization error bound for the end model that scales in the sampling error and a *model misspecification* term, which exists when the underlying data distribution \mathcal{D} cannot be represented with our graphical model. Lastly, we interpret these results, which are more fine-grained than prior weak supervision analyses, in terms of end model performance and label model tradeoffs. All proofs are provided in Appendix D.

In Appendix C.3.1, we give two further results for the online variant of the algorithm: selecting an optimal window size to

minimize sampling error, and providing a guarantee on end model performance even in the presence of distributional drift, sample noise, and model misspecification.

Sampling Error We first control the error in estimating the label model parameters $\hat{\mu}$. The noise comes from sampling in the empirical estimates of moments and probabilities used by Algorithm 2.

Theorem 1. *Let $\hat{\mu}$ be an estimate of μ produced by Algorithm 2 using n unlabeled data points. Then, assuming that cliques in G_{dep} are limited to 3 vertices,*

$$\mathbb{E} [\|\hat{\mu} - \mu\|_2] \leq \frac{1}{a_{\min}^5} \left(3.19C_1 \sqrt{\frac{m}{n}} + \frac{6.35C_2}{\sqrt{r}} \frac{m}{\sqrt{n}} \right),$$

where $a_{\min} > 0$ is a lower bound on the absolute value of the accuracies of the sources, and r is the minimum frequency at which sources abstain, if they do so.

If no sources abstain, \sqrt{r} is not present in the bound. For higher-order cliques, the error scales in m with the size of the largest clique. In the case of full conditional independence, only the first term in the bound is present, so the error scales as $\mathcal{O}(\sqrt{\frac{m}{n}})$.

Optimality We show that our method is sample optimal in both n and m up to constant factors for certain graphical models. We bound the minimax risk for the parameter estimates to be $\Omega(\sqrt{\frac{m}{n}})$ via Assouad’s Lemma (Yu, 1997). This bound holds for any binary Ising model used in our framework, but in particular it is tight when our observed variables are all conditionally independent and do not abstain.

Theorem 2. *Let $\mathcal{P} = \left\{ P(Y, \mathbf{v}) = \frac{1}{Z} \exp(\theta_Y Y + \sum_{i=1}^m \theta_i v_i Y) \right\}$, $\theta \in \mathbb{R}^{m+1}$ be a family of distributions. Using L_2 norm estimation of the minimax risk, the sampling error is lower bounded as*

$$\inf_{\hat{\mu}} \sup_{P \in \mathcal{P}} \mathbb{E}_P [\|\hat{\mu} - \mu(P)\|_2] \geq \frac{e_{\min}}{8} \sqrt{\frac{m}{n}}.$$

Here $\mu(P)$ is the set of label model parameters corresponding to a distribution P , and e_{\min} is the minimum eigenvalue of $\text{Cov}[Y, \mathbf{v}]$ for distributions in \mathcal{P} .

Generalization Bound We provide a bound quantifying the performance gap between the end model parametrization that uses outputs of our label model and the optimal end model parametrization over the true distribution of labels.

Let $P_{\hat{\mu}}(\cdot|\lambda)$ be the probabilistic output of our learned label model parametrized by $\hat{\mu}$ given some source labels λ . Define a loss function $L(w, \mathbf{X}, \mathbf{Y}) \in [0, 1]$, where w parametrizes the end model $f_w \in \mathcal{F} : \mathcal{X} \rightarrow \mathcal{Y}$, and choose

\hat{w} such that

$$\hat{w} = \operatorname{argmin}_w \frac{1}{n} \sum_{i=1}^n \mathbb{E}_{\tilde{\mathbf{Y}} \sim P_{\hat{\mu}}(\cdot|\lambda(\mathbf{X}^i))} [L(w, \mathbf{X}^i, \tilde{\mathbf{Y}})].$$

While previous approaches (Ratner et al., 2019) make the strong assumption that there exists some μ such that sampling $(\mathbf{X}, \tilde{\mathbf{Y}})$ from P_{μ} is equivalent to sampling from \mathcal{D} , our generalization error bound accounts for potential model misspecification:

Theorem 3. *Let $w^* = \operatorname{argmin}_w \mathbb{E}_{(\mathbf{X}, \mathbf{Y}) \sim \mathcal{D}} [L(w, \mathbf{X}, \mathbf{Y})]$. There exists a \hat{w} computed from the outputs of our label model such that the generalization error for \mathbf{Y} satisfies*

$$\begin{aligned} \mathbb{E}_{\mathcal{D}} [L(\hat{w}, \mathbf{X}, \mathbf{Y}) - L(w^*, \mathbf{X}, \mathbf{Y})] \\ \leq \gamma(n) + \frac{8|\mathcal{Y}|}{e_{\min}} \|\hat{\mu} - \mu\|_2 + \delta(\mathcal{D}, P_{\mu}), \end{aligned}$$

where $\delta(\mathcal{D}, P_{\mu}) = 2\sqrt{2KL(\mathcal{D}(\mathbf{Y}|\mathbf{X}) \| P_{\mu}(\mathbf{Y}|\mathbf{X}))}$, e_{\min} is the minimum eigenvalue of $\text{Cov}[Y, \mathbf{v}]$ over the construction of the binary Ising model, and $\gamma(n)$ is a decreasing function that bounds the error from performing empirical risk minimization to learn \hat{w} .

Interpreting the Bounds The generalization error in Theorem 3 has two components, involving the noise awareness of the model and the model misspecification. Using the sampling error result, the first two terms $\gamma(n)$ and $\|\hat{\mu} - \mu\|_2$ scale in $\mathcal{O}(1/\sqrt{n})$, which can be tight by Theorem 2 and is the same asymptotic rate as supervised approaches.

The third term $\delta(\mathcal{D}, P_{\mu})$ is a divergence between our model and \mathcal{D} . Richer models can represent more distributions and have a smaller KL term, but may suffer a higher sample complexity. This tradeoff suggests the importance of selecting an appropriately constrained graphical model in practice.

5. Evaluation

The primary goal of our evaluation is to validate that FLYINGSQUID can achieve the same or higher quality as state-of-the-art weak supervision frameworks (Section 5.1) while learning label model parameters orders of magnitude faster (Section 5.2). We also evaluate the online extension and discuss how online learning can be preferable to offline learning in the presence of distributional shift over time (Section 5.3).

Datasets We evaluate FLYINGSQUID on three benchmark datasets and four video analysis tasks. Each dataset consists of a large (187–64,130) unlabeled training set, a smaller (50–9,479) hand-labeled *development set*, and a held-out test set. We use the unlabeled training set to train the label model and end model, and use the labeled development set

Fast and Three-rious: Speeding Up Weak Supervision with Triplet Methods

	Task	D	m	Prop	End Model Performance (F1), Label Model Training Time (s)					Lift, Speedup			
					TS	MV	DP	SDP	FLYINGSQUID (Lm. in paren.)	TS	MV	DP	SDP
Benchmarks	Spouse	1	9	0.07	20.4 ± 0.2 –	19.3 ± 0.01 –	44.7 ± 1.7 7.5 ± 0.9	– –	49.6 ± 2.4 (47.0) 0.017 ± 0.003	+29.3 –	+30.3 –	+4.9 440×	– –
	Spam	1	10	0.49	91.5 –	88.3 –	91.8 0.76 ± 0.1	– –	92.3 (89.1) 0.014 ± 0.002	+0.8 –	+4.0 –	+0.5 54×	– –
	Weather	1	103	0.53	74.6 –	87.3 –	87.3 0.78 ± 0.1	– –	88.9 (77.6) 0.150 ± 0.03	+14.3 –	+1.6 –	+1.6 5.2×	– –
Video Analysis	Interview	6	24	0.03	80.0 ± 3.4 –	58.0 ± 5.3 –	8.7 ± 0.2 31.5 ± 1.0	92.0 ± 2.2 256.6 ± 5.4	91.9 ± 1.6 (93.0) 0.423 ± 0.04	+11.9 –	+33.9 –	+83.2 74.5×	-0.1 607×
	Commercial	6	24	0.32	90.9 ± 1.0 –	91.8 ± 0.2 –	90.5 ± 0.4 23.3 ± 1.0	89.8 ± 0.5 265.6 ± 6.2	92.3 ± 0.4 (88.4) 0.067 ± 0.01	+1.4 –	+0.5 –	+1.8 350×	+2.5 4,000×
	Tennis Rally	14	84	0.34	57.6 ± 3.4 –	80.2 ± 1.0 –	82.5 ± 0.3 41.1 ± 1.9	80.6 ± 0.7 398.4 ± 7.5	82.8 ± 0.4 (82.0) 0.199 ± 0.04	+25.2 –	+2.6 –	+0.3 210×	+2.2 2,000×
	Basketball	8	32	0.12	26.8 ± 1.3 –	8.1 ± 5.4 –	7.7 ± 3.3 28.7 ± 2.0	38.2 ± 4.1 248.6 ± 7.7	37.9 ± 1.9 (27.9) 0.092 ± 0.03	+11.1 –	+29.8 –	+30.2 310×	-0.3 2,700×

Table 1. FLYINGSQUID performance in terms of F1 score (first row of each task), and label model training time in seconds (second row). We report mean ± standard deviation across five random weight initializations of the end model (except for **Spam** and **Weather**, which use logistic regression). Improvement in terms of mean end model lift, speedup in terms of mean runtime. We compare FLYINGSQUID’s end model and label model (label model in parentheses) against traditionally supervised (TS) end models trained on the labeled dev set, majority vote (MV), data programming (DP) and sequential data programming (SDP). D : number of related elements modeled (contiguous sequences of frames for video tasks). m : number of supervision sources. Prop: proportion of positive examples.

for a) training a traditional supervision baseline, and b) for hyperparameter tuning of the label and end models. More details about each task and the experiments in Appendix E.

Benchmark Tasks. We draw three benchmark weak supervision datasets from a previous evaluation of a state-of-the-art weak supervision framework (Ratner et al., 2018). **Spouse** seeks to identify mentions of spouse relationships in a set of news articles (Corney et al., 2016), **Spam** classifies whether YouTube comments are spam (Alberto et al., 2015), and **Weather** is a weather sentiment task from Crowdflower (Cro, 2018).

Video Analysis Tasks. We use video analysis as another driving task: video data is large and expensive to label, and modeling temporal dependencies is important for quality but introduces significant slowdowns in label model parameter recovery (Sala et al., 2019). **Interview** and **Commercial** identify interviews with Bernie Sanders and commercials in a corpus of TV news, respectively (Fu et al., 2019; Int, 2018). **Tennis Rally** identifies tennis rallies during a match from broadcast footage. **Basketball** identifies basketball videos in a subset of ActivityNet (Caba Heilbron et al., 2015).

5.1. Quality

We now validate that end models trained with labels generated by FLYINGSQUID achieve the same or higher quality as previous state-of-the-art weak supervision frameworks. We also discuss the relative performance of FLYINGSQUID’s label model compared to the end model, and ablations of our method.

End Model Quality To evaluate end model quality, we use FLYINGSQUID to generate labels for the unlabeled train-

ing set and compare the end models trained with these labels against four baselines:

1. **Traditional Supervision [TS]:** We train the end model using the small hand-labeled development set.
2. **Majority Vote [MV]:** We generate training labels over the unlabeled training set using majority vote.
3. **Data Programming [DP]:** We use data programming, a state-of-the-art weak supervision framework that models each data point separately (Ratner et al., 2019).
4. **Sequential Data Programming [SDP]:** For the video tasks, we also use a state-of-the-art sequential weak supervision framework, which models sequences of frames (Sala et al., 2019).

Table 1 shows our results. We achieve the same or higher end model quality compared to previous weak supervision frameworks. Since FLYINGSQUID does not rely on SGD to learn label model parameters, there are fewer hyperparameters to tune, which can help us achieve higher quality than previous reported results.

Label Model vs. End Model Performance Table 1 also shows the performance of FLYINGSQUID’s label model. In four of the seven tasks, the end model outperforms the label model, since it can learn new features directly from the input data that are not available to the noisy sources. For example, the sources in the **Commercial** task rely on simple visual heuristics like the presence of black frames (in our dataset, commercials tend to be book-ended on either side by black frames); the end model, which is a deep network, is able to pick up on subtler features over the pixel space. In three tasks, however, the label model nearly matches

Task	Streaming End Model (F1)			Improvement	
	TS	MV	FLYINGSQUID	TS	MV
Interview	41.9 ± 4.0	37.8 ± 9.5	53.5 ± 0.5	+11.6	+15.7
Commercial	56.5 ± 1.7	78.9 ± 14.5	93.0 ± 0.5	+36.5	+14.1
Tennis Rally	41.5 ± 1.7	81.6 ± 0.6	82.7 ± 0.4	+25.2	+1.1
Basketball	20.7 ± 4.2	22.0 ± 11.3	26.7 ± 0.3	+6.0	+4.7

Table 2. We compare performance of an end model trained with an online pass over the training set, and then the test set with labels from FLYINGSQUID, against a model trained with majority vote (MV) labels over the training and test set, and a traditionally supervised (TS) model trained with ground truth labels over the test set. We report mean \pm standard deviation from five random weight initializations.

or slightly outperforms the end model. In these cases, the sources have access to features that are difficult for an end model to learn with the amount of unlabeled data available. For example, the sources in the **Interview** task rely on an identity classifier that has learned to identify Bernie Sanders from thousands of examples.

Ablations We describe the results of two ablation studies (detailed results in Appendix E.4). In the first study, we replace abstentions with random votes instead of augmenting G_{dep} . This results in a degradation of 25.6 points, demonstrating the importance of allowing supervision sources to abstain. In the second study, we examine the effect of using individual triplet assignments instead of taking the median or mean over all possible assignments. On average, taking random assignments results in a degradation of 23.8 points compared to taking an aggregate. Furthermore, there is a large degree of variance in label model performance when using individual triplet assignments. While the best assignments can match FLYINGSQUID, bad assignments result in significantly worse performance.

5.2. Speedup

We now evaluate the speedup that FLYINGSQUID provides over previous weak supervision frameworks. Table 1 shows measurements of how long it takes to train each label model. Since FLYINGSQUID learns source accuracies and correlations with a closed-form solution, it runs orders of magnitude faster than previous weak supervision frameworks, which rely on multiple iterations of stochastic gradient descent and thus scale superlinearly in the data. Speedup varies due to the optimal number of iterations for DP and SDP, which are SGD-based (number of iterations is tuned for accuracy), but FLYINGSQUID runs up to 440 times faster than data programming on benchmark tasks, and up to 4,000 times faster than sequential data programming on the video tasks (where modeling sequential dependencies results in much slower performance).

5.3. Online Weak Supervision

We now evaluate the ability of our online extension to simultaneously train a label model and end model online for our video analysis tasks. We also use synthetic experiments to demonstrate when training a model online can be preferable to training a model offline.

Core Validation We first validate our online extension by using the FLYINGSQUID PyTorch layer to simultaneously train a label model and end model online for our video analysis tasks. We train first on the training set and then on the test set (using probabilistic labels for both). We compare against online traditional supervision (TS) and majority vote (MV) baselines. Since the training set is unlabeled, the TS model is trained only on the ground-truth test set labels, while the MV baseline uses majority vote to label the training and test sets. To mimic the online setting, each datapoint is only seen once during training.

Table 2 shows our results. Our method outperforms MV by up to 15.7 F1 points, and TS by up to 36.5 F1 points. Even though TS is trained on ground-truth test set labels, it underperforms both other methods because it only does a single pass over the (relatively small) test set. MV and FLYINGSQUID, on the other hand, see many more examples in the weakly-labeled training set before having to classify the test set.

The online version of FLYINGSQUID often underperforms its offline equivalent (Table 1), since the online model can only perform a single iteration of SGD with each datapoint. However, in 2 cases, the online model overperforms the offline model, for two reasons: a) the training set is large enough to make up the difference in having multiple epochs with SGD, and b) online training over the test set enables continued specialization to the test set.

Distributional Drift Over Time We also study the effect of distributional drift over time using synthetic experiments. Distributional drift can mean that label model parameters learned on previous data points may not describe future data points. Figure 3 shows the results of online vs. offline training in two settings with different amounts of drift. On the left is a setting with limited drift; in this setting, the offline model learns better parameters than the online model, since it has access to more data, all of which is representative of the test set. On the right is a setting with large amounts of periodic drift; in this setting, the offline model cannot learn parameters that work for all data points. But the online model, which only learns parameters for a recent window of data points, is able to specialize to the periodic shifts.

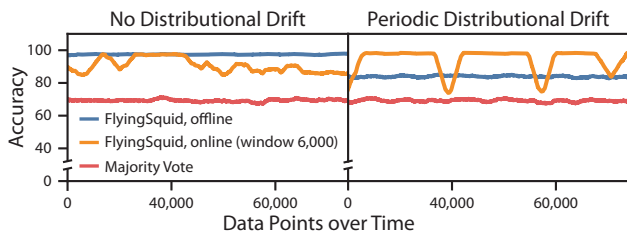


Figure 3. When there is large distributional drift, online learning can outperform offline learning by adapting over time (synthetic).

6. Related Work

Latent Variable Estimation Latent variable estimation is a classic problem in machine learning, used for hidden Markov Models, Markov random fields, topic modeling, and more (Wainwright & Jordan, 2008; Koller & Friedman, 2009). General algorithms do not admit closed-form solutions; classical techniques like expectation maximization and Gibbs sampling can require many iterations to converge, while techniques like tensor decomposition run the expensive power method (Anandkumar et al., 2014). We show that the weak supervision setting allows us to break down the parameter estimation problem into subproblems with closed-form solutions.

Our solution is similar to previous methods that have exploited triplets of conditionally-independent variables to solve latent variable estimation (Joglekar et al., 2013; Chaganty & Liang, 2014). Joglekar et al. (2013) focuses on the explicit context of crowdsourcing and is equivalent to a simplified version of Algorithm 1 when all the label sources are conditionally independent from each other and do not abstain. In contrast, our work handles a wider variety of use cases critical for weak supervision (such as sources that can abstain) and develops theoretical characterizations for downstream model behavior. Chaganty & Liang (2014) shows how to estimate the canonical parameters of a wide class of graphical models by applying tensor decomposition to recover conditional parameters. By comparison, our work is more specialized, which lets us replace tensor decomposition with a non-iterative closed-form solution, even for non-binary variables. A more detailed comparison against both of these methods is available in Appendix A.

Weak Supervision Our work is related to several such techniques, such as distant supervision (Mintz et al., 2009; Craven et al., 1999; Hoffmann et al., 2011; Takamatsu et al., 2012), co-training methods (Blum & Mitchell, 1998), pattern-based supervision (Gupta & Manning, 2014) and feature annotation (Mann & McCallum, 2010; Zaidan & Eisner, 2008; Liang et al., 2009). Recently, weak supervision frameworks rely on latent graphical models and other methods to systematically integrate multiple noisy sources (Ratner et al., 2016; 2018; Bach et al., 2017; 2019; Guan et al., 2018;

Khetan et al., 2018; Sheng et al., 2020; Ré et al., 2020). Two recent approaches have proposed new methods for modeling sequential dependencies in particular, which is important in applications like video (Zhan et al., 2019; Sala et al., 2019; Safranchik et al., 2020). These approaches largely rely on iterative methods like stochastic gradient descent, and do not run closed-form solutions to latent variable estimation.

Crowdsourcing Our work is related to crowdsourcing (crowd workers can be thought of as noisy label sources). A common approach in crowdsourcing is filtering crowd workers using a small set of gold tasks, or filtering based on number of previous tasks completed or with monetary incentives (Rashtchian et al., 2010; Shaw et al., 2011; Sorokin & Forsyth, 2008; Downs et al., 2010; Mitra et al., 2015; Kittur et al., 2008). In contrast, in our setting, we do not have access to ground truth data to estimate source accuracies, and we cannot filter out noisy sources *a priori*. Other techniques can estimate worker accuracies without ground truth annotations, but assume that workers are independent (Karger et al., 2011). We can also directly model crowd workers using our label model, as in the **Weather** task.

Online Learning Training models online traditionally requires hand labels (Cesa-Bianchi & Lugosi, 2006; Shalev-Shwartz et al., 2012), but recent approaches like Mullapudi et al. (2019) train models online using a student-teacher framework (training a student network online based on the outputs of a more powerful teacher network). In contrast, our method does not rely on a powerful network that has been pre-trained to carry out the end task. In both traditional and newer distillation settings, a critical challenge is updating model parameters to account for domain shift (Shalev-Shwartz et al., 2012). For our online setting, we deal with distributional drift via a standard rolling window.

7. Conclusion

We have proposed a method for latent variable estimation by decomposing it into minimal subproblems with closed-form solutions. We have used this method to build FLYINGSQUID, a new weak supervision framework that achieves the same or higher quality as previous approaches while running orders of magnitude faster, and presented an extension to online learning embodied in a novel FLYINGSQUID layer. We have proven generalization and sampling error bounds and shown that our method can be sample optimal. In future work, we plan to extend our insights to more problems where closed-form latent variable estimation can result in faster algorithms or new applications—problems such as structure learning and data augmentation.

Acknowledgments

We thank Avanika Narayan for helping with the Tennis dataset, and Avner May for helpful discussions. We gratefully acknowledge the support of DARPA under Nos. FA86501827865 (SDH) and FA86501827882 (ASED); NIH under No. U54EB020405 (Mobilize), NSF under Nos. CCF1763315 (Beyond Sparsity), CCF1563078 (Volume to Velocity), and 1937301 (RTML); ONR under No. N000141712266 (Unifying Weak Supervision); the Moore Foundation, NXP, Xilinx, LETI-CEA, Intel, IBM, Microsoft, NEC, Toshiba, TSMC, ARM, Hitachi, BASF, Accenture, Ericsson, Qualcomm, Analog Devices, the Okawa Foundation, American Family Insurance, Google Cloud, Swiss Re, Brown Institute for Media Innovation, the HAI-AWS Cloud Credits for Research program, Department of Defense (DoD) through the National Defense Science and Engineering Graduate Fellowship (NDSEG) Program, Fannie and John Hertz Foundation, National Science Foundation Graduate Research Fellowship under Grant No. DGE-1656518, Texas Instruments Stanford Graduate Fellowship in Science and Engineering, and members of the Stanford DAWN project: Teradata, Facebook, Google, Ant Financial, NEC, VMWare, and Infosys. The U.S. Government is authorized to reproduce and distribute reprints for Governmental purposes notwithstanding any copyright notation thereon. Any opinions, findings, and conclusions or recommendations expressed in this material are those of the authors and do not necessarily reflect the views, policies, or endorsements, either expressed or implied, of DARPA, NIH, ONR, or the U.S. Government.

References

- Weather sentiment: Dataset in crowdflower. <https://data.world/crowdflower/weather-sentiment>, 2018.
- Internet archive: Tv news archive. <https://archive.org/details/tv>, 2018.
- Alberto, T. C., Lochter, J. V., and Almeida, T. A. Tubesppam: Comment spam filtering on youtube. In *2015 IEEE 14th International Conference on Machine Learning and Applications (ICMLA)*, pp. 138–143. IEEE, 2015.
- Anandkumar, A., Ge, R., Hsu, D., Kakade, S. M., and Telgarsky, M. Tensor decompositions for learning latent variable models. *Journal of Machine Learning Research*, 15:2773–2832, 2014.
- Bach, S. H., He, B., Ratner, A., and Ré, C. Learning the structure of generative models without labeled data. In *ICML*, 2017.
- Bach, S. H., Rodriguez, D., Liu, Y., Luo, C., Shao, H., Xia, C., Sen, S., Ratner, A., Hancock, B., Alborzi, H., et al. Snorkel drybell: A case study in deploying weak supervision at industrial scale. In *Proceedings of the 2019 International Conference on Management of Data*, pp. 362–375, 2019.
- Blum, A. and Mitchell, T. Combining labeled and unlabeled data with co-training. In *Proceedings of the eleventh annual conference on Computational learning theory*, pp. 92–100. ACM, 1998.
- Bunea, F. and Xiao, L. On the sample covariance matrix estimator of reduced effective rank population matrices, with applications to fPCA. *Bernoulli*, 21(5):1200–1230, 2015.
- Caba Heilbron, F., Escorcía, V., Ghanem, B., and Carlos Niebles, J. Activitynet: A large-scale video benchmark for human activity understanding. In *Proceedings of the IEEE Conference on Computer Vision and Pattern Recognition*, pp. 961–970, 2015.
- Cesa-Bianchi, N. and Lugosi, G. *Prediction, learning, and games*. Cambridge university press, 2006.
- Chaganty, A. T. and Liang, P. Estimating latent-variable graphical models using moments and likelihoods. In *International Conference on Machine Learning*, pp. 1872–1880, 2014.
- Chandrasekaran, V., Srebro, N., and Harsha, P. Complexity of inference in graphical models. In *Proceedings of the Twenty-Fourth Conference on Uncertainty in Artificial Intelligence*, pp. 70–78. AUAI Press, 2008.
- Corney, D., AlBakour, D., Martinez-Alvarez, M., and Moussa, S. What do a million news articles look like? In *NewsIR@ ECIR*, pp. 42–47, 2016.
- Craven, M., Kumlien, J., et al. Constructing biological knowledge bases by extracting information from text sources. In *ISMB*, pp. 77–86, 1999.
- Dawid, A. P. and Skene, A. M. Maximum likelihood estimation of observer error-rates using the EM algorithm. *Applied statistics*, pp. 20–28, 1979.
- Dehghani, M., Severyn, A., Rothe, S., and Kamps, J. Learning to learn from weak supervision by full supervision. In *NIPS workshop on Meta-Learning (MetaLearn 2017)*, 2017a.
- Dehghani, M., Zamani, H., Severyn, A., Kamps, J., and Croft, W. B. Neural ranking models with weak supervision. In *Proceedings of the 40th International ACM SIGIR Conference on Research and Development in Information Retrieval*, pp. 65–74. ACM, 2017b.

- Devlin, J., Chang, M.-W., Lee, K., and Toutanova, K. Bert: Pre-training of deep bidirectional transformers for language understanding. *arXiv preprint arXiv:1810.04805*, 2018.
- Downs, J. S., Holbrook, M. B., Sheng, S., and Cranor, L. F. Are your participants gaming the system? screening mechanical turk workers. In *Proceedings of the SIGCHI conference on human factors in computing systems*, pp. 2399–2402, 2010.
- Fu, D. Y., Crichton, W., Hong, J., Yao, X., Zhang, H., Truong, A., Narayan, A., Agrawala, M., Ré, C., and Fatahalian, K. Recall: Specifying video events using compositions of spatiotemporal labels. *arXiv preprint arXiv:1910.02993*, 2019.
- Guan, M. Y., Gulshan, V., Dai, A. M., and Hinton, G. E. Who said what: Modeling individual labelers improves classification. In *Thirty-Second AAAI Conference on Artificial Intelligence*, 2018.
- Gupta, S. and Manning, C. Improved pattern learning for bootstrapped entity extraction. In *Proceedings of the Eighteenth Conference on Computational Natural Language Learning*, pp. 98–108, 2014.
- Hearst, M. A. Automatic acquisition of hyponyms from large text corpora. In *Proceedings of the 14th conference on Computational linguistics-Volume 2*, pp. 539–545. Association for Computational Linguistics, 1992.
- Hochreiter, S. and Schmidhuber, J. Long short-term memory. *Neural Comput.*, 9(8):1735–1780, November 1997.
- Hoffmann, R., Zhang, C., Ling, X., Zettlemoyer, L., and Weld, D. S. Knowledge-based weak supervision for information extraction of overlapping relations. In *Proceedings of the 49th Annual Meeting of the Association for Computational Linguistics: Human Language Technologies-Volume 1*, pp. 541–550. Association for Computational Linguistics, 2011.
- Jia, Z., Huang, X., Eric, I., Chang, C., and Xu, Y. Constrained deep weak supervision for histopathology image segmentation. *IEEE transactions on medical imaging*, 36(11):2376–2388, 2017.
- Joglekar, M., Garcia-Molina, H., and Parameswaran, A. Evaluating the crowd with confidence. In *Proceedings of the 19th ACM SIGKDD international conference on Knowledge discovery and data mining*, pp. 686–694, 2013.
- Karger, D. R., Oh, S., and Shah, D. Iterative learning for reliable crowdsourcing systems. In *Advances in neural information processing systems*, pp. 1953–1961, 2011.
- Khetan, A., Lipton, Z. C., and Anandkumar, A. Learning from noisy singly-labeled data. In *International Conference on Learning Representations*, 2018.
- Kittur, A., Chi, E. H., and Suh, B. Crowdsourcing user studies with mechanical turk. In *Proceedings of the SIGCHI conference on human factors in computing systems*, pp. 453–456, 2008.
- Koller, D. and Friedman, N. *Probabilistic graphical models: principles and techniques*. MIT press, 2009.
- Lauritzen, S. *Graphical Models*. Clarendon Press, 1996.
- Liang, P., Jordan, M. I., and Klein, D. Learning from measurements in exponential families. In *Proceedings of the 26th annual international conference on machine learning*, pp. 641–648. ACM, 2009.
- Long, P. M. The complexity of learning according to two models of a drifting environment. *Machine Learning*, 37(3):337–354, Dec 1999. ISSN 1573-0565. doi: 10.1023/A:1007666507971. URL <https://doi.org/10.1023/A:1007666507971>.
- Mahajan, D., Girshick, R., Ramanathan, V., He, K., Paluri, M., Li, Y., Bharambe, A., and van der Maaten, L. Exploring the limits of weakly supervised pretraining. In *Proceedings of the European Conference on Computer Vision (ECCV)*, pp. 181–196, 2018.
- Mann, G. S. and McCallum, A. Generalized expectation criteria for semi-supervised learning with weakly labeled data. *Journal of machine learning research*, 11(Feb):955–984, 2010.
- Mintz, M., Bills, S., Snow, R., and Jurafsky, D. Distant supervision for relation extraction without labeled data. In *Proceedings of the Joint Conference of the 47th Annual Meeting of the ACL and the 4th International Joint Conference on Natural Language Processing of the AFNLP: Volume 2-Volume 2*, pp. 1003–1011. Association for Computational Linguistics, 2009.
- Mitra, T., Hutto, C. J., and Gilbert, E. Comparing person- and process-centric strategies for obtaining quality data on amazon mechanical turk. In *Proceedings of the 33rd Annual ACM Conference on Human Factors in Computing Systems*, pp. 1345–1354, 2015.
- Mullapudi, R. T., Chen, S., Zhang, K., Ramanan, D., and Fatahalian, K. Online model distillation for efficient video inference. In *Proceedings of the IEEE International Conference on Computer Vision*, pp. 3573–3582, 2019.
- Niu, F., Zhang, C., Ré, C., and Shavlik, J. W. Deepdive: Web-scale knowledge-base construction using statistical learning and inference. *VLDS*, 12:25–28, 2012.

- Raghunathan, A., Frostig, R., Duchi, J., and Liang, P. Estimation from indirect supervision with linear moments. In *International conference on machine learning*, pp. 2568–2577, 2016.
- Rashtchian, C., Young, P., Hodosh, M., and Hockenmaier, J. Collecting image annotations using amazon’s mechanical turk. In *Proceedings of the NAACL HLT 2010 Workshop on Creating Speech and Language Data with Amazon’s Mechanical Turk*, pp. 139–147. Association for Computational Linguistics, 2010.
- Ratner, A., Bach, S. H., Ehrenberg, H., Fries, J., Wu, S., and Ré, C. Snorkel: Rapid training data creation with weak supervision. In *Proceedings of the 44th International Conference on Very Large Data Bases (VLDB)*, Rio de Janeiro, Brazil, 2018.
- Ratner, A. J., Sa, C. M. D., Wu, S., Selsam, D., and Ré, C. Data programming: Creating large training sets, quickly. In *Proceedings of the 29th Conference on Neural Information Processing Systems (NIPS 2016)*, Barcelona, Spain, 2016.
- Ratner, A. J., Hancock, B., Dunnmon, J., Sala, F., Pandey, S., and Ré, C. Training complex models with multi-task weak supervision. In *Proceedings of the AAAI Conference on Artificial Intelligence*, Honolulu, Hawaii, 2019.
- Ré, C., Niu, F., Gudipati, P., and Srisuwananukorn, C. Overton: A data system for monitoring and improving machine-learned products. In *Proceedings of the 10th Annual Conference on Innovative Data Systems Research*, 2020.
- Safranich, E., Luo, S., and Bach, S. H. Weakly supervised sequence tagging from noisy rules. In *Thirty-Fourth AAAI Conference on Artificial Intelligence*, 2020.
- Sala, F., Varma, P., Fries, J., Fu, D. Y., Sagawa, S., Khattar, S., Ramamoorthy, A., Xiao, K., Fatahalian, K., Priest, J., and Ré, C. Multi-resolution weak supervision for sequential data. In *Advances in Neural Information Processing Systems 32*, pp. 192–203, 2019.
- Shalev-Shwartz, S. et al. Online learning and online convex optimization. *Foundations and Trends® in Machine Learning*, 4(2):107–194, 2012.
- Shaw, A. D., Horton, J. J., and Chen, D. L. Designing incentives for inexpert human raters. In *Proceedings of the ACM 2011 conference on Computer supported cooperative work*, pp. 275–284, 2011.
- Sheng, Y., Vo, N. H., Wendt, J. B., Tata, S., and Najork, M. Migrating a privacy-safe information extraction system to a software 2.0 design. In *Proceedings of the 10th Annual Conference on Innovative Data Systems Research*, 2020.
- Sorokin, A. and Forsyth, D. Utility data annotation with amazon mechanical turk. In *2008 IEEE Computer Society Conference on Computer Vision and Pattern Recognition Workshops*, pp. 1–8. IEEE, 2008.
- Takamatsu, S., Sato, I., and Nakagawa, H. Reducing wrong labels in distant supervision for relation extraction. In *Proceedings of the 50th Annual Meeting of the Association for Computational Linguistics: Long Papers-Volume 1*, pp. 721–729. Association for Computational Linguistics, 2012.
- Wainwright, M. J. and Jordan, M. I. Graphical models, exponential families, and variational inference. *Foundations and Trends® in Machine Learning*, 1(1-2):1–305, 2008.
- Xiao, T., Xia, T., Yang, Y., Huang, C., and Wang, X. Learning from massive noisy labeled data for image classification. In *Proceedings of the IEEE Conference on Computer Vision and Pattern Recognition*, pp. 2691–2699, 2015.
- Yu, B. Assouad, fano, and le cam. In *Festschrift for Lucien Le Cam*, pp. 423–435. Springer, 1997.
- Zaidan, O. F. and Eisner, J. Modeling annotators: A generative approach to learning from annotator rationales. In *Proceedings of the Conference on Empirical Methods in Natural Language Processing*, pp. 31–40. Association for Computational Linguistics, 2008.
- Zhan, E., Zheng, S., Yue, Y., Sha, L., and Lucey, P. Generating multi-agent trajectories using programmatic weak supervision. In *7th International Conference on Learning Representations, ICLR 2019, New Orleans, LA, USA, May 6-9, 2019*, 2019.
- Zhang, C., Ré, C., Cafarella, M., De Sa, C., Ratner, A., Shin, J., Wang, F., and Wu, S. DeepDive: Declarative knowledge base construction. *Commun. ACM*, 60(5): 93–102, 2017.
- Zhou, X. On the fenchel duality between strong convexity and lipschitz continuous gradient. *arXiv preprint arXiv:1803.06573*, 2018.

First, we provide an extended discussion of related work. Next, we provide a glossary of terms and notation that we use throughout this paper for easy summary. Next, we discuss additional algorithmic details, and we give the proofs of our main results (each theorem). Finally, we give additional experimental details.

A. Extended Related Work

The notion of the “triplet” of (conditionally) independent variables as the source of minimal signal in latent variable models was observed and exploited in two innovative works, both using moments to deal with the challenge of the latent variable. These are

- [Joglekar et al. \(2013\)](#), in the explicit context of crowdsourcing, and
- [Chaganty & Liang \(2014\)](#), for estimating the parameters of certain latent variable graphical models.

The “3-Differences Scheme” described in 3.1 of [Joglekar et al. \(2013\)](#) is equivalent to our approach in Algorithm 1 in the basic case where there are no abstains and the signs of the accuracies are non-negative. [Joglekar et al. \(2013\)](#) focuses on crowdsourcing, and thus offers two contributions for this setting: (i) computing confidence intervals for worker accuracies and (ii) a set of techniques for extending the three-voters case by collapsing multiple voters into a pair ‘super-voters’ in order to build a better triplet for a particular worker. Both of these are useful directions for extensions of our work. In contrast, our approach focuses on efficiently handling the non-binary abstains case critical for weak supervision and develops theoretical characterizations for the downstream model behavior when using our generated labels.

A more general approach to learning latent variable graphical models is described in [Chaganty & Liang \(2014\)](#). Here there is an explicit description of the “three-views” approach. It is shown how to estimate the canonical parameters of a remarkably wide class of graphical models (e.g., both directed and undirected) by applying the tensor decomposition idea (developed in [Anandkumar et al. \(2014\)](#)) to recover conditional parameters. By comparison, our work is more specialized, looking at undirected (in fact, specifically Ising) models in the context of weak supervision. The benefits of this specialization are that we can replace the use of the tensor power iteration technique with a non-iterative closed-form solution, even for non-binary variables. Nevertheless, the techniques in [Chaganty & Liang \(2014\)](#) can be useful for weak supervision as well, and their pseudolikelihood approach to recover canonical parameters suggests that forward methods of inference could be used in our label model. We also note that closed-form triplet methods can be used to estimate *part* of the parameters of a more complex exponential family model (where some variables are involved in pairwise interactions at most, others in more complex patterns), so that resorting to tensor power iterations can be minimized.

A further work that builds on the approach of [Chaganty & Liang \(2014\)](#) is [Raghunathan et al. \(2016\)](#), where moments are used in combination with a linear technique. However, the setting here is different from weak supervision. The authors of [Raghunathan et al. \(2016\)](#) study *indirect* supervision. Here, for any unlabeled data point x , the label y is not seen, but a variable o is observed. So far this framework resembles weak supervision, but in the indirect setting, the supervision distribution $S(o|y)$ is known—while for weak supervision, it is not. Instead, in [Chaganty & Liang \(2014\)](#), the S distribution is given for two particular applications: local privacy and a light-weight annotation scheme for POS tagging.

B. Glossary

The glossary is given in Table 3 below.

C. Further Algorithmic Details

In this section, we present more details on the main algorithm, extensions to more complex models, and the online variant.

C.1. Core Algorithm

We first present the general binary Ising model and the proof of Proposition 1 that follows from this construction. We also prove another independence property over this general class of Ising models that can be used to factorize expectations over arbitrarily large cliques. Next, we detail the exact setup of the graphical model when sources can abstain, as well as the special case when they never abstain, and define the mappings necessary to convert between values over v, G and λ, G_{dep} .

Symbol	Used for
\mathbf{X}	Unlabeled data vector, $\mathbf{X} = [X_1, X_2, \dots, X_D] \in \mathcal{X}$
\mathbf{X}^i	i th unlabeled data vector
X_i	i th data element
D	Length of the unlabeled data vector
\mathbf{Y}	Latent, ground-truth label vector, $\mathbf{Y} = [Y_1, Y_2, \dots, Y_D] \in \mathcal{Y}$, also referred to as hidden variables
\mathbf{Y}^i	i th ground-truth label vector
Y_i	Ground-truth label for i th task, $Y_i \in \{-1, +1\}$
\mathcal{D}	Distribution from which we assume (\mathbf{X}, \mathbf{Y}) data points are sampled i.i.d.
S_i	i th weak supervision source
m	Number of weak supervision sources
λ_i	Label of S_i for \mathbf{X} where $\lambda_i \in \{-1, 0, 1\}$; all m labels per \mathbf{X} collectively denoted λ
n	Number of data vectors
$\tilde{\mathbf{Y}}$	Probabilistic training labels for a label vector
f_w	Discriminative classifier used as end model, parametrized by w
G_{dep}	Source dependency graph
G	Augmented graph $G = (V, E)$ used for binary Ising model, where $V = \{\mathbf{Y}, \mathbf{v}\}$
\mathbf{v}	Observed variables of the graphical model corresponding to λ
L	Label matrix containing n samples of source labels $\lambda_1, \dots, \lambda_m$
\mathcal{L}	Augmented label matrix computed from L
$Y^{dep}(i)$	Task that λ_i labels
$Y(i)$	Hidden variable that the observed variable v_i acts on
$\tilde{\mathcal{C}}_{dep}$	Cliqueset (maximal and non-maximal) of G_{dep}
$\tilde{\mathcal{C}}_{dep}, \mathcal{S}_{dep}$	The maximal cliques and separator sets of the junction tree over G_{dep}
μ	The label model parameters collectively over all μ_C, μ_S , the marginal distributions of $C \in \tilde{\mathcal{C}}_{dep}, S \in \mathcal{S}_{dep}$
$P(\tilde{\mathbf{Y}})$	Class prior for the \mathbf{Y} label vector
a_i	$\mathbb{E}[v_i Y(i)]$, the unobservable mean parameters of binary Ising model G
Ω_G	Set of vertices in V to which the triplet method can be applied
\mathcal{C}	Cliqueset (maximal and non-maximal) of G
a_C	The expectation over the product of observed variables in clique $C \in \mathcal{C}$ and $Y(C)$
$a_{C_{dep}}$	The expectation over the product of sources in clique $C_{dep} \in \mathcal{C}_{dep}$ and $Y^{dep}(C_{dep})$

Table 3. Glossary of variables and symbols used in this paper.

We then formalize the linear transformation from $a_{C_{dep}}$ to $\mu_{C_{dep}}$, and finally we explain the RESOLVESIGNS function used in Algorithm 1.

First, we give the explicit form of the density for the Ising model we use. Given the graph $G = (V, E)$, we can write the corresponding joint distribution of \mathbf{Y}, \mathbf{v} as

$$f_G(\mathbf{Y}, \mathbf{v}) = \frac{1}{Z} \exp \left(\sum_{k=1}^D \theta_{Y_k} Y_k + \sum_{(Y_k, Y_l) \in E} \theta_{Y_k, Y_l} Y_k Y_l + \sum_{v_i \in \mathbf{v}} \theta_i v_i Y(i) + \sum_{(v_k, v_l) \in E} \theta_{k,l} v_k v_l \right), \quad (3)$$

where Z is the partition function, and the θ terms collectively are the canonical parameters of the model. Note that this is the most general definition of the binary Ising model with multiple dependent hidden variables and observed variables that we use.

C.1.1. PROOF OF PROPOSITION 1

We present the proof of Proposition 1, which is the underlying independence property of (3) that enables us to use the triplet method. We aim to show that for any $a, b \in \{-1, +1\}^2$,

$$P(v_i Y(i) = a, v_j Y(i) = b) = P(v_i Y(i) = a) \cdot P(v_j Y(i) = b), \quad (4)$$

where $v_i \perp\!\!\!\perp v_j | Y(i)$. For now, assume that $Y(j) \neq Y(i)$.

Because v_i and v_j are conditionally independent given $Y(i)$, we have that $P(v_i = a, v_j = b | Y(i) = 1) = P(v_i = a | Y(i) =$

1) $\cdot P(v_j = b|Y(i) = 1)$, and similarly for $v_i = -a, v_j = -b$ conditional on $Y(i) = -1$. Then

$$\begin{aligned} P(v_i = a, v_j = b, Y(i) = 1) \cdot P(Y = 1) &= P(v_i = a, Y(i) = 1) \cdot P(v_j = b, Y(i) = 1) \\ P(v_i = -a, v_j = -b, Y(i) = -1) \cdot P(Y = -1) &= P(v_i = -a, Y(i) = -1) \cdot P(v_j = -b, Y(i) = -1). \end{aligned} \quad (5)$$

Note that terms in (4) can be split depending on if $Y(i)$ is 1 or -1 , so proving independence of $v_i Y(i)$ and $v_j Y(i)$ is equivalent to

$$\begin{aligned} &P(v_i = a, v_j = b, Y(i) = 1) + P(v_i = -a, v_j = -b, Y(i) = -1) \\ &= (P(v_i = a, Y(i) = 1) + P(v_i = -a, Y(i) = -1)) \cdot (P(v_j = b, Y(i) = 1) + P(v_j = -b, Y(i) = -1)). \end{aligned}$$

We substitute (5) into the right hand side. After rearranging, our equation to prove is

$$\begin{aligned} &P(v_i = a, v_j = b, Y(i) = 1) \cdot P(Y(i) = -1) + P(v_i = -a, v_j = -b, Y(i) = -1) \cdot P(Y(i) = 1) \\ &= P(v_i = -a, Y(i) = -1) \cdot P(v_j = b, Y(i) = 1) + P(v_i = a, Y(i) = 1) \cdot P(v_j = -b, Y(i) = -1). \end{aligned}$$

Due to symmetry of the terms above, it is thus sufficient to prove

$$P(v_i = a, v_j = b, Y(i) = 1) \cdot P(Y(i) = -1) = P(v_i = -a, Y(i) = -1) \cdot P(v_j = b, Y(i) = 1). \quad (6)$$

Let $N(v_i)$ be the set of v_i 's neighbors in \mathbf{v} , and $N(Y_i)$ be the set of Y_i 's neighbors in \mathbf{Y} . Let \mathcal{S} be the event space for the hidden and observed variables, such that each element of the set \mathcal{S} is a sequence of +1s and -1s of length equal to $|V|$. Denote $\mathcal{S}(v_i, v_j, Y(i))$ to be the event space for V besides v_i, v_j , and $Y(i)$; we also have similar definitions used for $\mathcal{S}(Y(i)), \mathcal{S}(v_i, Y(i)), \mathcal{S}(v_j, Y(i))$.

Our approach is to write each probability in (6) as a summation of joint probabilities over $\mathcal{S}(v_i, Y(i)), \mathcal{S}(v_j, Y(i))$, and $\mathcal{S}(v_i, v_j, Y(i))$ using (3). To do this more efficiently, we can factor each joint probability defined according to (3) into a product over *isolated variables* and a product over *non-isolated variables*. Recall that our marginal variables are v_i, v_j and $Y(i)$. Define the set of non-isolated variables to be the marginal variables, plus all variables that interact directly with the marginal variables according to the potentials in the binary Ising model. Per this definition, the non-isolated variables are $V_{NI} = \{v_i, v_j, Y(i), Y(j), N(Y(i)), N(v_i), N(v_j), v_{Y(i)}\}$ where $v_{Y(i)} = \{v : Y(v) = Y(i)\}$ and the isolated variables are all other variables not in this set, $V_I = V \setminus V_{NI}$. We can thus factorize each probability into a term $\psi(\cdot)$ corresponding to factors of the binary Ising model that only have isolated variables and a term $\zeta(\cdot)$ corresponding to factors that have non-isolated variables.

$$\begin{aligned} P(v_i = a, v_j = b, Y(i) = 1) &= \frac{1}{Z} \sum_{s^{(a,b)} \in \mathcal{S}(v_i, v_j, Y(i))} \psi(s^{(a,b)}) \cdot \zeta(v_i = a, v_j = b, Y(i) = 1, s^{(a,b)}) \\ P(Y(i) = -1) &= \frac{1}{Z} \sum_{s^{(Y)} \in \mathcal{S}(Y(i))} \psi(s^{(Y)}) \cdot \zeta(Y(i) = -1, s^{(Y)}) \\ P(v_i = -a, Y(i) = -1) &= \frac{1}{Z} \sum_{s^{(a)} \in \mathcal{S}(v_i, Y(i))} \psi(s^{(a)}) \cdot \zeta(v_i = -a, Y(i) = -1, s^{(a)}) \\ P(v_j = b, Y(i) = 1) &= \frac{1}{Z} \sum_{s^{(b)} \in \mathcal{S}(v_j, Y(i))} \psi(s^{(b)}) \cdot \zeta(v_j = b, Y(i) = 1, s^{(b)}) \end{aligned}$$

To be precise, $\psi(\cdot)$ is

$$\psi(s^{(a,b)}) = \exp \left(\sum_{\substack{Y_k \notin N(Y(i)) \\ \cup Y(i) \cup Y(j)}} \theta_{Y_k} Y_k^{(a,b)} + \sum_{\substack{Y_k, Y_l \notin \\ N(Y(i)) \cup Y(i) \cup Y(j)}} \theta_{Y_k, Y_l} Y_k^{(a,b)} Y_l^{(a,b)} + \sum_{\substack{Y(k) \notin N(Y(i)) \cup Y(i) \cup Y(j), \\ k \notin N(v_j) \cup v_j}} \theta_k v_k^{(a,b)} Y(k)^{(a,b)} + \sum_{\substack{v_k, v_l \notin N(v_i) \cup v_i \\ \cup N(v_j) \cup v_j}} \theta_{l,k} v_k^{(a,b)} v_l^{(a,b)} \right),$$

where $s^{(a,b)} = \{Y_1^{(a,b)}, \dots, Y_D^{(a,b)}, v_1^{(a,b)}, \dots\}$, and similar definitions hold for $s^{(a)}$, $s^{(b)}$, and $s^{(Y)}$. Then, (6) is equivalent to showing

$$\begin{aligned} & \sum_{s^{(a,b)}, s^{(Y)}} \psi(s^{(a,b)}) \cdot \psi(s^{(Y)}) \cdot \zeta(v_i = a, v_j = b, Y(i) = 1, s^{(a,b)}) \cdot \zeta(Y(i) = -1, s^{(Y)}) \\ &= \sum_{s^{(a)}, s^{(b)}} \psi(s^{(a)}) \cdot \psi(s^{(b)}) \cdot \zeta(v_i = -a, Y(i) = -1, s^{(a)}) \cdot \zeta(v_j = b, Y(i) = 1, s^{(b)}). \end{aligned}$$

We can show this by finding values of $s^{(a)}$ and $s^{(b)}$ that correspond to each $s^{(a,b)}$ and $s^{(Y)}$. Note that the ψ terms will cancel each other out if we directly set $s^{(a)}[V_I] = s^{(Y)}[V_I]$ and $s^{(b)}[V_I] = s^{(a,b)}[V_I]$. Therefore, we want to set $s^{(a)}[V_{NI}]$ and $s^{(b)}[V_{NI}]$ such that the products of ζ s are equivalent. We write them out explicitly first:

$$\begin{aligned} \zeta(v_i = a, v_j = b, Y(i) = 1, s^{(a,b)}) &= \exp \left(\theta_{Y(i)} + \sum_{Y_k \in N(Y(i)) \cup Y(j)} \theta_{Y_k} Y_k^{(a,b)} + \sum_{Y_k \in N(Y(i))} \theta_{Y_k, Y(i)} Y_k^{(a,b)} + \sum_{\substack{Y_k \in N(Y(i)) \cup Y(j), \\ Y_l \notin N(Y(i)) \cup Y(i) \cup Y(j)}} \theta_{Y_k, Y_l} Y_k^{(a,b)} Y_l^{(a,b)} \right. \\ &\quad \left. + \theta_i a + \theta_j b Y(j)^{(a,b)} + \sum_{\substack{k \neq i, j, \\ Y(k) = Y(i)}} \theta_k v_k^{(a,b)} + \sum_{\substack{k \neq i, j, \\ Y(k) \in N(Y(i)) \cup Y(j) \\ |k \in N(v_j)}} \theta_k v_k^{(a,b)} Y(k)^{(a,b)} + \sum_{v_k \in N(v_i)} \theta_{i,k} a v_k^{(a,b)} \right. \\ &\quad \left. + \sum_{v_k \in N(v_j)} \theta_{j,k} b v_k^{(a,b)} \right) \end{aligned}$$

$$\begin{aligned} \zeta(Y(i) = -1, s^{(Y)}) &= \exp \left(-\theta_{Y(i)} + \sum_{Y_k \in N(Y(i)) \cup Y(j)} \theta_{Y_k} Y_k^{(Y)} - \sum_{Y_k \in N(Y(i))} \theta_{Y_k, Y(i)} Y_k^{(Y)} + \sum_{\substack{Y_k \in N(Y(i)) \cup Y(j), \\ Y_l \notin N(Y(i)) \cup Y(i) \cup Y(j)}} \theta_{Y_k, Y_l} Y_k^{(Y)} Y_l^{(Y)} \right. \\ &\quad \left. - \theta_i v_i^{(Y)} + \theta_j v_j^{(Y)} Y(j)^{(Y)} - \sum_{\substack{k \neq i, j, \\ Y(k) = Y(i)}} \theta_k v_k^{(Y)} + \sum_{\substack{k \neq i, j, \\ Y(k) \in N(Y(i)) \cup Y(j) \\ |k \in N(v_j)}} \theta_k v_k^{(Y)} Y(k)^{(Y)} + \sum_{\substack{v_k \in N(v_i), \\ v_l \neq v_i}} \theta_{k,l} v_k^{(Y)} v_l^{(Y)} \right. \\ &\quad \left. + \sum_{\substack{v_k \in N(v_j), \\ v_l \neq v_j}} \theta_{k,l} v_k^{(Y)} v_l^{(Y)} \right) \end{aligned}$$

$$\begin{aligned} \zeta(v_i = -a, Y(i) = -1, s^{(a)}) &= \exp \left(-\theta_{Y(i)} + \sum_{Y_k \in N(Y(i)) \cup Y(j)} \theta_{Y_k} Y_k^{(a)} - \sum_{Y_k \in N(Y(i))} \theta_{Y_k, Y(i)} Y_k^{(a)} + \sum_{\substack{Y_k \in N(Y(i)) \cup Y(j), \\ Y_l \notin N(Y(i)) \cup Y(i) \cup Y(j)}} \theta_{Y_k, Y_l} Y_k^{(a)} Y_l^{(a)} \right. \\ &\quad \left. + \theta_i a + \theta_j v_j^{(a)} Y(j)^{(a)} - \sum_{\substack{k \neq i, j, \\ Y(k) = Y(i)}} \theta_k v_k^{(a)} + \sum_{\substack{k \neq i, j, \\ Y(k) \in N(Y(i)) \cup Y(j) \\ |k \in N(v_j)}} \theta v_k^{(a)} Y(k)^{(a)} + \sum_{\substack{v_k \in N(v_j), \\ v_l \neq v_j}} \theta_{k,l} v_k^{(a)} v_l^{(a)} \right. \\ &\quad \left. - \sum_{v_k \in N(v_i)} \theta_{i,k} a v_k^{(a)} \right) \end{aligned}$$

$$\begin{aligned} \zeta(v_j = b, Y(i) = 1, s^{(b)}) &= \exp \left(\theta_{Y(i)} + \sum_{Y_k \in N(Y(i)) \cup Y(j)} \theta_{Y_k} Y_k^{(b)} + \sum_{Y_k \in N(Y(i))} \theta_{Y_k, Y(i)} Y_k^{(b)} + \sum_{\substack{Y_k \in N(Y(i)) \cup Y(j), \\ Y_l \notin N(Y(i)) \cup Y(i) \cup Y(j)}} \theta_{Y_k, Y_l} Y_k^{(b)} Y_l^{(b)} \right. \\ &\quad \left. + \theta_i v_i^{(b)} + \theta_j b Y(j)^{(b)} + \sum_{\substack{k \neq i, j, \\ Y(k) = Y(i)}} \theta_k v_k^{(b)} + \sum_{\substack{k \neq i, j, \\ Y(k) \in N(Y(i)) \cup Y(j) \\ |k \in N(v_j)}} \theta_k v_k^{(b)} Y(k)^{(b)} + \sum_{\substack{v_k \in N(v_i), \\ v_l \neq v_i}} \theta_{k,l} v_k^{(b)} v_l^{(b)} \right. \\ &\quad \left. + \sum_{v_k \in N(v_j)} \theta_{j,k} b v_k^{(b)} \right) \end{aligned}$$

We present a simple mapping from $s^{(a,b)}$ and $s^{(Y)}$ to $s^{(a)}$ and $s^{(b)}$ such that $\zeta(v_i = a, v_j = b, Y(i) = 1, s^{(a,b)}) \cdot \zeta(Y(i) = -1, s^{(Y)}) = \zeta(v_i = -a, Y(i) = -1, s^{(a)}) \cdot \zeta(v_j = b, Y(i) = 1, s^{(b)})$ holds:

	$s^{(a)}$	$s^{(b)}$
v_i	—	$-v_i^{(Y)}$
v_j	$v_j^{(Y)}$	—
$Y_k \in N(Y(i)) \cup Y(j)$	$Y_k^{(Y)}$	$Y_k^{(a,b)}$
$v_k \in N(v_i)$	$-v_k^{(a,b)}$	$-v_k^{(Y)}$
$v_k \in N(v_j)$	$v_k^{(Y)}$	$v_k^{(a,b)}$
$v_{Y(i)}$	$-v_k^{(a,b)}$	$-v_k^{(Y)}$

With this construction of $s^{(a)}$ and $s^{(b)}$, we have shown that $v_i Y(i)$ and $v_j Y(i)$ are independent. (In the case that $Y(j) = Y(i)$, the proof is almost exactly the same).

C.1.2. HANDLING LARGER CLIQUES

We discuss how arbitrarily large cliques can be factorized into mean parameters and observable statistics to compute values of a_C in Algorithm 2. This is due to the following general independence property that arises from construction of the Ising model in (3):

Proposition 2. *For a clique C of v_k 's all connected to a single $Y(C)$, we have that $\prod_{k \in C} v_k \perp\!\!\!\perp Y(C)$ if $|C|$ is even, and $\prod_{k \in C} v_k Y(C) \perp\!\!\!\perp Y(C)$ if $|C|$ is odd.*

Therefore, if $|C|$ is even, then $a_C = \mathbb{E} [\prod_{k \in C} v_k] \cdot \mathbb{E} [Y(C)]$. If $|C|$ is odd, then $a_C = \mathbb{E} [\prod_{k \in C} v_k] / \mathbb{E} [Y(C)]$.

Proof. We assume that there is only one hidden variable Y , although generalizing to the case where $D > 1$ is straightforward because our proposed independence property only acts on the hidden variable associated with a clique of observed variables.

We first prove the case where $|C|$ is even. We aim to show that for any $a, b \in \{-1, +1\}^2$,

$$P\left(\prod_{k \in C} v_k = a, Y = b\right) = P\left(\prod_{k \in C} v_k = a\right)P(Y = b).$$

Using the concept of isolated variables and non-isolated variables earlier, the set of all observed variables V_I besides those in C and their neighbors can be ignored. Furthermore, suppose that $\mathcal{S}^{(C,a)}$ is the set of all $k \in C$ such that $\prod_{k \in C} v_k = a$. For example, if $C = \{i, j\}$ and $a = -1$, $\mathcal{S}^{(C,-1)} = \{(v_i, v_j) = (1, -1), (-1, 1)\}$. We write out each of the above probabilities as well as the partition function Z :

$$\begin{aligned} P\left(\prod_{i \in C} v_i = a, Y = b\right) &= \frac{1}{Z} \sum_{s^{(a,b)} \in \mathcal{S}(C,Y)} \psi(s^{(a,b)}) \sum_{s^{(C_1,a)} \in \mathcal{S}(C)} \exp\left(\theta_Y b + \sum_{i \in C} \theta_i b s_{v_i}^{(C_1)} + \sum_{i \notin C} \theta_i b v_i^{(a,b)}\right) \\ &\quad + \sum_{(i,j) \in C} \theta_{i,j} s_{v_i}^{(C_1)} s_{v_j}^{(C_1)} + \sum_{i \in C} \sum_{j \in N(v_i) \setminus v_C} \theta_{i,j} s_{v_i}^{(C_1)} v_j^{(a,b)} \end{aligned}$$

$$\begin{aligned} P\left(\prod_{i \in C} v_i = a\right) &= \frac{1}{Z} \sum_{s^{(a)} \in \mathcal{S}(C)} \psi(s^{(a)}) \sum_{s^{(C_2,a)} \in \mathcal{S}(C)} \exp\left(\theta_Y Y^{(a)} + \sum_{i \in C} \theta_i s_{v_i}^{(C_1)} Y^{(a)} + \sum_{i \notin C} \theta_i v_i^{(a)} Y^{(a)}\right) \\ &\quad + \sum_{(i,j) \in C} \theta_{i,j} s_{v_i}^{(C_2)} s_{v_j}^{(C_2)} + \sum_{i \in C} \sum_{j \in N(v_i) \setminus v_C} \theta_{i,j} s_{v_i}^{(C_1)} v_j^{(a)} \end{aligned}$$

$$\begin{aligned}
 P(Y = b) &= \sum_{s^{(b)} \in \mathcal{S}(Y)} \psi(s^{(b)}) \exp\left(\theta_Y b + \sum_{i \in C} \theta_i b v_i^{(b)} + \sum_{i \notin C} \theta_i v_i^{(b)} Y^{(b)}\right) \\
 &\quad + \sum_{(i,j) \in C} \theta_{i,j} v_i^{(b)} v_j^{(b)} + \sum_{i \in C} \sum_{j \in N(v_i) \setminus v_C} \theta_{i,j} v_i^{(b)} v_j^{(b)} \\
 Z &= \sum_{s^{(z)} \in \mathcal{S}} \psi(s^{(z)}) \exp\left(\theta_Y Y^{(z)} + \sum_{i \in C} \theta_i v_i^{(z)} Y^{(z)} + \sum_{i \notin C} \theta_i v_i^{(z)} Y^{(z)} + \sum_{(i,j) \in C} \theta_{i,j} v_i^{(z)} v_j^{(z)}\right) \\
 &\quad + \sum_{i \in C} \sum_{j \in N(v_i) \setminus v_C} \theta_{i,j} v_i^{(z)} v_j^{(z)}
 \end{aligned}$$

We want to show that we can map from each $s^{(a,b)}$, $s^{(z)}$ and $s^{(C_1)}$ to a respective $s^{(a)}$, $s^{(b)}$, and $s^{(C_2)}$. The $\psi(\cdot)$ terms can be ignored since we can just directly set $s^{(a)}[V_I] = s^{(a,b)}[V_I]$ and $s^{(b)}[V_I] = s^{(z)}[V_I]$. Using the above expressions for probabilities and the cumulant function, our desired statement to prove for each $s^{(a,b)}$, $s^{(z)}$ and $s^{(C_1)}$ is

$$\begin{aligned}
 &\exp\left(\theta_Y(b + Y^{(z)}) + \sum_{i \in C} \theta_i (b s_{v_i}^{(C_1)} + v_i^{(z)} Y^{(z)}) + \sum_{i \notin C} \theta_i (b v_i^{(a,b)} + v_i^{(z)} Y^{(z)})\right) \\
 &\quad + \sum_{(i,j) \in C} \theta_{i,j} (s_{v_i}^{(C_1)} s_{v_j}^{(C_1)} + v_i^{(z)} v_j^{(z)}) + \sum_{i \in C} \sum_{j \in N(v_i) \setminus v_C} \theta_{i,j} (s_{v_i}^{(C_1)} v_k^{(a,b)} + v_i^{(z)} v_k^{(z)}) \\
 &= \exp\left(\theta_Y(b + Y^{(a)}) + \sum_{i \in C} \theta_i (s_{v_i}^{(C_2)} Y^{(a)} + b v_i^{(b)}) + \sum_{i \notin C} \theta_i (v_i^{(a)} Y^{(a)} + b v_i^{(b)})\right) \\
 &\quad + \sum_{(i,j) \in C} \theta_{i,j} (s_{v_i}^{(C_2)} s_{v_j}^{(C_2)} + v_i^{(b)} v_j^{(b)}) + \sum_{i \in C} \sum_{j \in N(v_i) \setminus v_C} \theta_{i,j} (s_{v_i}^{(C_2)} v_j^{(a)} + v_i^{(b)} v_j^{(b)}) \tag{7}
 \end{aligned}$$

We can ensure that the above expression is satisfied with the following relationship between $s^{(a,b)}$, $s^{(z)}$, $s^{(C_1)}$ and $s^{(a)}$, $s^{(b)}$, $s^{(C_2)}$. If $Y^{(z)} = b$, then we set $Y^{(a)} = b$, $s_{v_i}^{(C_2)} = s_{v_i}^{(C_1)}$ for $i \in C$, and $v_i^{(b)} = v_i^{(z)}$, $v_i^{(a)} = v_i^{(a,b)}$ for all v_i . If $Y^{(z)} = -b$, then we set $Y^{(a)} = -b$, $s_{v_i}^{(C_2)} = -s_{v_i}^{(C_1)}$ for $i \in C$, and $v_i^{(b)} = -v_i^{(z)}$, $v_i^{(a)} = -v_i^{(a,b)}$ for all v_i . However, note that setting either all $s_{v_i}^{(C_2)}$ to be $s_{v_i}^{(C_1)}$ or $-s_{v_i}^{(C_1)}$ means that both $s^{(C_1)}$ and $-s^{(C_1)}$ are in $\mathcal{S}^{(C)}$. This is only true when $|C|$ is even because $\prod_{i \in C} (-v_i) = (-1)^{|C|} \prod_{i \in C} v_i = (-1)^{|C|} a$.

Our proof approach is similar when $|C|$ is odd. We aim to show that for any $a, b \in \{-1, +1\}^2$,

$$P\left(\prod_{k \in C} v_k Y = a, Y = b\right) = P\left(\prod_{k \in C} v_k Y = a\right) P(Y = b).$$

$P(\prod_{k \in C} v_k Y = a, Y = b)$ can be written as $P(\prod_{k \in C} v_k = \frac{a}{b}, Y = b)$, which follows the same format of the probability we used for the case where $|C|$ is even. We will end up with a desired equation to prove that is identical to (7), except that we must modify $s^{(C_1)}$ and $s^{(C_2)}$. $s^{(C_1)}$ is now from the set $\mathcal{S}^{(C, a/b)}$, and $s^{(C_2)}$ is from the set $\mathcal{S}^{(C, a/b)}$ when $Y^{(a)} = b$ and from the set $\mathcal{S}^{(C, -a/b)}$ when $Y^{(a)} = -b$. We can set $s^{(a)}$, $s^{(b)}$, and $s^{(C_2)}$ the exact same way as before; in particular, $s_{v_i}^{(C_2)} = s_{v_i}^{(C_1)}$ when $Y^{(a)} = b$ and $s_{v_i}^{(C_2)} = -s_{v_i}^{(C_1)}$ when $Y^{(a)} = -b$. Both $s_{v_i}^{(C_1)}$, $Y^{(a)} = b$ and $-s_{v_i}^{(C_1)}$, $Y^{(a)} = -b$ satisfy $\prod_{i \in C} v_i Y = a$, since $\prod_{i \in C} (-v_i)(-Y) = (-1)^{|C|+1} \prod_{i \in C} v_i Y = a$ when $|C|$ is odd. \square

C.1.3. AUGMENTING THE DEPENDENCY GRAPH

We define the graphical model particular to how G_{dep} is augmented, which gives way to a concise mapping between each a_C and $a_{C_{dep}}$.

In the case where no sources can abstain at all, λ_i takes on values $\{\pm 1\}$ and thus the augmentation is not necessary. We have that $G = G_{dep}$, $\mathbf{v} = \boldsymbol{\lambda}$, and the graphical model's joint distribution (3) reduces to

$$f_G(Y, \boldsymbol{\lambda}) = \frac{1}{Z} \exp\left(\sum_{k=1}^D \theta_{Y_k} Y_k + \sum_{(Y_k, Y_l) \in E} \theta_{Y_k, Y_l} Y_k Y_l + \sum_{i=1}^m \theta_i \lambda_i Y(i) + \sum_{(\lambda_i, \lambda_j) \in E} \theta_{i,j} \lambda_i \lambda_j\right). \tag{8}$$

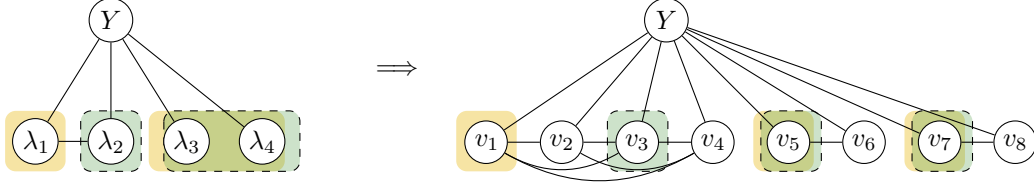


Figure 4. Example of mapping from G_{dep} to G . Left: G_{dep} , where boxes indicate valid triplet groupings of sources. Right: G , where boxes indicate the triplets of observed variables that are sufficient to recover all mean parameters.

All of Algorithm 2 will be done on $\{\mathbf{Y}, \boldsymbol{\lambda}\}$. While the triplet method is still used for recovering mean parameters, the mapping from a_C to $a_{C_{dep}}$ is trivial, and the linear transformation back to $\mu_{C_{dep}}$ will have terms containing $\lambda_i = 0$ reduced to 0.

In the case where sources abstain, we have discussed how to generate \mathbf{v} from $\boldsymbol{\lambda}$ and G from G_{dep} , of which an example is shown in Figure 4. Most importantly, we suppose that when $\lambda_i = 0$, we set (v_{2i-1}, v_{2i}) to either $(1, 1)$ or $(-1, -1)$ with equal probability such that

$$P((v_{2i-1}, v_{2i}) = (1, 1), V \setminus \{v_{2i-1}, v_{2i}\}) = P((v_{2i-1}, v_{2i}) = (-1, -1), V \setminus \{v_{2i-1}, v_{2i}\}) = \frac{1}{2} P(\lambda_i = 0, V \setminus \{v_{2i-1}, v_{2i}\}). \quad (9)$$

The joint distribution over $\{\mathbf{Y}, \mathbf{v}\}$ follows from (3):

$$f_G(\mathbf{Y}, \mathbf{v}) = \frac{1}{Z} \exp \left(\sum_{k=1}^D \theta_{Y_k} Y_k + \sum_{(Y_k, Y_l) \in E} \theta_{Y_k, Y_l} Y_k Y_l + \sum_{i=1}^m \theta_i \begin{bmatrix} 1 & -1 \\ & \end{bmatrix} \begin{bmatrix} v_{2i-1} \\ v_{2i} \end{bmatrix} Y^{dep}(i) \right. \\ \left. + \sum_{i=1}^m \theta_{i,i} v_{2i-1} v_{2i} + \sum_{i,j: (\lambda_i, \lambda_j) \in E_{dep}} \theta_{i,j} \begin{bmatrix} v_{2i-1} & v_{2i} \\ & \end{bmatrix} \begin{bmatrix} 1 & -1 \\ -1 & 1 \end{bmatrix} \begin{bmatrix} v_{2j-1} \\ v_{2j} \end{bmatrix} \right), \quad (10)$$

where E_{dep} is G_{dep} 's edge set. Note that this graphical model has the same absolute values of the canonical parameters for both $v_{2i-1} Y^{dep}(i)$ and for all four terms $(v_{2i-1}, v_{2i}) \times (v_{2j-1}, v_{2j})$ due to the balancing in (9). As a result, the mean parameters also exhibit the same symmetry, which we show in the following lemma.

Lemma 1. For each λ_i , we have that $\mathbb{E}[\lambda_i Y^{dep}(i)] = \mathbb{E}[v_{2i-1} Y^{dep}(i)] = -\mathbb{E}[v_{2i} Y^{dep}(i)]$.

Proof. First, we can write out $\mathbb{E}[\lambda_i Y^{dep}(i)]$ as

$$\begin{aligned} \mathbb{E}[\lambda_i Y^{dep}(i)] &= P(\lambda_i Y^{dep}(i) = 1) - P(\lambda_i Y^{dep}(i) = -1) = P(\lambda_i Y^{dep}(i) = 1) \\ &\quad - (1 - P(\lambda_i Y^{dep}(i) = 1) - P(\lambda_i Y^{dep}(i) = 0)) \\ &= 2P(\lambda_i Y^{dep}(i) = 1) + P(\lambda_i = 0) - 1. \end{aligned}$$

We know that if we have $v_{2i-1} = 1$ or $v_{2i} = -1$, then λ_i is either 1 or 0, but never -1 ; similarly, $v_{2i-1} = -1$ and $v_{2i} = 1$ imply that $\lambda_i \neq 1$. We write out $\mathbb{E}[v_{2i-1} Y^{dep}(i)]$:

$$\begin{aligned} \mathbb{E}[v_{2i-1} Y^{dep}(i)] &= 2(P(v_{2i-1} = 1, Y^{dep}(i) = 1) + P(v_{2i-1} = -1, Y^{dep}(i) = -1)) - 1 \\ &= 2(P((v_{2i-1}, v_{2i}) = (1, 1), Y^{dep}(i) = 1) + P(\lambda_i = 1, Y^{dep}(i) = 1) \\ &\quad + P(\lambda_i = -1, Y^{dep}(i) = -1) + P((v_{2i-1}, v_{2i}) = (-1, -1), Y^{dep}(i) = -1)) - 1 \\ &= 2\left(P(\lambda_i Y^{dep}(i) = 1) + \frac{1}{2}P(\lambda_i = 0, Y^{dep}(i) = 1) + \frac{1}{2}P(\lambda_i = 0, Y^{dep}(i) = -1)\right) - 1 \\ &= 2P(\lambda_i Y^{dep}(i) = 1) + P(\lambda_i = 0) - 1 = \mathbb{E}[\lambda_i Y^{dep}(i)]. \end{aligned}$$

Similarly, $\mathbb{E} [v_{2i}Y^{dep}(i)]$ is

$$\begin{aligned}
 \mathbb{E} [v_{2i}Y^{dep}(i)] &= 2(P((v_{2i-1}, v_{2i}) = (1, 1), Y^{dep}(i) = 1) + P(\lambda_i = -1, Y^{dep}(i) = 1)) \\
 &\quad + P(\lambda_i = 1, Y^{dep}(i) = -1) + P((v_{2i-1}, v_{2i}) = (-1, -1), Y^{dep}(i) = -1)) - 1 \\
 &= 2\left(P(\lambda_i Y^{dep}(i) = -1) + \frac{1}{2}P(\lambda_i = 0, Y^{dep}(i) = 1) + \frac{1}{2}P(\lambda_i = 0, Y^{dep}(i) = -1)\right) - 1 \\
 &= 2P(\lambda_i Y^{dep}(i) = -1) + P(\lambda_i = 0) - 1 \\
 &= P(\lambda_i Y^{dep}(i) = -1) - (1 - P(\lambda_i = 0) - P(\lambda_i Y^{dep}(i) = -1)) \\
 &= P(\lambda_i Y^{dep}(i) = -1) - P(\lambda_i Y^{dep}(i) = 1) = -\mathbb{E} [\lambda_i Y^{dep}(i)].
 \end{aligned}$$

□

The triplets in Algorithm 1 thus only need to be computed over exactly half of \mathbf{v} , each corresponding to one source, as shown in Figure 4. Moreover, this augmentation method for \mathbf{v} and G allows us to conclude for any clique of sources $C_{dep} \in \mathcal{C}_{dep}$,

$$\mathbb{E} \left[\prod_{k \in C_{dep}} v_{2k-1} Y^{dep}(C_{dep}) \right] = \mathbb{E} \left[\prod_{k \in C_{dep}} \lambda_k Y^{dep}(C_{dep}) \right].$$

In general, the expectation over a clique in G_{dep} containing $\{\lambda_i\}_{i \in C_{dep}}$ is equal to the expectation over the corresponding clique C in G containing $\{v_{2i-1}\}_{i \in C_{dep}}$ such that $a_C = a_{C_{dep}}$.

C.1.4. LINEAR TRANSFORMATION TO LABEL MODEL PARAMETERS

To convert these $a_{C_{dep}}$ into $\mu_{C_{dep}}$, we present a way to linearly map from these product probabilities and expectations back to marginal distributions, focusing on the unobservable distributions over a clique of sources and a task that the sources vote on. We first restate our example stated in Section 3.2. Define $\mu_i(a, b) = P(Y^{dep}(i) = a, \lambda_i = b)$ for $a \in \{-1, 1\}$ and $b \in \{-1, 0, 1\}$. We can set up a series of linear equations and denote it as $A_1 \mu_i = r_i$:

$$\begin{bmatrix} 1 & 1 & 1 & 1 & 1 & 1 \\ 1 & 0 & 1 & 0 & 1 & 0 \\ 1 & 1 & 0 & 0 & 0 & 0 \\ 1 & 0 & 0 & 0 & 0 & 1 \\ 0 & 0 & 1 & 1 & 0 & 0 \\ 0 & 0 & 1 & 0 & 0 & 0 \end{bmatrix} \begin{bmatrix} \mu_i(1, 1) \\ \mu_i(-1, 1) \\ \mu_i(1, 0) \\ \mu_i(-1, 0) \\ \mu_i(1, -1) \\ \mu_i(-1, -1) \end{bmatrix} = \begin{bmatrix} 1 \\ P(Y^{dep}(i) = 1) \\ P(\lambda_i = 1) \\ P(\lambda_i Y^{dep}(i) = 1) \\ P(\lambda_i = 0) \\ P(\lambda_i = 0, Y^{dep}(i) = 1) \end{bmatrix}. \quad (11)$$

Note that four entries on the right of the equation are observable or known. $P(\lambda_i Y^{dep}(i) = 1)$ can be written in terms of a_i , and by construction of (v_{2i-1}, v_{2i}) and (9), we can factorize $P(\lambda_i = 0, Y^{dep}(i) = 1)$ into observable terms:

$$\begin{aligned}
 P(\lambda_i = 0, Y^{dep}(i) = 1) &= P((v_{2i-1}, v_{2i}) = (1, 1), Y^{dep}(i) = 1) + P((v_{2i-1}, v_{2i}) = (-1, -1), Y^{dep}(i) = 1) \\
 &= (P((v_{2i-1}, v_{2i}) = (1, 1)) + P((v_{2i-1}, v_{2i}) = (-1, -1)))P(Y^{dep}(i) = 1) \\
 &= P(\lambda_i = 0)P(Y^{dep}(i) = 1).
 \end{aligned}$$

Here we use the fact that $v_{2i-1}v_{2i}$ and $Y^{dep}(i)$ are independent by Proposition 2. We can verify that A_1 is invertible, so $\mu_i(a, b)$ can be obtained from this system.

There is a way to extend this system to the general case. We form a system of linear equations $A_s \mu_C = r_C$ for each clique of sources C in G_{dep} , where $s = |C|$ is the number of weak sources λ_i in the clique and μ_C is the marginal distribution over these s sources and 1 task. A_s is a $2(3^s) \times 2(3^s)$ matrix of 0s and 1s that will help map from r_C , a vector of probabilities known from prior steps of the algorithms or from direct estimation, to the desired label model parameter μ_C . Define

$$A_0 = \begin{bmatrix} 1 & 1 \\ 1 & 0 \end{bmatrix} \quad B_0 = \begin{bmatrix} 0 & 0 \\ 0 & 1 \end{bmatrix}$$

$$D = \begin{bmatrix} 1 & 1 & 1 \\ 1 & 0 & 0 \\ 0 & 1 & 0 \end{bmatrix} \quad E = \begin{bmatrix} 0 & 0 & 0 \\ 0 & 0 & 1 \\ 0 & 0 & 0 \end{bmatrix}$$

Then A_s and B_s can be recursively constructed with

$$\begin{aligned} A_s &= D \otimes A_{s-1} + E \otimes B_{s-1} \\ B_s &= E \otimes A_{s-1} + D \otimes B_{s-1}, \end{aligned}$$

where \otimes is the Kronecker product. To define r_C , we first specify an ordering of elements of μ_C . Let the last λ_{C_s} in the joint probability μ_C take on value $\lambda_{C_s} = 1$ for the first $2 \times 3^{s-1}$ entries, $\lambda_{C_s} = 0$ for the next $2 \times 3^{s-1}$ entries, and $\lambda_{C_s} = -1$ for the last $2 \times 3^{s-1}$ entries. In general, the i th λ_{C_i} in μ_C will alternate among 1, 0, -1 every $2 \times 3^{i-1}$ entries. Finally, the $Y(i)$ entry of μ_C alternates every other value between 1 and -1 .

The ordering of r_C follows a similar structure. If we rename the Y and λ variables to z_1, \dots, z_{s+1} for generality, each entry $r_C(U, Z)$ is equal to $P(\prod_{z_i \in Z} z_i = 1, z_j = 0 \forall z_j \in U)$, where $U \cap Z = \emptyset$, and $U \subseteq C \setminus Y(i)$, $Z \subseteq C$. We also write $r_C(\emptyset, \emptyset) = 1$. The entries of r_C will alternate similarly to μ_C , for each λ_{C_i} , the first $2 \times 3^{i-1}$ terms will not contain λ_{C_i} in either U or Z , the second $2 \times 3^{i-1}$ terms will have $\lambda_{C_i} \in Z$, and the last $2 \times 3^{i-1}$ terms will have $\lambda_{C_i} \in U$. For $Y(i)$, elements of r_C will alternate every other value between not having $Y(i)$ in Z and having $Y(i)$ in Z . (11) illustrates an example of the orderings for μ_C and r_C .

Furthermore, we also have the system $B_s \mu_C = r_C^B$, where $r_C^B(U, Z) = P(\prod_{z_i \in Z} z_i = -1, z_j = 0 \forall z_j \in U)$ when $Z \neq \emptyset$, and $r_C^B(U, \emptyset) = 0$. The ordering of r_C^B is the same as that of r_C .

Lemma 2. *With the setup above, $A_s \mu_C = r_C$.*

Proof. We prove that $A_s \mu_C = r_C$ and $B_s \mu_C = r_C^B$ by induction on s . For the base case $s = 0$, we examine a clique over just a single Y :

$$\begin{bmatrix} 1 & 1 \\ 1 & 0 \end{bmatrix} \begin{bmatrix} P(Y = 1) \\ P(Y = -1) \end{bmatrix} = \begin{bmatrix} 1 \\ P(Y = 1) \end{bmatrix} \quad \begin{bmatrix} 0 & 0 \\ 0 & 1 \end{bmatrix} \begin{bmatrix} P(Y = 1) \\ P(Y = -1) \end{bmatrix} = \begin{bmatrix} 0 \\ P(Y = -1) \end{bmatrix},$$

which are both clearly true. Next, we assume that $A_k \mu_C = r_C$ and $B_k \mu_C = r_C^B$ for $s = k$. We want to show that $A_{k+1} \mu_{C'} = r_{C'}$ and $B_{k+1} \mu_{C'} = r_{C'}^B$, for a larger clique C' where $C \subset C'$ and $|C'| = s + 1$. By construction of A_{k+1} and B_{k+1} ,

$$A_{k+1} = \begin{bmatrix} A_k & A_k & A_k \\ A_k & 0 & B_k \\ 0 & A_k & 0 \end{bmatrix} \quad B_{k+1} = \begin{bmatrix} B_k & B_k & B_k \\ B_k & 0 & A_k \\ 0 & B_k & 0 \end{bmatrix}.$$

$\mu_{C'}$, $r_{C'}$, and $r_{C'}^B$ can be written as

$$\mu_{C'} = \begin{bmatrix} \mu_C(\lambda_{C'_{k+1}} = 1) \\ \mu_C(\lambda_{C'_{k+1}} = 0) \\ \mu_C(\lambda_{C'_{k+1}} = -1) \end{bmatrix} \quad r_{C'} = \begin{bmatrix} r_C \\ r_C(\lambda_{C'_{k+1}} \in Z') \\ r_C(\lambda_{C'_{k+1}} \in U') \end{bmatrix} \quad r_{C'}^B = \begin{bmatrix} r_C^B \\ r_C^B(\lambda_{C'_{k+1}} \in Z') \\ r_C^B(\lambda_{C'_{k+1}} \in U') \end{bmatrix},$$

where $\mu_C(\lambda_{C'_{k+1}} = 1) = P(Y, \lambda_{C_1}, \dots, \lambda_{C_k}, \lambda_{C'_{k+1}} = 1)$, $r_C(\lambda_{C'_{k+1}} \in Z') = r_C(U, Z \cup \{\lambda_{C'_{k+1}}\})$, and so on. U' , Z' for C' are constructed similarly to U, Z for C .

Then the three equations for A_k we want to show are

$$\begin{aligned} A_k(\mu_C(\lambda_{C'_{k+1}} = 1) + \mu_C(\lambda_{C'_{k+1}} = 0) + \mu_C(\lambda_{C'_{k+1}} = -1)) &= r_C \\ A_k(\mu_C(\lambda_{C'_{k+1}} = 1)) + B_k(\mu_C(\lambda_{C'_{k+1}} = -1)) &= r_C(\lambda_{C'_{k+1}} \in Z') \\ A_k(\mu_C(\lambda_{C'_{k+1}} = 0)) &= r_C(\lambda_{C'_{k+1}} \in U'). \end{aligned}$$

The first equation is true because $\lambda_{C'_{k+1}}$ is marginalized out to yield $A_k \mu_C = r_C$, which is true by our inductive hypothesis. In the third equation, the term $\lambda_{C'_{k+1}} = 0$ is added as a joint probability to all probabilities in μ_C and r_C , so this also holds by the inductive hypothesis. In the second equation, $A_k(\mu_C(\lambda_{C'_{k+1}} = 1))$ is equal to r_C with each probability having $\lambda_{C'_{k+1}} = 1$ as an additional joint probability, and similarly $B_k(\mu_C(\lambda_{C'_{k+1}} = -1))$ is equal to r_C^B with each nonzero probability having $\lambda_{C'_{k+1}} = -1$ as an additional joint probability. For entries where $Z \neq \emptyset$, summing these up yields

$$\begin{aligned} & P\left(\prod_{z_i \in Z} z_i = 1, \lambda_{C'_{k+1}} = 1, z_j = 0 \forall z_j \in U\right) + P\left(\prod_{z_i \in Z} z_i = -1, \lambda_{C'_{k+1}} = -1, z_j = 0 \forall z_j \in U\right) \\ &= P\left(\prod_{z_i \in Z} z_i \lambda_{C'_{k+1}} = 1, z_j = 0 \forall z_j \in U\right). \end{aligned}$$

And when $Z = \emptyset$, we have $P(\lambda_{C'_{k+1}} = 1, z_j = 0 \forall z_j \in U)$, so all together these probabilities make up $r_C(\lambda_{C'_{k+1}} \in Z')$.

The three equations for B_k are similar:

$$\begin{aligned} B_k(\mu_C(\lambda_{C'_{k+1}} = 1) + \mu_C(\lambda_{C'_{k+1}} = 0) + \mu_C(\lambda_{C'_{k+1}} = -1)) &= r_C^B \\ B_k(\mu_C(\lambda_{C'_{k+1}} = 1)) + A_k(\mu_C(\lambda_{C'_{k+1}} = -1)) &= r_C^B(\lambda_{C'_{k+1}} \in Z') \\ B_k(\mu_C(\lambda_{C'_{k+1}} = 0)) &= r_C^B(\lambda_{C'_{k+1}} \in U'). \end{aligned}$$

Again, the first and third equations are clearly true using the inductive hypothesis, and the second equation is also true when we decompose $\prod_{z_i \in Z'} z_i = -1$ into $\prod_{z_i \in Z} z_i = 1, \lambda_{C'_{k+1}} = -1$ and $\prod_{z_i \in Z} z_i = -1, \lambda_{C'_{k+1}} = 1$.

We complete this proof by induction to conclude that $A_s \mu_C = r_C$ and $B_s \mu_C = r_C^B$, showing a recursive approach for mapping from r_C to μ_C for any clique or separator set C . \square

Finally, we note that each r_C is made up of computable terms. Entries of the form $r_C(\emptyset, Z) = P(\prod_{z_i \in Z} z_i = 1)$ are immediately calculated from a_c for cliques $c \subseteq C$, and entries where $Y(i) \notin Z$ can be directly estimated. Entries where $Z = \{Y(i)\}, U \neq \emptyset$ can be factorized into known or directly estimated probabilities, and all other entries can be computed by calculating each a_c conditional on U .

As an example, to construct r_{ij} for a clique $\{\lambda_i, \lambda_j, Y^{dep}(i, j)\}$, the only entries of r_{ij} that are unobservable from the data are $P(\lambda_i Y^{dep}(i, j) = 1), P(\lambda_j Y^{dep}(i, j) = 1), P(\lambda_i \lambda_j Y^{dep}(i, j) = 1), P(\lambda_i = 0, Y^{dep}(i, j) = 1), P(\lambda_j = 0, Y^{dep}(i, j) = 1), P(\lambda_i = 0, \lambda_j Y^{dep}(i, j) = 1), P(\lambda_j = 0, \lambda_i Y^{dep}(i, j) = 1),$ and $P(\lambda_i = 0, \lambda_j = 0, Y^{dep}(i, j) = 1)$. We have discussed how to estimate all but the last three.

To estimate $P(\lambda_i = 0, \lambda_j Y^{dep}(i, j) = 1)$, we can write this as

$$\begin{aligned} P(\lambda_j Y^{dep}(i, j) = 1, \lambda_i = 0) &= P(\lambda_j Y^{dep}(i, j) = 1 | \lambda_i = 0) P(\lambda_i = 0) \\ &= \frac{1 + \mathbb{E}[\lambda_j Y^{dep}(i, j) | \lambda_i = 0] - P(\lambda_j = 0 | \lambda_i = 0)}{2} \cdot P(\lambda_i = 0) \\ &= \frac{1}{2} P(\lambda_i = 0) + \frac{1}{2} \mathbb{E}[\lambda_j Y^{dep}(i, j) | \lambda_i = 0] P(\lambda_i = 0) + \frac{1}{2} P(\lambda_j = 0, \lambda_i = 0). \end{aligned}$$

We can solve $\mathbb{E}[\lambda_j Y^{dep}(i, j) | \lambda_i = 0]$ using the triplet method conditional on samples where λ_i abstains. $P(\lambda_i = 0, \lambda_j = 0, Y^{dep}(i, j) = 1)$ can be written as $P(\lambda_i = 0, \lambda_j = 0) P(Y^{dep}(i, j) = 1)$, of which all probabilities are observable, by Proposition 2.

C.1.5. RESOLVESIGNS

This function is used to determine the signs after we have recovered the magnitudes of accuracy terms such as $|\mathbb{E}[v_i Y(i)]|$. One way to implement this function is to use one known accuracy sign per Y . We observe that if we know the sign of $a_i = \mathbb{E}[v_i Y(i)]$, then we are able to obtain the sign of any other term $a_j = \mathbb{E}[v_j Y(j)]$ where $Y(j) = Y(i)$. If v_i and v_j are conditionally independent given $Y(i)$, we directly use $a_i a_j = \mathbb{E}[v_i v_j]$ and knowledge of a_i 's sign to get the sign of a_j . If v_i and v_j are not conditionally independent given $Y(i)$, we need two steps to recover the sign: for some v_k that is

conditionally independent of both v_i and v_j given $Y(i)$, we first use $a_i \mathbb{E}[v_k Y(i)] = \mathbb{E}[v_i v_k]$ to get the sign of $\mathbb{E}[v_k Y(i)]$. Then we use $a_j \mathbb{E}[v_k Y(i)] = \mathbb{E}[v_j v_k]$ to get the sign of a_j . Therefore, knowing the sign of one accuracy per Y is sufficient to recover all signs.

The RESOLVESIGNS used in Algorithm 1 uses another approach and follows from the assumption that on average per Y , the accuracies a_i are better than zero. We apply this procedure to the sets of accuracies corresponding to each hidden variable; for each set, we have two sign choices, and we check which of these two produces a non-negative sum for the accuracies. In the common case where there is just one task, there are only two choices to check overall.

C.2. Extensions to More Complex Graphical Models

Recall that our Ising model is constructed for binary task labels, with sufficient conditional independence on G and G_{dep} such that $\Omega_G = V$, and without singleton potentials. We address how to extend our method when each of these conditions do not hold.

Multiclass Case We have given an algorithm for binary classes for Y (and ternary for the sources, since these can also abstain). To extend this to higher-class cases, we can apply a one-versus-all reduction repeatedly to apply our core algorithm.

Extension to More Complex Graphs In Algorithm 1, we rely on the fact $\Omega_G = V$ to compute all accuracies. However, certain a_i 's cannot be recovered when there are fewer than 3 conditionally independent subgraphs in G , where a subgraph V_a is defined as a set of vertices such that if $v_i \in V_a$ and $v_j \notin V_a$, $v_i \perp v_j | Y(i)$. Instead, when there are only 1 or 2 subgraphs, we use another independence property, which states that $v_i Y(i) \perp Y(i)$ for all v_i . This means that $\mathbb{E}[v_i Y(i)] \cdot \mathbb{E}[Y(i)] = \mathbb{E}[v_i Y(i)^2] = \mathbb{E}[v_i]$, and thus $a_i = \frac{\mathbb{E}[v_i]}{\mathbb{E}[Y(i)]}$. This independence property does not require us to choose triplets of sources; instead we can directly divide to compute a_i . However, this approach fails in the presence of singleton potentials and can be very inaccurate when $\mathbb{E}[Y(i)]$ is close to 0. One can use this independence property in addition to Proposition 1 on G with 2 conditionally independent subgraphs, and when G only consists of 1 subgraph, we require that there are no singleton potentials on any of the sources.

Dealing with Singleton Potentials Our current Ising model does not include singleton potentials except on Y_i terms. However, we can handle cases where sources are modeled to have singleton potentials. Proposition 1 holds as long as either v_i or v_j belongs to a subgraph that has no potentials on individual observed variables. Therefore, the triplet method is able to recover mean parameters as long as we have at least two conditionally independent subgraph with no singleton potentials on observed variables. For example, just two sources conditionally independent of all the others with no singleton potential suffices to guarantee that this modified graphical model still allows for our algorithm to recover label model parameters.

In the case where we have singleton potentials on possibly every source, we have the following alternative approach. We use a slightly different parametrization and a quadratic version of the triplet method. Instead of tracking mean parameters (and thus accuracies like $\mathbb{E}[v_i Y(i)]$), we shall instead directly compute parameters that involve *class-conditional* probabilities. These are, in particular, for v_i ,

$$\mu_i = \begin{bmatrix} P(v_i = 1 | Y(i) = 1) & P(v_i = 1 | Y(i) = -1) \\ P(v_i = -1 | Y(i) = 1) & P(v_i = -1 | Y(i) = -1) \end{bmatrix}.$$

Note that these parameters are minimal (the terms $P(v_i = 0 | Y(i) = \pm 1)$, indicating the conditional abstain rate, are determined by the columns above.

We set

$$O_{ij} = \begin{bmatrix} P(\lambda_i = 1 | \lambda_j = 1) & P(\lambda_i = 1 | \lambda_j = -1) \\ P(\lambda_i = -1 | \lambda_j = 1) & P(\lambda_i = -1 | \lambda_j = -1) \end{bmatrix} \text{ and } P = \begin{bmatrix} P(Y = 1) & 0 \\ 0 & P(Y = -1) \end{bmatrix}.$$

For a pair of conditionally independent sources, we have that

$$\mu_i P \mu_j^T = O_{ij}. \quad (12)$$

Because we can observe terms like O_{ij} , we can again form triplets with i, j, k as before, and solve. Note that this alternative parametrization does not depend on the presence or absence of singleton potentials in the Ising model, only on the conditional independences directly defined by it.

Moreover, there is a closed form solution to the resulting system of non-linear equations. To see this, consider the following. Note that

$$P(v_i = 1|Y(i) = -1) = \frac{P(v_i = 1)}{P(Y(i) = -1)} - \frac{P(v_i = 1|Y(i) = 1)P(Y(i) = 1)}{P(Y(i) = -1)}.$$

Note that everything is observable (or known, for class balances), so that we can write the top row of μ_i as a function of a single variable. That is, we set $\alpha = P(v_i = 1|Y(i) = 1)$, $c_i = \frac{P(v_i=1)}{P(Y(i)=-1)}$ and $d_i = \frac{P(Y(i)=1)}{P(Y(i)=-1)}$. Then, the top row of μ_i becomes $[\alpha \quad c_i - d_i\alpha]$, and c_i and d_i are known.

Next, consider some triplets i, j, k , with corresponding μ 's. Similarly, we set the top-left corner in the corresponding μ 's to be α, β, γ , and the corresponding terms for the top-right corner are c_i, c_j, c_k and d_i, d_j, d_k . Then, by considering the upper-left position in (12), we get the system

$$\begin{aligned} (1 + d_i d_j)\alpha\beta + c_i c_j - c_i d_j \beta - c_j d_i \alpha &= O_{ij}/P(Y = 1), \\ (1 + d_i d_k)\alpha\gamma + c_i c_k - c_i d_k \gamma - c_k d_i \alpha &= O_{ik}/P(Y = 1), \\ (1 + d_j d_k)\beta\gamma + c_j c_k - c_j d_k \gamma - c_k d_j \beta &= O_{jk}/P(Y = 1). \end{aligned}$$

To solve this system, we express α and γ in terms of β , using the first and third equations, and then we can plug these into the second and multiply (for example, when using α , by $((1 + d_i d_j)\beta - c_j d_i)^2$) to obtain a quadratic in terms of β . Solving this quadratic and selecting the correct root, then obtaining the remaining parameters (α, γ) and filling in the rest of the μ_i, μ_j, μ_k terms completes the procedure. Note that we have to carry out the triplet procedure here twice per μ_i , since there are two rows. Lastly, we can convert probabilities over \mathbf{v} into equivalent probabilities over λ as discussed in Appendix C.1.3.

C.3. Online Algorithm

The online learning setting presents new challenges for weak supervision. In the offline setting, the weak supervision pipeline has two distinct components: first, computing all probabilistic labels for a dataset and then using them to train an end model. In the online setting however, samples are introduced one by one, so we see each \mathbf{X}^i only once and are not able to store it.

Fortunately, Algorithm 1 and Algorithm 2 both rely on computing estimates of expected moments over the observable weak sources. Since these are just averages, we can efficiently produce an estimate of the label model parameters at each time step. For each new sample, we update the averages of the moments using a rolling window and use them to output its probabilistic label; then the end model is trained on this sample, and the data point itself is no longer needed for further computation. Our method is fast enough that we can “interleave” the two components of the weak supervision pipeline, in comparison to Ratner et al. (2019) and Sala et al. (2019), which require a full covariance matrix inversion and SGD.

The online learning environment is also subject to *distributional drift* over time, where old samples may come from very different distributions compared to more recent samples. Formally, define distributional drift as the following property: for $(\mathbf{X}^t, \mathbf{Y}^t) \sim P_t$, the KL-divergence between P_i and P_{i+1} is less than $KL(P_t, P_{t+1}) \leq \Delta$ for any t . If there were no distributional drift, i.e., $\Delta = 0$, we would invoke Algorithm 1 or 2 at each time step t for the new sample's output label, where the estimates of $\hat{\mathbb{E}}[v_i v_j]$ and other observable moments would be cumulatively over t rather than n . However, because of distributional drift, it is important to prioritize most recent samples. We propose a rolling window of size W , which can be optimized theoretically, to average over rather than all past t samples. Algorithm 3 describes the general meta-algorithm for the online setting.

C.3.1. THEORETICAL ANALYSIS

Similar to the offline setting, we analyze our method for online label model parameter recovery and provide bounds on its performance. First, we derive a bound on the sampling error $\|\mu_t - \hat{\mu}_t\|_2$ in terms of the window size W , concluding that there exists an optimal W^* to minimize this error. Then, we present an online generalization result that describes how well our end model can “track” new samples coming from a drifting distribution.

Controlling the Online Sampling Error with W The sampling error at each time step t $\|\mu_t - \hat{\mu}_t\|_2$ is dependent on the window size W which we average samples over to produce estimates. On one hand, a small window will ensure that the

Algorithm 3 Online Weak Supervision

Input: dependency graph G_{dep} , window W for rolling averages
for $t = 1, 2, \dots$ **do**
 Receive source output vector l_t and distribution prior $P_t(\bar{Y})$.
 Run Algorithm 1 and Algorithm 2 with estimates computed over W samples $l_{t-W+1:t}$ and their augmented equivalents to output $\hat{\mu}_t$.
 Use junction tree formula to produce probabilistic output $\tilde{Y}^t \sim P_{\hat{\mu}_t}(\cdot | l_t)$.
 Use \tilde{Y}^t to update w_t , the parametrization of the end model f_w .
end for

estimate will be computed using samples from distributions close to P_t , but using few samples results in a high empirical estimation error. On the other hand, a larger window will allow us to use many samples; however, samples farther in the past will be from distributions that may not be similar to P_t . Hence, W must be selected to minimize both the effect of using drifting distributions and the estimation error in the number of samples used.

Theorem 4. *Let $\hat{\mu}_t$ be an estimate of μ_t , the label model parameters at time t , over W previous samples from the product distribution $\mathbf{Pr}_W = \prod_{i=t-W+1}^t P_i$, which suffers a Δ -distributional drift. Then, still assuming cliques in G_{dep} are limited to 3 vertices,*

$$\mathbb{E}_{\mathbf{Pr}_W} [\|\hat{\mu}_t - \mu_t\|_2] = \frac{1}{a_{\min}^5} \left(3.19C_1 \sqrt{\frac{m}{W}} + \frac{6.35C_2}{\sqrt{r}} \frac{m}{\sqrt{W}} \right) + \frac{2c(|\mathcal{C}_{dep}| + |\mathcal{S}_{dep}|)\Delta W^{3/2}}{\sqrt{6\alpha_{P_t}}}.$$

where α_{P_t} is the minimum non-zero probability that P_t takes. A global minimum for the sampling error as a function of W exists, so the window size can be set such that $W^* = \operatorname{argmin}_W \mathbb{E} [\|\hat{\mu}_t - \mu_t\|_2]$.

Proof. Denote $P_t^W = \underbrace{P_t \times \dots \times P_t}_W$. We first bound the difference between $\mathbb{E}_{\mathbf{Pr}_W} [\|\hat{\mu}_t - \mu_t\|_2]$ and $\mathbb{E}_{P_t^W} [\|\hat{\mu}_t - \mu_t\|_2]$.

$$\begin{aligned} \left| \mathbb{E}_{\mathbf{Pr}_W} [\|\hat{\mu}_t - \mu_t\|_2] - \mathbb{E}_{P_t^W} [\|\hat{\mu}_t - \mu_t\|_2] \right| &= \left| \sum_{\{x_i\}_{i=t-W+1}^t} \|\hat{\mu}_t - \mu_t\|_2 \cdot (\mathbf{Pr}_W(x_{t-W+1}, \dots, x_t) - P_t^W(x_{t-W+1}, \dots, x_t)) \right| \\ &\leq \max \|\hat{\mu}_t - \mu_t\|_2 \cdot \sum_{\{x_i\}_{i=t-W+1}^t} |\mathbf{Pr}_W(x_{t-W+1}, \dots, x_t) - P_t^W(x_{t-W+1}, \dots, x_t)| \\ &= \max \|\hat{\mu}_t - \mu_t\|_2 \cdot 2TV(\mathbf{Pr}_W, P_t^W). \end{aligned}$$

Since the label model parameters are all probabilities, $\|\hat{\mu}_t - \mu_t\|_2$ is bounded by $c \cdot (|\mathcal{C}_{dep}| + |\mathcal{S}_{dep}|)$, where c is a constant. To compute $TV(\mathbf{Pr}_W, P_t^W)$, we use Pinsker's inequality and tensorization of the KL-divergence:

$$\begin{aligned} TV(\mathbf{Pr}_W, P_t^W) &\leq \sqrt{\frac{1}{2} KL(\mathbf{Pr}_W \| P_t^W)} = \sqrt{\frac{1}{2} KL(P_{t-W+1} \times \dots \times P_t \| P_t \times \dots \times P_t)} \\ &= \sqrt{\frac{1}{2} \sum_{i=t-W+1}^t KL(P_i \| P_t)}. \end{aligned}$$

Each $KL(P_i \| P_t)$ can be bounded above by $\frac{2}{\alpha_{P_t}} TV(P_i, P_t)^2$ by the inverse of Pinsker's inequality, where $\alpha_{P_t} = \min_{x \in \mathcal{X}, P_t(x) > 0} P_t(x)$. Since the triangle inequality is satisfied for total variation distance, $TV(P_i, P_t) \leq \Delta(t-i)$. Plugging this back in, we get

$$\begin{aligned} TV(\mathbf{Pr}_W, P_t^W) &\leq \sqrt{\frac{1}{2} \cdot \frac{2}{\alpha_{P_t}} \Delta^2 \sum_{i=t-W+1}^t (t-i)^2} = \sqrt{\frac{\Delta^2}{\alpha_{P_t}} \sum_{i=0}^{W-1} i^2} \\ &= \sqrt{\frac{\Delta^2}{\alpha_{P_t}} \cdot \frac{(W-1)W(2W-1)}{6}} \leq \frac{\Delta W^{3/2}}{\sqrt{6\alpha_{P_t}}}. \end{aligned}$$

Therefore,

$$\left| \mathbb{E}_{\mathbf{Pr}_W} [\|\hat{\boldsymbol{\mu}}_t - \boldsymbol{\mu}_t\|_2] - \mathbb{E}_{P_t^W} [\|\hat{\boldsymbol{\mu}}_t - \boldsymbol{\mu}_t\|_2] \right| \leq \frac{2c(|\mathcal{C}_{dep}| + |\mathcal{S}_{dep}|)\Delta W^{3/2}}{\sqrt{6\alpha_{P_t}}}.$$

Furthermore, the offline sampling error result applies over P_t^W , so $\mathbb{E}_{P_t^W} [\|\hat{\boldsymbol{\mu}}_t - \boldsymbol{\mu}_t\|_2] \leq \frac{1}{a_{\min}^5} \left(3.19C_1\sqrt{\frac{m}{W}} + \frac{6.35C_2}{\sqrt{r}} \frac{m}{\sqrt{W}} \right)$. Hence,

$$\mathbb{E}_{\mathbf{Pr}_W} [\|\hat{\boldsymbol{\mu}}_t - \boldsymbol{\mu}_t\|_2] \leq \frac{1}{a_{\min}^5} \left(3.19C_1\sqrt{\frac{m}{W}} + \frac{6.35C_2}{\sqrt{r}} \frac{m}{\sqrt{W}} \right) + \frac{2c(|\mathcal{C}_{dep}| + |\mathcal{S}_{dep}|)\Delta W^{3/2}}{\sqrt{6\alpha_{P_t}}},$$

and we set a window size W^* to minimize this expression. \square

Online Generalization Bound We provide a bound quantifying the gap in probability of incorrectly classifying an unseen $t + 1$ th sample between our learned end model parametrization and an optimal end model parametrization.

Because the online learning setting is subject to distributional drift over time, our methods must be able to predict the next time step's label with some guarantee despite the changing environment. The Δ drift is aggravated by (1) potential model misspecification for each P_t and (2) sample noise. However, we are able to take into account these additional conditions by modeling the overall drift Δ^μ to be a combination of intrinsic distributional drift Δ , model misspecification, and estimation error of parameters.

Recall that $\mathbf{X}^i \sim P_i$ is drawn from the true distribution at time i , while $\tilde{\mathbf{Y}}^i \sim P_{\hat{\boldsymbol{\mu}}_i}(\cdot|\lambda(\mathbf{X}^i))$ is the probabilistic output of our label model. Define the joint distribution of a sample to be $(\mathbf{X}^i, \tilde{\mathbf{Y}}^i) \sim P_{i, \hat{\boldsymbol{\mu}}_i}$. At each time step t , our goal is train our end model $f_w \in \mathcal{F}$ and evaluate its performance against the true $(\mathbf{X}^t, \mathbf{Y}^t) \sim P_t$, given that we have $t - 1$ previous samples drawn from $P_{i, \hat{\boldsymbol{\mu}}_i}$.

We define a binary loss function $L(w, x, y) = |f_w(x) - y|$ and choose \hat{w}_t to minimize over the past s samples such that

$$\hat{w}_t = \operatorname{argmin}_w \frac{1}{s} \sum_{i=t-s}^{t-1} L(w, \mathbf{X}^i, \tilde{\mathbf{Y}}^i).$$

We present a new generalization result that bounds the probability that $f_{\hat{w}_t}(\mathbf{X}^t)$ does not equal the true \mathbf{Y}^t and also accounts for model misspecification and error from parameter estimation.

Theorem 5. Define $\Delta^\mu := d_{TV}(P_{i, \hat{\boldsymbol{\mu}}_i}, P_{i+1, \hat{\boldsymbol{\mu}}_{i+1}})$ to be the distributional drift between the two samples and $D^\mu := \max_i d_{TV}(P_i, P_{i, \hat{\boldsymbol{\mu}}_i})$ to be an upper bound for the total variational distance between the true distribution and the noise aware misspecified distribution. If $\Delta^\mu \leq \frac{c(\epsilon - 8D^\mu)^3}{\sqrt{\text{CDim}(\mathcal{F})}}$ for some constant $c > 0$, there exists a \hat{w}_t computed over the past $s = \left\lceil \frac{\epsilon - 8D^\mu}{16\Delta^\mu} \right\rceil$ samples such that, for any time $t > s$ and $\epsilon \in (8D^\mu, 1)$,

$$\mathbf{Pr}_{\hat{\boldsymbol{\mu}}, t}(L(\hat{w}_t, \mathbf{X}^t, \mathbf{Y}^t) = 1) \leq \epsilon + \min_{w^*} P_t(L(w^*, \mathbf{X}^t, \mathbf{Y}^t) = 1),$$

where $\mathbf{Pr}_{\hat{\boldsymbol{\mu}}, t} = \prod_{i=t-s}^{t-1} P_{i, \hat{\boldsymbol{\mu}}_i} \cdot P_t$. Furthermore,

$$D^\mu \leq \sqrt{\frac{1}{2} \max_i KL(P_i(\mathbf{Y}|\mathbf{X}) \parallel P_{\boldsymbol{\mu}_i}(\mathbf{Y}|\mathbf{X}))} + m^{\frac{1}{4}} \sqrt{\frac{1}{e_{\min}} \max_i \|\boldsymbol{\mu}_i - \hat{\boldsymbol{\mu}}_i\|_2}.$$

Proof. We adapt Theorem 2 from Long (1999). Choose $\epsilon \leq 1$. Let $s = \left\lceil \frac{\epsilon - 8D^\mu}{16(\Delta + 2D^\mu)} \right\rceil$ and $\Delta^\mu = \Delta + 2D^\mu \leq \frac{(\epsilon - 8D^\mu)^3}{5000000d}$, where d is the end model's VC dimension. Let $L(w, x, y) = |y - f_w(x)| \in \{0, 1\}$, where $f_w(x)$ is the output of the end model parametrized by w when given input x .

At time t , the sequence of inputs to the end model so far is $(\mathbf{X}^1, \tilde{\mathbf{Y}}^1), (\mathbf{X}^2, \tilde{\mathbf{Y}}^2), \dots, (\mathbf{X}^{t-1}, \tilde{\mathbf{Y}}^{t-1})$, where $(\mathbf{X}^i, \tilde{\mathbf{Y}}^i) \sim P_{i, \hat{\boldsymbol{\mu}}_i}$. We evaluate the end model's performance by using a parametrization w_t that is a function of the $t - 1$ inputs so far

and computing $L(w_t, \mathbf{X}^t, \mathbf{Y}^t)$ where $(\mathbf{X}^t, \mathbf{Y}^t) \sim P_t$. In particular, let $w_t^* = \operatorname{argmin}_w \mathbb{E}_{(\mathbf{X}^t, \mathbf{Y}^t) \sim P_t} [L(w, \mathbf{X}^t, \mathbf{Y}^t)]$, and $\hat{w}_t = \operatorname{argmin}_w \frac{1}{s} \sum_{i=t-s}^{t-1} L(w, x_i, \tilde{y}_i)$ where x_i, \tilde{y}_i are the values of the random variables \mathbf{X}^i and $\tilde{\mathbf{Y}}^i$.

Suppose that $TV(P_i, P_{i+1}) \leq \Delta$. Then $TV(P_i, \hat{P}_i, P_{i+1}, \hat{P}_{i+1})$ is

$$TV(P_i, \hat{P}_i, P_{i+1}, \hat{P}_{i+1}) \leq TV(P_i, \hat{P}_i, P_i) + \Delta + TV(P_{i+1}, P_{i+1}, \hat{P}_{i+1}) \leq \Delta + 2D^\mu = \Delta^\mu.$$

Let $\beta \geq 6\Delta^\mu s + 4D^\mu$, and $\alpha = \frac{\beta}{2} - 2D^\mu \geq 3\Delta^\mu s$. Note that $TV(P_i, \hat{P}_i, P_t, \hat{P}_t) \leq \Delta^\mu s = \kappa$ for any $i = t-s, \dots, t-1$. Denote $\mathbf{Pr}_{\hat{\mu}} = \prod_{i=t-s}^{t-1} P_i, \hat{P}_i$. Then by Lemma 12 of Long (1999),

$$\mathbf{Pr}_{\hat{\mu}} \left\{ \exists w : \left| \frac{1}{s} \sum_{i=t-s}^{t-1} L(w, \mathbf{X}^i, \tilde{\mathbf{Y}}^i) - \mathbb{E}_{(\mathbf{X}^t, \tilde{\mathbf{Y}}^t) \sim P_t, \hat{P}_t} [L(w, \mathbf{X}^t, \tilde{\mathbf{Y}}^t)] \right| > \alpha \right\} \leq 8 \cdot 41^d \exp \left(-\frac{(\alpha - \kappa)^2 s}{1600} \right).$$

For any real numbers a, b, c , and $x > y$, if $|a - b| \geq x$ and $|b - c| \leq y$, then $|a - b| - |b - c| \geq x - y$ and thus $|a - c| = |a - b + b - c| \geq ||a - b| - |b - c|| \geq x - y$. Applying this,

$$\begin{aligned} & \mathbf{Pr}_{\hat{\mu}} \left\{ \exists w : \left| \frac{1}{s} \sum_{i=t-s}^{t-1} L(w, \mathbf{X}^i, \tilde{\mathbf{Y}}^i) - \mathbb{E}_{(\mathbf{X}^t, \mathbf{Y}^t) \sim P_t} [L(w, \mathbf{X}^t, \mathbf{Y}^t)] \right| > \alpha + 2D^\mu, \right. \\ & \left. \left| \mathbb{E}_{(\mathbf{X}^t, \mathbf{Y}^t) \sim P_t} [L(w, \mathbf{X}^t, \mathbf{Y}^t)] - \mathbb{E}_{(\mathbf{X}^t, \tilde{\mathbf{Y}}^t) \sim P_t, \hat{P}_t} [L(w, \mathbf{X}^t, \tilde{\mathbf{Y}}^t)] \right| < 2D^\mu \right\} \\ & \leq \mathbf{Pr}_{\hat{\mu}} \left\{ \exists w : \left| \frac{1}{s} \sum_{i=t-s}^{t-1} L(w, \mathbf{X}^i, \tilde{\mathbf{Y}}^i) - \mathbb{E}_{(\mathbf{X}^t, \tilde{\mathbf{Y}}^t) \sim P_t, \hat{P}_t} [L(w, \mathbf{X}^t, \tilde{\mathbf{Y}}^t)] \right| > \alpha \right\} \leq 8 \cdot 41^d \exp \left(-\frac{(\alpha - \kappa)^2 s}{1600} \right). \end{aligned}$$

By Lemma 3, the difference in the expected loss $\mathbb{E}[L(w, \mathbf{X}^t, \mathbf{Y}^t)]$ when $\mathbf{X}^t, \mathbf{Y}^t$ is from P_t versus P_t, \hat{P}_t is always less than $2D^\mu$, so the above becomes

$$\begin{aligned} & \mathbf{Pr}_{\hat{\mu}} \left\{ \exists w : \left| \frac{1}{s} \sum_{i=t-s}^{t-1} L(w, \mathbf{X}^i, \tilde{\mathbf{Y}}^i) - \mathbb{E}_{(\mathbf{X}^t, \mathbf{Y}^t) \sim P_t} [L(w, \mathbf{X}^t, \mathbf{Y}^t)] \right| > \alpha + 2D^\mu \right\} \\ & \leq 8 \cdot 41^d \exp \left(-\frac{(\alpha - \kappa)^2 s}{1600} \right). \end{aligned}$$

We can write this in terms of β . Note that $\Delta^\mu s \leq \frac{\beta}{6} - \frac{2D^\mu}{3}$. The RHS is equivalent to

$$\begin{aligned} & 8 \cdot 41^d \exp \left(-\frac{(\alpha - \kappa)^2 m}{1600} \right) = 8 \cdot 41^d \exp \left(-\frac{s}{1600} \left(\frac{\beta}{2} - 2D^\mu - \Delta^\mu s \right)^2 \right) \\ & \leq 8 \cdot 41^d \exp \left(-\frac{s}{1600} \left(\frac{\beta}{2} - 2D^\mu - \frac{\beta}{6} + \frac{2D^\mu}{3} \right)^2 \right) = 8 \cdot 41^d \exp \left(-\frac{s}{14400} (\beta - 4D^\mu)^2 \right). \end{aligned}$$

So the probability becomes

$$\mathbf{Pr}_{\hat{\mu}} \left\{ \exists w : \left| \frac{1}{s} \sum_{i=t-s}^{t-1} L(w, \mathbf{X}^i, \tilde{\mathbf{Y}}^i) - \mathbb{E}_{(\mathbf{X}^t, \mathbf{Y}^t) \sim P_t} [L(w, \mathbf{X}^t, \mathbf{Y}^t)] \right| > \frac{\beta}{2} \right\} \leq 8 \cdot 41^d \exp \left(-\frac{s}{14400} (\beta - 4D^\mu)^2 \right).$$

Next, note that the probability that at least one of \hat{w}_t or w_t^* satisfies $\left| \frac{1}{s} \sum_{i=t-s}^{t-1} L(w, \mathbf{X}^i, \tilde{\mathbf{Y}}^i) - \mathbb{E}_{(\mathbf{X}^t, \mathbf{Y}^t) \sim P_t} [L(w, \mathbf{X}^t, \mathbf{Y}^t)] \right| > \frac{\beta}{2}$ is less than the probability that there exists a w that satisfies the above inequality. In

general, if $|a - b| > \beta$, then $|a| > \frac{\beta}{2}$ or $|b| > \frac{\beta}{2}$ (or both). Then

$$\begin{aligned}
 & \Pr_{\hat{\mu}} \left\{ \left| \frac{1}{s} \sum_{i=t-s}^{t-1} L(w_t^*, \mathbf{X}^i, \tilde{\mathbf{Y}}^i) - \mathbb{E}_{(\mathbf{X}^t, \mathbf{Y}^t) \sim P_t} [L(w_t^*, \mathbf{X}^t, \mathbf{Y}^t)] \right. \right. \\
 & \quad \left. \left. - \frac{1}{s} \sum_{i=t-s}^{t-1} L(\hat{w}_t, \mathbf{X}^i, \tilde{\mathbf{Y}}^i) + \mathbb{E}_{(\mathbf{X}^t, \mathbf{Y}^t) \sim P_t} [L(\hat{w}_t, \mathbf{X}^t, \mathbf{Y}^t)] \right| > \beta \right\} \\
 & \leq \Pr_{\hat{\mu}} \left\{ \left| \frac{1}{s} \sum_{i=t-s}^{t-1} L(w_t^*, \mathbf{X}^i, \tilde{\mathbf{Y}}^i) - \mathbb{E}_{(\mathbf{X}^t, \mathbf{Y}^t) \sim P_t} [L(w_t^*, \mathbf{X}^t, \mathbf{Y}^t)] \right| > \frac{\beta}{2}, \cup \right. \\
 & \quad \left. \left| -\frac{1}{s} \sum_{i=t-s}^{t-1} L(\hat{w}_t, \mathbf{X}^i, \tilde{\mathbf{Y}}^i) + \mathbb{E}_{(\mathbf{X}^t, \mathbf{Y}^t) \sim P_t} [L(\hat{w}_t, \mathbf{X}^t, \mathbf{Y}^t)] \right| > \frac{\beta}{2} \right\} \\
 & \leq 8 \cdot 41^d \exp \left(-\frac{s}{14400} (\beta - 4D^\mu)^2 \right).
 \end{aligned}$$

By definition of w_t^* and \hat{w}_t , $\frac{1}{s} \sum_{i=t-s}^{t-1} L(w_t^*, \mathbf{X}^i, \tilde{\mathbf{Y}}^i) > \frac{1}{s} \sum_{i=t-s}^{t-1} L(\hat{w}_t, \mathbf{X}^i, \tilde{\mathbf{Y}}^i)$ and $\mathbb{E}_{(\mathbf{X}^t, \mathbf{Y}^t) \sim P_t} [L(\hat{w}_t, \mathbf{X}^t, \mathbf{Y}^t)] > \mathbb{E}_{(\mathbf{X}^t, \mathbf{Y}^t) \sim P_t} [L(w_t^*, \mathbf{X}^t, \mathbf{Y}^t)]$. Therefore,

$$\begin{aligned}
 & \Pr_{\hat{\mu}} \left\{ \mathbb{E}_{(\mathbf{X}^t, \mathbf{Y}^t) \sim P_t} [L(\hat{w}_t, \mathbf{X}^t, \mathbf{Y}^t)] - \mathbb{E}_{(\mathbf{X}^t, \mathbf{Y}^t) \sim P_t} [L(w_t^*, \mathbf{X}^t, \mathbf{Y}^t)] > \beta \right\} \\
 & \leq 8 \cdot 41^d \exp \left(-\frac{s}{14400} (\beta - 4D^\mu)^2 \right).
 \end{aligned}$$

Now we apply Lemma 13 from Long (1999). Define

$$\phi(\beta) = \begin{cases} 8 \cdot 41^d \exp \left(-\frac{s}{14400} (\beta - 4D^\mu)^2 \right) & \beta \geq 6\Delta^\mu s + 4D^\mu \\ 1 & o.w. \end{cases}.$$

Let $a_0 = 0$ and $a_1 = 6\Delta^\mu s + 4D^\mu$. For all other a_i where $i > 1$ until some a_n where $a_{n+1} > 1$, define $a_i = \sqrt{\frac{14400(\ln 8 + (\ln 41)d + i \ln 2)}{s}} + 4D^\mu$. This way, $\phi(a_{i>1}) = 2^{-i}$. Then Lemma 13 states

$$\begin{aligned}
 & \mathbb{E}_{\{(\mathbf{X}^i, \tilde{\mathbf{Y}}^i) \sim P_{i, \hat{\mu}_i}\}_{i=t-s}^{t-1}} [P_t(L(\hat{w}_t, \mathbf{X}^t, \mathbf{Y}^t) = 1) - P_t(L(w_t^*, \mathbf{X}^t, \mathbf{Y}^t) = 1)] \\
 & \leq 1 \cdot a_1 + \sum_{i=1}^{\infty} \left(\sqrt{\frac{14400(\ln 8 + (\ln 41)d + i \ln 2)}{s}} + 4D^\mu \right) 2^{-i} \\
 & \leq 6\Delta^\mu s + 4D^\mu + 341 \sqrt{\frac{d}{s}} + 4D^\mu = 6\Delta^\mu s + 8D^\mu + 341 \sqrt{\frac{d}{s}}.
 \end{aligned}$$

Plugging in our values of s and Δ^μ , we get that $6\Delta^\mu s + 8D^\mu + 341 \sqrt{\frac{d}{s}} \leq \epsilon$. Therefore, if the drift between two consecutive samples is less than $TV(P_{i, \hat{\mu}_i}, P_{i+1, \hat{\mu}_{i+1}}) \leq \Delta^\mu \leq \frac{(\epsilon - 8D^\mu)^3}{5000000d}$, there exists an algorithm that computes a \hat{w}_t over the past $s = \left\lfloor \frac{\epsilon - 8D^\mu}{16(\Delta + 2D^\mu)} \right\rfloor$ inputs to the end model, such that

$$\Pr_{\hat{\mu}, t} (L(\hat{w}_t, \mathbf{X}^t, \mathbf{Y}^t) = 1) \leq \epsilon + \min_w P_t(L(w, \mathbf{X}^t, \mathbf{Y}^t) = 1),$$

where $D^\mu \leq \sqrt{\frac{1}{2} \max_i \mathbb{E}_{\mathbf{X} \sim P_i} [KL(P_i(\mathbf{Y}|\mathbf{X}) || P_{\mu_i}(\mathbf{Y}|\mathbf{X}))]} + m^{1/4} \sqrt{\frac{1}{\sigma_{min}} \max_i \|\mu_i - \hat{\mu}_i\|_2}$ by Lemma 4. \square

Lemma 3. The difference in the expected value of $L(w, \mathbf{X}, \mathbf{Y})$ when samples are drawn from $P_{t, \hat{\mu}_t}$ versus P_t is

$$\left| \mathbb{E}_{(\mathbf{X}^t, \tilde{\mathbf{Y}}^t) \sim P_{t, \hat{\mu}_t}} [L(w, \mathbf{X}^t, \tilde{\mathbf{Y}}^t)] - \mathbb{E}_{(\mathbf{X}^t, \mathbf{Y}^t) \sim P_t} [L(w, \mathbf{X}^t, \mathbf{Y}^t)] \right| \leq 2D^\mu.$$

Proof. We use the definition of total variation distance:

$$\begin{aligned}
 & \left| \mathbb{E}_{(\mathbf{X}^t, \tilde{\mathbf{Y}}^t) \sim P_{t, \hat{\boldsymbol{\mu}}_t}} [L(w, \mathbf{X}^t, \tilde{\mathbf{Y}}^t)] - \mathbb{E}_{(\mathbf{X}^t, \mathbf{Y}^t) \sim P_t} [L(w, \mathbf{X}^t, \mathbf{Y}^t)] \right| \\
 &= \left| \sum_{x, y} L(w, x, y) (P_{t, \hat{\boldsymbol{\mu}}_t}(x, y) - P_t(x, y)) \right| \\
 &\leq \sum_{x, y} L(w, x, y) |P_{t, \hat{\boldsymbol{\mu}}_t}(x, y) - P_t(x, y)| \\
 &\leq \sum_{x, y} |P_{t, \hat{\boldsymbol{\mu}}_t}(x, y) - P_t(x, y)| = 2TV(P_{t, \hat{\boldsymbol{\mu}}_t}, P_t) \leq 2D^\mu.
 \end{aligned}$$

□

Lemma 4.

$$D^\mu \leq \sqrt{\frac{1}{2} \max_i KL(P_i(\mathbf{Y}|\mathbf{X}) \| P_{\boldsymbol{\mu}_i}(\mathbf{Y}|\mathbf{X}))} + m^{1/4} \sqrt{\frac{1}{\sigma_{min}} \max_i \|\boldsymbol{\mu}_i - \hat{\boldsymbol{\mu}}_i\|_2}.$$

Here, σ_{min} is the minimum singular value of the covariance matrix Σ of the variables $V = \{\mathbf{Y}, \mathbf{v}\}$ in the graphical model.

Proof. We first use the triangle inequality on TV distance to split D^μ into two KL-divergences.

$$\begin{aligned}
 D^\mu &\leq \max_i TV(P_{i, \hat{\boldsymbol{\mu}}_i}, P_i) \leq \max_i TV(P_{i, \hat{\boldsymbol{\mu}}_i}, P_{i, \boldsymbol{\mu}_i}) + \max_i TV(P_{i, \boldsymbol{\mu}_i}, P_i) \\
 &\leq \sqrt{\frac{1}{2} \max_i KL(P_{i, \boldsymbol{\mu}_i} \| P_{i, \hat{\boldsymbol{\mu}}_i})} + \sqrt{\frac{1}{2} \max_i KL(P_i \| P_{i, \boldsymbol{\mu}_i})}.
 \end{aligned}$$

To simplify the first divergence, we use the binary Ising model definition in (3), which for simplicity we write as $f_G(\mathbf{Y}, \mathbf{v}) = \frac{1}{Z} \exp(\theta^T \phi(V))$, where $\phi(V)$ is the vector of all potentials.

$$\begin{aligned}
 KL(P_{i, \boldsymbol{\mu}_i} \| P_{i, \hat{\boldsymbol{\mu}}_i}) &= (\hat{\theta}_i - \theta_i)^T \mathbb{E}[\phi(V)] + \ln \frac{\hat{Z}}{Z} \leq |\hat{\theta}_i - \theta_i|_1 + \ln \frac{\hat{Z}}{Z} \leq \sqrt{m} \|\hat{\theta}_i - \theta_i\|_2 + \ln \frac{\sum_{s \in \mathcal{S}} \exp(\hat{\theta}_i^T \phi(s))}{\sum_{s \in \mathcal{S}} \exp(\theta_i^T \phi(s))} \\
 &\leq \sqrt{m} \|\hat{\theta}_i - \theta_i\|_2 + \frac{1}{\hat{Z}} \sum_{s \in \mathcal{S}} \exp(\hat{\theta}_i^T \phi(s)) \ln \frac{\exp(\hat{\theta}_i^T \phi(s))}{\exp(\theta_i^T \phi(s))} \\
 &\leq \sqrt{m} \|\hat{\theta}_i - \theta_i\|_2 + \frac{1}{\hat{Z}} \sum_{s \in \mathcal{S}} \exp(\hat{\theta}_i^T \phi(s)) ((\hat{\theta}_i - \theta_i)^T \phi(s)) \\
 &\leq \sqrt{m} \|\hat{\theta}_i - \theta_i\|_2 + \frac{1}{\hat{Z}} \sum_{s \in \mathcal{S}} \exp(\hat{\theta}_i^T \phi(s)) \sqrt{m} \|\hat{\theta}_i - \theta_i\|_2 \leq 2\sqrt{m} \|\hat{\theta}_i - \theta_i\|_2 \\
 &\leq \frac{2\sqrt{m}}{\sigma_{min}} \|\hat{\boldsymbol{\mu}}_i - \boldsymbol{\mu}_i\|_2.
 \end{aligned}$$

Here we used $\phi(s), \mathbb{E}[\phi(V)] \in [-1, +1]$, the log sum inequality, and Lemma 8. The second divergence can be simplified into a conditional KL-divergence.

$$\begin{aligned}
 KL(P_i \| P_{i, \boldsymbol{\mu}_i}) &= \sum_{x, y} P_i(x, y) \ln \frac{P_i(x, y)}{P_{i, \boldsymbol{\mu}_i}(x, y)} = \sum_{x, y} P_i(x, y) \ln \frac{P_i(y|x)P_i(x)}{P_{i, \boldsymbol{\mu}_i}(y|x)P_{i, \boldsymbol{\mu}_i}(x)} \\
 &= \sum_{x, y} P_i(x, y) \ln \frac{P_i(y|x)P_i(x)}{P_{\boldsymbol{\mu}_i}(y|x)P_i(x)} = \sum_x P_i(x) \sum_y P_i(y|x) \ln \frac{P_i(y|x)}{P_{\boldsymbol{\mu}_i}(y|x)} \\
 &= \sum_x P_i(x) KL(P_i(\mathbf{Y}|x) \| P_{\boldsymbol{\mu}_i}(\mathbf{Y}|x)) = KL(P_i(\mathbf{Y}|\mathbf{X}) \| P_{\boldsymbol{\mu}_i}(\mathbf{Y}|\mathbf{X})),
 \end{aligned}$$

where

$$KL(P_i(\mathbf{Y}|\mathbf{X}) \parallel P_{\mu_i}(\mathbf{Y}|\mathbf{X})) = \mathbb{E}_{P_i}[KL(P_i(\mathbf{Y}|x) \parallel P_{\mu_i}(\mathbf{Y}|x))].$$

□

This result suggests that, with a small enough Δ^μ , our parametrization of the end model using past data will perform only ϵ worse in probability than the best possible parametrization of the end model on the next data point. Furthermore, note that s is decreasing in D^μ ; more model misspecification and sampling error intuitively suggests that we want to use fewer previous data points to compute \hat{w}_t , so again having a simple yet suitable graphical model allows the end model to train on more data for better prediction.

D. Proofs of Main Results

D.1. Proof of Theorem 1 (Sampling Error)

We first present three concentration inequalities - one on the accuracies estimated via the triplet method, and the other two on directly observable values. Afterwards, we discuss how to combine these inequalities into a sampling error result for μ when G_{dep} has small cliques of size 3 or less.

Estimation error for a_i using Algorithm 1

Lemma 5. Denote M as the second moment matrix over all observed variables, e.g. $M_{ij} = \mathbb{E}[v_i v_j]$. Let \hat{a} be an estimate of the m desired accuracies a using \hat{M} computed from n samples. Define $a_{\min} = \min\{\min_i |\hat{a}_i|, \min_i |a_i|\}$, and assume $\text{sign}(a_i) = \text{sign}(\hat{a}_i)$ for all a_i . Furthermore, assume that the number of samples n is greater than some n_0 such that $a_{\min} > 0$, and $\hat{M}_{ij} \neq 0$. Then the estimation error of the accuracies is

$$\Delta_a = \mathbb{E}[\|\hat{a} - a\|_2] \leq C_a \frac{1}{a_{\min}^5} \sqrt{\frac{m}{n}},$$

for some constant C_a .

Proof. We start with a few definitions. Denote a triplet as $T_i(1), T_i(2), T_i(3)$, and in total suppose we need τ number of triplets. Recall that our estimate of a can be obtained with

$$|\hat{a}_{T_i(1)}| = \left(\frac{|\hat{M}_{T_i(1)T_i(2)}| |\hat{M}_{T_i(1)T_i(3)}|}{|\hat{M}_{T_i(2)T_i(3)}|} \right)^{\frac{1}{2}}.$$

Because we assume that signs are completely recoverable,

$$\|\hat{a} - a\|_2 = \|\hat{a} - |a|\|_2 = \left(\sum_{i=1}^{\tau} (|\hat{a}_{T_i(1)}| - |a_{T_i(1)}|)^2 + (|\hat{a}_{T_i(2)}| - |a_{T_i(2)}|)^2 + (|\hat{a}_{T_i(3)}| - |a_{T_i(3)}|)^2 \right)^{\frac{1}{2}}. \quad (13)$$

Note that $|\hat{a}_i^2 - a_i^2| = |\hat{a}_i - a_i| |\hat{a}_i + a_i|$. By the reverse triangle inequality, $(|\hat{a}_i| - |a_i|)^2 = \|\hat{a}_i - |a_i|\|^2 \leq |\hat{a}_i - a_i|^2 = \left(\frac{|\hat{a}_i^2 - a_i^2|}{|\hat{a}_i + a_i|} \right)^2 \leq \frac{1}{4a_{\min}^2} |\hat{a}_i^2 - a_i^2|^2$, because $|\hat{a}_i + a_i| = |\hat{a}_i| + |a_i| \geq 2a_{\min}$. For ease of notation, suppose we examine a

particular $T_i = \{1, 2, 3\}$. Then

$$\begin{aligned}
 (|\hat{a}_1| - |a_1|)^2 &\leq \frac{1}{4a_{\min}^2} |\hat{a}_1^2 - a_1^2|^2 = \frac{1}{c^2} \left| \frac{|\hat{M}_{12}||\hat{M}_{13}|}{|\hat{M}_{23}|} - \frac{|M_{12}||M_{13}|}{|M_{23}|} \right|^2 \\
 &= \frac{1}{4a_{\min}^2} \left| \frac{|\hat{M}_{12}||\hat{M}_{13}|}{|\hat{M}_{23}|} - \frac{|\hat{M}_{12}||\hat{M}_{13}|}{|M_{23}|} + \frac{|\hat{M}_{12}||\hat{M}_{13}|}{|M_{23}|} - \frac{|\hat{M}_{12}||M_{13}|}{|M_{23}|} + \frac{|\hat{M}_{12}||M_{13}|}{|M_{23}|} - \frac{|M_{12}||M_{13}|}{|M_{23}|} \right|^2 \\
 &\leq \frac{1}{4a_{\min}^2} \left(\left| \frac{\hat{M}_{12}\hat{M}_{13}}{\hat{M}_{23}M_{23}} \right| \left| |\hat{M}_{23}| - |M_{23}| \right| + \left| \frac{\hat{M}_{12}}{M_{23}} \right| \left| |\hat{M}_{13}| - |M_{13}| \right| + \left| \frac{M_{13}}{M_{23}} \right| \left| |\hat{M}_{12}| - |M_{12}| \right| \right)^2 \\
 &\leq \frac{1}{4a_{\min}^2} \left(\left| \frac{\hat{M}_{12}\hat{M}_{13}}{\hat{M}_{23}M_{23}} \right| |\hat{M}_{23} - M_{23}| + \left| \frac{\hat{M}_{12}}{M_{23}} \right| |\hat{M}_{13} - M_{13}| + \left| \frac{M_{13}}{M_{23}} \right| |\hat{M}_{12} - M_{12}| \right)^2. \tag{14}
 \end{aligned}$$

Clearly, all elements of \hat{M} and M must be less than 1. We further know that elements of $|M|$ are at least a_{\min}^2 , since $\mathbb{E}[v_i v_j] = \mathbb{E}[v_i Y] \mathbb{E}[v_j Y] \geq a_{\min}^2$. Furthermore, elements of $|\hat{M}|$ are also at least a_{\min}^2 because $|\hat{M}_{ij}| = \hat{a}_i \hat{a}_j \geq a_{\min}^2$ by construction of our algorithm. Define $\Delta_{ij} = \hat{M}_{ij} - M_{ij}$. Then

$$\begin{aligned}
 (|\hat{a}_1| - |a_1|)^2 &\leq \frac{1}{4a_{\min}^2} \left(\frac{1}{a_{\min}^4} |\Delta_{23}| + \frac{1}{a_{\min}^2} |\Delta_{13}| + \frac{1}{a_{\min}^2} |\Delta_{12}| \right)^2 \\
 &\leq \frac{1}{4a_{\min}^2} (\Delta_{23}^2 + \Delta_{13}^2 + \Delta_{12}^2) \left(\frac{1}{a_{\min}^8} + \frac{2}{a_{\min}^4} \right).
 \end{aligned}$$

(13) is now

$$\|\hat{a} - a\|_2 \leq \left(\frac{3}{4a_{\min}^2} \left(\frac{1}{a_{\min}^8} + \frac{2}{a_{\min}^4} \right) \sum_{i=1}^{\tau} \left(\Delta_{T_i(1)T_i(2)}^2 + \Delta_{T_i(1)T_i(3)}^2 + \Delta_{T_i(2)T_i(3)}^2 \right) \right)^{\frac{1}{2}}.$$

To bound the maximum absolute value between elements of \hat{M} and M , note that the Frobenius norm of the 3×3 submatrix defined over T_i is

$$\|\hat{M}_{T_i} - M_{T_i}\|_F = \left(2 \left(\Delta_{T_i(1)T_i(2)}^2 + \Delta_{T_i(1)T_i(3)}^2 + \Delta_{T_i(2)T_i(3)}^2 \right) \right)^{\frac{1}{2}}.$$

Moreover, $\|\hat{M}_{T_i} - M_{T_i}\|_F = \sqrt{\sum_{j=1}^3 \sigma_j^2(\hat{M}_{T_i} - M_{T_i})} \leq \sqrt{3} \|\hat{M}_{T_i} - M_{T_i}\|_2$. Putting everything together,

$$\begin{aligned}
 \|\hat{a} - a\|_2 &\leq \left(\frac{3}{4a_{\min}^2} \left(\frac{1}{a_{\min}^8} + \frac{2}{a_{\min}^4} \right) \cdot \frac{1}{2} \sum_{i=1}^{\tau} \|\hat{M}_{T_i} - M_{T_i}\|_F^2 \right)^{\frac{1}{2}} \\
 &\leq \left(\frac{3}{4a_{\min}^2} \left(\frac{1}{a_{\min}^8} + \frac{2}{a_{\min}^4} \right) \cdot \frac{3}{2} \sum_{i=1}^{\tau} \|\hat{M}_{T_i} - M_{T_i}\|_2^2 \right)^{\frac{1}{2}}.
 \end{aligned}$$

Lastly, to compute $\mathbb{E}[\|\hat{a} - a\|_2]$, we use Jensen's inequality and linearity of expectation:

$$\mathbb{E}[\|\hat{a} - a\|_2] \leq \left(\frac{3}{4a_{\min}^2} \left(\frac{1}{a_{\min}^8} + \frac{2}{a_{\min}^4} \right) \cdot \frac{3}{2} \sum_{i=1}^{\tau} \mathbb{E}[\|\hat{M}_{T_i} - M_{T_i}\|_2^2] \right)^{\frac{1}{2}}.$$

We use the matrix Hoeffding inequality as described in [Ratner et al. \(2019\)](#), which says

$$P(\|\hat{M} - M\|_2 \geq \gamma) \leq 2m \exp\left(-\frac{n\gamma^2}{32m^2}\right).$$

To get the probability distribution over $\|\hat{M} - M\|_2^2$, we just note that $P(\|\hat{M} - M\|_2 \geq \gamma) = P(\|\hat{M} - M\|_2^2 \geq \gamma^2)$ to get

$$P(\|\hat{M} - M\|_2^2 \geq \gamma) \leq 2m \exp\left(-\frac{n\gamma}{32m^2}\right).$$

From which we can integrate to get

$$\mathbb{E}[\|\hat{M}_{T_i} - M_{T_i}\|_2^2] = \int_0^\infty P(\|\hat{M}_{T_i} - M_{T_i}\|_2^2 \geq \gamma) d\gamma \leq \frac{64(3)^3}{n}.$$

Substituting this back in, we get

$$\begin{aligned} \mathbb{E}[\|\hat{a} - a\|_2] &\leq \left(\frac{3}{4a_{\min}^2} \left(\frac{1}{a_{\min}^8} + \frac{2}{a_{\min}^4}\right) \cdot \frac{3\tau}{2} \frac{1728}{n}\right)^{\frac{1}{2}} \\ &\leq \left(\frac{1944}{a_{\min}^2} \cdot \left(\frac{1}{a_{\min}^8} + \frac{2}{a_{\min}^4}\right) \cdot \frac{\tau}{n}\right)^{\frac{1}{2}}. \end{aligned}$$

Finally, note that

$$\frac{1}{a_{\min}^2} \cdot \left(\frac{1}{a_{\min}^8} + \frac{2}{a_{\min}^4}\right) = \frac{1}{a_{\min}^2} \cdot \frac{1 + 2a_{\min}^4}{a_{\min}^8} \leq \frac{3}{a_{\min}^{10}}.$$

Therefore, the sampling error for the accuracy is bounded by

$$\mathbb{E}[\|\hat{a} - a\|_2] \leq \left(\frac{1944 \cdot 3}{a_{\min}^{10}} \cdot \frac{\tau}{n}\right)^{\frac{1}{2}} \leq C_a \frac{1}{a_{\min}^5} \sqrt{\frac{m}{n}}.$$

This is because at most we will use a triplet to compute each relevant a_i , meaning that $\tau \leq m$. The term C_a here is $18\sqrt{6}$. \square

Remark 1. Although a lower bound on accuracy a_{\min} invariably appears in this result, the dependence on a single low-accuracy source λ_{\min} can be reduced. We improve our bound from having a $\frac{1}{a_{\min}^5}$ dependency to one additive term of order $\frac{1}{a_{\min}\sqrt{n}}$, while other terms are not dependent on a_{\min} and are overall of order $\sqrt{\frac{m-1}{n}}$. In (14), the $4a_{\min}^2$ can be tightened to $4a_i^2$ for each λ_i , and M_{23} and \hat{M}_{23} are not in terms of a_{\min} if neither of the two labeling functions at hand are λ_{\min} . Therefore, for any $\lambda_i \neq \lambda_{\min}$, we do not have a dependency on a_{\min} if we ensure that the triplet used to recover its accuracy in Algorithm 1 does not include λ_{\min} . Then only one term in our final bound will have a $\frac{1}{a_{\min}\sqrt{n}}$ dependency compared to the previous $\frac{1}{a_{\min}^5} \sqrt{\frac{m}{n}}$.

Concentration inequalities on observable data

Lemma 6. Define $p^{(i)}(x) = P(\lambda_i = x)$ and $\hat{p}^{(i)}(x) = \frac{1}{n} \sum_{k=1}^n \mathbb{1}\{L_k^{(i)} = x\}$, and let $p(x), \hat{p}(x) \in \mathbb{R}^m$ denote the vectors over all i . Then

$$\Delta_p := \mathbb{E}[\|\hat{p}(x) - p(x)\|_2] \leq \sqrt{\frac{m}{n}}.$$

Proof. Note that $\mathbb{E}[\mathbb{1}\{L_k^{(i)} = x\}] = P(\lambda_i = x)$. Then using Hoeffding's inequality, we have that

$$P(|\hat{p}^{(i)}(x) - p^{(i)}(x)| \geq \epsilon) \leq 2 \exp\left(-\frac{2n^2\epsilon^2}{n(1)^2}\right) \leq 2 \exp(-2n\epsilon^2).$$

This expression is equivalent to

$$P(|\hat{p}^{(i)}(x) - p^{(i)}(x)|^2 \geq \epsilon) \leq 2 \exp(-2n\epsilon).$$

We can now compute $\mathbb{E} [|\hat{p}^{(i)}(x) - p^{(i)}(x)|^2]$:

$$\mathbb{E} [|\hat{p}^{(i)}(x) - p^{(i)}(x)|^2] \leq \int_0^\infty 2 \exp(-2n\epsilon) d\epsilon = -2 \cdot \frac{1}{2n} \exp(-2n\epsilon) \Big|_0^\infty = \frac{1}{n}.$$

The overall L2 error for $p(x)$ is then

$$\mathbb{E} [\|\hat{p}(x) - p(x)\|_2] = \mathbb{E} \left[\left(\sum_{i=1}^m |\hat{p}^{(i)}(x) - p^{(i)}(x)|^2 \right)^{1/2} \right] \leq \sqrt{\sum_{i=1}^m \mathbb{E} [|\hat{p}^{(i)}(x) - p^{(i)}(x)|^2]} \leq \sqrt{\frac{m}{n}}.$$

□

Lemma 7. Define $M(a, b)$ to be a second moment matrix where $M(a, b)_{ij} = \mathbb{E} [a_i b_j]$ for some random variables $a_i, b_j \in \{-1, 0, 1\}$ each corresponding to λ_i, λ_j . Let $\|\cdot\|_{ij}$ be the Frobenius norm over elements indexed at (i, j) , where λ_i and λ_j share an edge in the dependency graph. If G_{dep} has d conditionally independent subgraphs, the estimation error of M is

$$\Delta_M := \mathbb{E} [\|\hat{M}(a, b) - M(a, b)\|_{ij}] \leq C_m \sqrt{\frac{d-1 + (m-d+1)^2}{n}} \leq C_m \frac{m}{\sqrt{n}}.$$

For some constant C_m .

Proof. Recall that the subgraphs are defined as sets V_1, \dots, V_d , and let E_1, \dots, E_d be the corresponding sets of edges within the subgraphs. We can split up the norm $\|\hat{M}(a, b) - M(a, b)\|_{ij}$ into summations over sets of edges.

$$\begin{aligned} \|\hat{M}(a, b) - M(a, b)\|_{ij} &= \left(\sum_{(i,j) \in E_{dep}} (\hat{M}(a, b)_{ij} - M(a, b)_{ij})^2 \right)^{\frac{1}{2}} = \left(\sum_{k=1}^d \sum_{(i,j) \in E_k} (\hat{M}(a, b)_{ij} - M(a, b)_{ij})^2 \right)^{\frac{1}{2}} \\ &\leq \left(\sum_{k=1}^d \sum_{i,j \in V_k} (\hat{M}(a, b)_{ij} - M(a, b)_{ij})^2 \right)^{\frac{1}{2}} = \left(\sum_{k=1}^d \frac{1}{2} \|\hat{M}(a, b)_{V_k} - M(a, b)_{V_k}\|_F^2 \right)^{\frac{1}{2}}. \end{aligned}$$

We take the expectation of both sides by using linearity of expectation and Jensen's inequality:

$$\mathbb{E} [\|\hat{M}(a, b) - M(a, b)\|_{ij}] \leq \left(\sum_{k=1}^d \frac{1}{2} \mathbb{E} [\|\hat{M}(a, b)_{V_k} - M(a, b)_{V_k}\|_F^2] \right)^{\frac{1}{2}}.$$

We are able to modify Proposition A.3 of [Bunea & Xiao \(2015\)](#) into a concentration inequality for the second moment matrix rather than the covariance matrix, which states that $\mathbb{E} [\|\hat{M}(a, b)_{V_k} - M(a, b)_{V_k}\|_F^2] \leq (32e^{-4} + e + 64) \left(\frac{4c_1 \text{tr}(M_{V_k})}{\sqrt{n}} \right)^2$ for some constant c_1 . We are able to use this result because our random variables are sub-Gaussian and have bounded higher order moments. Then our bound becomes

$$\mathbb{E} [\|\hat{M}(a, b) - M(a, b)\|_{ij}] \leq \left(\sum_{k=1}^d \frac{1}{2} (32e^{-4} + e + 64) \frac{16c_1^2 |V_k|^2}{n} \right)^{\frac{1}{2}} \leq \left(\frac{8c_1^2 (32e^{-4} + e + 64)}{n} \sum_{k=1}^d |V_k|^2 \right)^{\frac{1}{2}}.$$

$\sum_{k=1}^d |V_k|^2$ is maximized when we have $d-1$ subgraphs of size 1 and 1 subgraph of size $m-d+1$, in which case the summation is $d-1 + (m-d+1)^2$. Intuitively, when there are more subgraphs, this value will be smaller and closer to an order of m rather than m^2 . Putting this together, our bound is

$$\mathbb{E} [\|\hat{M}(a, b) - M(a, b)\|_{ij}] \leq \left(8c_1^2 (32e^{-4} + e + 64) \frac{d-1 + (m-d+1)^2}{n} \right)^{\frac{1}{2}} \leq C_m \frac{m}{\sqrt{n}}.$$

Where $C_m = \sqrt{8c_1^2 (32e^{-4} + e + 64)}$.

□

Estimating μ_i We first estimate $\mu_i = P(\lambda_i, Y^{dep}(i))$ for all relevant λ_i . For ease of notation, let Y refer to $Y^{dep}(i)$ in this section. Denote $\boldsymbol{\mu}_i$ to be the vector of all μ_i across all $\boldsymbol{\lambda}$. Note that

$$\|\hat{\boldsymbol{\mu}}_i - \boldsymbol{\mu}_i\|_2 \leq \|\text{diag}_m(A_1^{-1})\|_2 \|\hat{\rho} - \rho\|_2.$$

ρ is the vector of all r_i for $i = 1, \dots, m$, and $\text{diag}_m(A_1^{-1})$ is a block matrix containing m A_1^{-1} on its diagonal; note that the 2-norm of a block diagonal matrix is just the maximum 2-norm over all of the block matrices, which is $\|A_1^{-1}\|_2$. Recall that $r_i = [1 \ P(\lambda_i = 1) \ P(\lambda_i = 0) \ P(Y = 1) \ P(\lambda_i Y = 1) \ P(\lambda_i = 0, Y = 1)]^T$. For each term of r_i , we have a corresponding sampling error to compute over ρ :

- $P(\lambda_i = 1)$: We need to compute $\hat{P}(\lambda_i = 1) - P(\lambda_i = 1)$ for each λ_i . All together, the sampling error for this term is equivalent to $\|\hat{p}(1) - p(1)\|_2$.
- $P(\lambda_i = 0)$: The sampling error over all $\hat{P}(\lambda_i = 0) - P(\lambda_i = 0)$ is equivalent to $\|\hat{p}(0) - p(0)\|_2$.
- $P(\lambda_i Y = 1)$: Since $a_i = \mathbb{E}[v_{2i-1}Y] = \mathbb{E}[\lambda_i Y] = P(\lambda_i Y = 1) - P(\lambda_i Y = -1) = 2P(\lambda_i Y = 1) + P(\lambda_i = 0) - 1$ and the sampling error over all $\hat{P}(\lambda_i Y = 1) - P(\lambda_i Y = 1)$ is at most $\frac{1}{2}\|(\hat{a} - a) - (\hat{p}(0) - p(0))\|_2 \leq \frac{1}{2}(\|\hat{a} - a\|_2 + \|\hat{p}(0) - p(0)\|_2)$.
- $P(\lambda_i = 0, Y = 1)$: This expression is equal to $P(\lambda_i = 0)P(Y = 1)$, so the sampling error is $P(Y = 1)\|\hat{p}(0) - p(0)\|_2 \leq \|\hat{p}(0) - p(0)\|_2$.

Putting these error terms together, we have an expression for the sampling error for ρ :

$$\begin{aligned} \|\hat{\rho} - \rho\|_2 &= \sqrt{\|\hat{p}(1) - p(1)\|_2^2 + 2\|\hat{p}(0) - p(0)\|_2^2 + \frac{1}{4}(\|\hat{a} - a\|_2 + \|\hat{p}(0) - p(0)\|_2)^2} \\ &\leq \|\hat{p}(1) - p(1)\|_2 + \sqrt{2}\|\hat{p}(0) - p(0)\|_2 + \frac{1}{2}(\|\hat{a} - a\|_2 + \|\hat{p}(0) - p(0)\|_2) \\ &= \|\hat{p}(1) - p(1)\|_2 + \left(\frac{1}{2} + \sqrt{2}\right)\|\hat{p}(0) - p(0)\|_2 + \frac{1}{2}\|\hat{a} - a\|_2, \end{aligned}$$

where we use concavity of the square root in the first step. Therefore,

$$\begin{aligned} \mathbb{E}[\|\hat{\rho} - \rho\|_2] &\leq \mathbb{E}[\|\hat{p}(1) - p(1)\|_2] + \left(\frac{1}{2} + \sqrt{2}\right)\mathbb{E}[\|\hat{p}(0) - p(0)\|_2] + \frac{1}{2}\mathbb{E}[\|\hat{a} - a\|_2] \\ &= \left(\frac{3}{2} + \sqrt{2}\right)\Delta_p + \frac{1}{2}\Delta_a. \end{aligned}$$

Plugging this back into our error for $\boldsymbol{\mu}_i$ and using Lemmas 5 and 6,

$$\mathbb{E}[\|\hat{\boldsymbol{\mu}}_i - \boldsymbol{\mu}_i\|_2] \leq \|A_1^{-1}\|_2 \left(\left(\frac{3}{2} + \sqrt{2}\right) \sqrt{\frac{m}{n}} + \frac{C_a}{2a_{\min}^5} \sqrt{\frac{m}{n}} \right).$$

Therefore, if there are no cliques of size 3 or greater in G_{dep} , the sampling error is $\mathcal{O}(\sqrt{m/n})$.

Estimating all μ_{ij} Now we estimate $\mu_{ij} = P(\lambda_i, \lambda_j, Y^{dep}(i, j))$ for λ_i, λ_j sharing an edge in G_{dep} . For ease of notation, let Y refer to $Y^{dep}(i, j)$ in this section. Denote $\boldsymbol{\mu}_{ij}$ to be the vector of all μ_{ij} . Note that

$$\|\hat{\boldsymbol{\mu}}_{ij} - \boldsymbol{\mu}_{ij}\|_2 \leq \|\text{diag}_{|E|}(A_2)^{-1}\|_2 \|\hat{\psi} - \psi\|_2 = \|A_2^{-1}\|_2 \|\hat{\psi} - \psi\|_2.$$

ψ is the vector of all r_{ij} for all $(i, j) \in E$. Recall that $a_i = \mathbb{E}[v_i Y]$, $a_{ij} = \mathbb{E}[v_i v_j Y]$. We also define $X_i^{(a)} = \mathbb{1}\{\lambda_i = a\}$ and $M(X^{(a)}, X^{(b)})_{ij} = \mathbb{E}[X_i^{(a)} X_j^{(b)}] = P(\lambda_i = a, \lambda_j = b)$. For each term of r_i , we have a corresponding estimation error to compute.

- $P(\lambda_i = 1)$: We need to compute $\hat{P}(\lambda_i = 1) - P(\lambda_i = 1)$ over all $(i, j) \in E$, so the sampling error for this term is $\sqrt{\sum_{(i,j) \in E} (\hat{P}(\lambda_i = 1) - P(\lambda_i = 1))^2} \leq \sqrt{\sum_{i=1}^m m (\hat{P}(\lambda_i = 1) - P(\lambda_i = 1))^2} = \sqrt{m} \|\hat{p}(1) - p(1)\|_2$.
- $P(\lambda_i = 0)$: The sampling error is equivalent to $\sqrt{m} \|\hat{p}(0) - p(0)\|_2$.
- $P(\lambda_j = 1)$: The sampling error is equivalent to $\sqrt{m} \|\hat{p}(1) - p(1)\|_2$.
- $P(\lambda_j = 0)$: The sampling error is equivalent to $\sqrt{m} \|\hat{p}(0) - p(0)\|_2$.
- $P(\lambda_i \lambda_j = 1)$: This probability can be written as $P(\lambda_i = 1, \lambda_j = 1) + P(\lambda_i = -1, \lambda_j = -1)$, so we would need to compute $\hat{P}(\lambda_i = 1, \lambda_j = 1) - P(\lambda_i = 1, \lambda_j = 1) + \hat{P}(\lambda_i = -1, \lambda_j = -1) - P(\lambda_i = -1, \lambda_j = -1)$. Then the sampling error is equivalent to $\|\hat{M}(X^{(1)}, X^{(1)}) - M(X^{(1)}, X^{(1)}) + \hat{M}(X^{(-1)}, X^{(-1)}) - M(X^{(-1)}, X^{(-1)})\|_{ij}$.
- $P(\lambda_i = 0, \lambda_j = 1)$: Using the definition of M , the sampling error over all $(i, j) \in E$ for this is $\|\hat{M}(X^{(0)}, X^{(1)}) - M(X^{(0)}, X^{(1)})\|_{ij}$.
- $P(\lambda_i = 1, \lambda_j = 0)$: Similarly, the sampling error is $\|\hat{M}(X^{(1)}, X^{(0)}) - M(X^{(1)}, X^{(0)})\|_{ij}$.
- $P(\lambda_i = 0, \lambda_j = 0)$: Similarly, the sampling error is $\|\hat{M}(X^{(0)}, X^{(0)}) - M(X^{(0)}, X^{(0)})\|_{ij}$.
- $P(\lambda_i Y = 1)$: Similar to before, the sampling error is $\frac{1}{2} \sqrt{m} (\|\hat{a} - a\|_2 + \|\hat{p}(0) - p(0)\|_2)$.
- $P(\lambda_i = 0, Y = 1)$: Similar to our estimate of μ_i , the sampling error is $\sqrt{m} \|\hat{p}(0) - p(0)\|_2$.
- $P(\lambda_j Y = 1)$: The sampling error is $\frac{1}{2} \sqrt{m} (\|\hat{a} - a\|_2 + \|\hat{p}(0) - p(0)\|_2)$.
- $P(\lambda_j = 0, Y = 1)$: The sampling error is $\sqrt{m} \|\hat{p}(0) - p(0)\|_2$.
- $P(\lambda_i \lambda_j Y = 1)$: Note that $\mathbb{E}[\lambda_i \lambda_j Y] = 2P(\lambda_i \lambda_j Y = 1) + P(\lambda_i \lambda_j = 0) - 1$. Moreover, $\mathbb{E}[\lambda_i \lambda_j Y]$ can be expressed as $\mathbb{E}[Y] \cdot \mathbb{E}[\lambda_i \lambda_j]$. Then the sampling error over all $\hat{P}(\lambda_i \lambda_j Y = 1) - P(\lambda_i \lambda_j Y = 1)$ is at least $\frac{1}{2} \|\mathbb{E}[Y] (\hat{\mathbb{E}}[\lambda_i \lambda_j] - \mathbb{E}[\lambda_i \lambda_j]) - (\hat{P}(\lambda_i \lambda_j = 0) - P(\lambda_i \lambda_j = 0))\|_{ij}$. Furthermore, we can write $P(\lambda_i \lambda_j = 0)$ as $P(\lambda_i = 0) + P(\lambda_j = 0) - P(\lambda_i = 0, \lambda_j = 0)$, so our sampling error is now less than $\frac{1}{2} \|\hat{M}(\lambda, \lambda) - M(\lambda, \lambda)\|_{ij} + \frac{1}{2} \sqrt{m} \|\hat{p}(0) - p(0)\|_2 + \frac{1}{2} \sqrt{m} \|\hat{p}(0) - p(0)\|_2 + \frac{1}{2} \|\hat{M}(X^{(0)}, X^{(0)}) - M(X^{(0)}, X^{(0)})\|_{ij}$.
- $P(\lambda_i = 0, \lambda_j Y = 1)$: Note that this can be written as $\frac{1}{2} (P(\lambda_i = 0) + \mathbb{E}[\lambda_j Y | \lambda_i = 0] P(\lambda_i = 0) - P(\lambda_i = 0, \lambda_j = 0))$. Then the sampling error over all $\hat{P}(\lambda_i = 0, \lambda_j Y = 1) - P(\lambda_i = 0, \lambda_j Y = 1)$ is equivalent to

$$\begin{aligned} & \frac{1}{2} \sqrt{m} \|\hat{p}(0) - p(0)\|_2 + \frac{1}{2} \|\hat{\mathbb{E}}[\lambda_j Y | \lambda_i = 0] \hat{P}(\lambda_i = 0) - \mathbb{E}[\lambda_j Y | \lambda_i = 0] P(\lambda_i = 0) \\ & \quad - (\hat{M}(X^{(0)}, X^{(0)}) - M(X^{(0)}, X^{(0)}))\|_{ij} \\ & = \frac{1}{2} \sqrt{m} \|\hat{p}(0) - p(0)\|_2 + \frac{1}{2} \|\hat{M}(X^{(0)}, X^{(0)}) - M(X^{(0)}, X^{(0)})\|_{ij} + \frac{1}{2} \|\hat{\mathbb{E}}[\lambda_j Y | \lambda_i = 0] (\hat{P}(\lambda_i = 0) - P(\lambda_i = 0)) \\ & \quad - (\mathbb{E}[\lambda_j Y | \lambda_i = 0] - \hat{\mathbb{E}}[\lambda_j Y | \lambda_i = 0]) P(\lambda_i = 0)\|_{ij} \\ & \leq \frac{\sqrt{m}}{2} \|\hat{p}(0) - p(0)\|_2 + \frac{1}{2} \|\hat{M}(X^{(0)}, X^{(0)}) - M(X^{(0)}, X^{(0)})\|_{ij} + \frac{\sqrt{m}}{2} \|\hat{p}(0) - p(0)\|_2 \\ & \quad + \frac{1}{2} \|\mathbb{E}[\lambda_j Y | \lambda_i = 0] - \hat{\mathbb{E}}[\lambda_j Y | \lambda_i = 0]\|_{ij} \\ & = \sqrt{m} \|\hat{p}(0) - p(0)\|_2 + \frac{1}{2} \|\hat{M}(X^{(0)}, X^{(0)}) - M(X^{(0)}, X^{(0)})\|_{ij} + \frac{1}{2} \|\mathbb{E}[\lambda_j Y | \lambda_i = 0] - \hat{\mathbb{E}}[\lambda_j Y | \lambda_i = 0]\|_{ij} \end{aligned}$$
- $P(\lambda_j = 0, \lambda_i Y = 1)$: Symmetric to the previous case, the sampling error is $\sqrt{m} \|\hat{p}(0) - p(0)\|_2 + \frac{1}{2} \|\hat{M}(X^{(0)}, X^{(0)}) - M(X^{(0)}, X^{(0)})\|_{ij} + \frac{1}{2} \|\mathbb{E}[\lambda_j Y | \lambda_i = 0] - \hat{\mathbb{E}}[\lambda_j Y | \lambda_i = 0]\|_{ij}$.
- $P(\lambda_i = 0, \lambda_j = 0, Y = 1)$: This expression is equal to $P(\lambda_i = 0, \lambda_j = 0) P(Y = 1)$, so the sampling error is $P(Y = 1) \|\hat{M}(X^{(0)}, X^{(0)}) - M(X^{(0)}, X^{(0)})\|_{ij} \leq \|\hat{M}(X^{(0)}, X^{(0)}) - M(X^{(0)}, X^{(0)})\|_{ij}$.

After combining terms and taking the expectation, we have that

$$\begin{aligned} \mathbb{E} \left[\|\hat{\psi} - \psi\|_2 \right] &\leq 2\sqrt{2m}\Delta_p + 2\Delta_M + 3\Delta_M + \frac{1}{\sqrt{2}}(\sqrt{m}\Delta_a + \sqrt{m}\Delta_p) + \sqrt{2m}\Delta_p + \frac{1}{2}(\Delta_M + 2\sqrt{m}\Delta_p + \Delta_M) \\ &\quad + \frac{1}{\sqrt{2}}(2\sqrt{m}\Delta_p + \|\hat{\mathbb{E}}[\lambda_i Y | \lambda_j = 0] - \mathbb{E}[\lambda_i Y | \lambda_j = 0]\|_{ij} + \Delta_M) + \Delta_M \\ &= \left(7 + \frac{1}{\sqrt{2}}\right)\Delta_M + \left(\frac{9}{2}\sqrt{2m} + \sqrt{m}\right)\Delta_p + \sqrt{\frac{m}{2}}\Delta_a + \frac{1}{\sqrt{2}}\|\hat{\mathbb{E}}[\lambda_i Y | \lambda_j = 0] - \mathbb{E}[\lambda_i Y | \lambda_j = 0]\|_{ij}. \end{aligned}$$

For $\mathbb{E}[\lambda_i Y | \lambda_j = 0]$, this term is equal to 0 when no sources can abstain. Otherwise, suppose that among the sources that do abstain, each label abstains with frequency at least r . Then $\|\hat{\mathbb{E}}[\lambda_i Y | \lambda_j = 0] - \mathbb{E}[\lambda_i Y | \lambda_j = 0]\|_{ij} \leq \sqrt{m} \cdot \frac{C_a}{a_{\min}^5} \sqrt{\frac{m}{rn}}$ since there are rn samples used to produce the estimate. Using Lemma 5, 6, and 7, we now get that

$$\mathbb{E} \left[\|\hat{\mu}_{ij} - \mu_{ij}\|_2 \right] \leq \|A_2^{-1}\| \left(\left(7 + \frac{1}{\sqrt{2}}\right) C_m \frac{m}{\sqrt{n}} + \left(\frac{9\sqrt{2}}{2} + 1\right) \frac{m}{\sqrt{n}} + \frac{C_a}{a_{\min}^5} \cdot \frac{m}{\sqrt{n}} \left(\frac{1}{\sqrt{2}} + \frac{1}{\sqrt{2r}}\right) \right).$$

Finally, we can compute $\|A_1^{-1}\|$ and $\|A_2^{-1}\|$ since both matrices are constants, so the total estimation error is

$$\begin{aligned} \mathbb{E} \left[\|\hat{\mu} - \mu\|_2 \right] &\leq 3.19 \left(\left(\frac{3}{2} + \sqrt{2}\right) \sqrt{\frac{m}{n}} + \frac{C_a}{2a_{\min}^5} \sqrt{\frac{m}{n}} \right) + \\ &\quad 6.35 \left(\left(7 + \frac{1}{\sqrt{2}}\right) C_m \frac{m}{\sqrt{n}} + \left(\frac{9\sqrt{2}}{2} + 1\right) \frac{m}{\sqrt{n}} + \frac{C_a}{a_{\min}^5} \cdot \frac{m}{\sqrt{n}} \left(\frac{1}{\sqrt{2}} + \frac{1}{\sqrt{2r}}\right) \right). \end{aligned}$$

D.2. Proof of Theorem 2 (Information Theoretical Lower Bound)

For Theorem 2 and Theorem 3, we will need the following lemma.

Lemma 8. *Let θ_1 and θ_2 be two sets of canonical parameters for an exponential family model, and let μ_1 and μ_2 be the respective mean parameters. If we define e_{\min} to be the smallest eigenvalue of the covariance matrix Σ for the random variables in the graphical model,*

$$\|\theta_1 - \theta_2\| \leq \frac{1}{e_{\min}} \|\mu_1 - \mu_2\|$$

Proof. Let $A(\theta)$ be the log partition function. Now, recall that the Hessian $\nabla^2 A(\theta)$ is equal to Σ above. Next, since e_{\min} is the smallest eigenvalue, $\nabla^2 A(\theta) - e_{\min} I = \Sigma - e_{\min} I$ is positive semi-definite, so $A(\theta)$ is strongly convex with parameter e_{\min} .

Note that since $A(\cdot)$ is strongly convex with parameter e_{\min} , then $A^*(\cdot)$, its Fenchel dual, has Lipschitz continuous gradients with parameter $\frac{1}{e_{\min}}$ (Zhou, 2018). This means that

$$\|\nabla A^*(\mu_1) - \nabla A^*(\mu_2)\| \leq \frac{1}{e_{\min}} \|\mu_1 - \mu_2\|.$$

But $\nabla A^*(\mu)$ is the inverse mapping from mean parameters to canonical parameters, so this is just

$$\|\theta_1 - \theta_2\| \leq \frac{1}{e_{\min}} \|\mu_1 - \mu_2\|$$

□

Now, we provide the proof for Theorem 2. Consider the following family of distributions for a graphical model with one hidden variable Y , m observed variables that are all conditionally independent given Y , and no sources abstaining:

$$\mathcal{P} = \left\{ P = \frac{1}{z} \exp(\theta_Y Y + \sum_{j=1}^m \theta_j \lambda_j Y) : \theta \in \mathbb{R}^{m+1} \right\}$$

We define a set of canonical parameters $\theta_v = \delta v$, where $\delta > 0$, $v \in \{-1, 1\}^m$ (θ_Y is fixed since it maps to a known mean parameter), and P_v is the corresponding distribution in \mathcal{P} . \mathcal{P} induces a $\frac{\delta}{\sqrt{m}}$ -Hamming separation for the L2 loss because

$$\begin{aligned} \|\theta - \theta_v\|_2 &= \left(\sum_{j=1}^m |\theta_j - [\theta_v]_j|^2 \right)^{1/2} \geq \frac{\sum_{j=1}^m \mathbf{1} \cdot |\theta_j - [\theta_v]_j|}{\left(\sum_{j=1}^m 1^2 \right)^{1/2}} \\ &= \frac{1}{\sqrt{m}} \sum_{j=1}^m |\theta_j - [\theta_v]_j| \geq \frac{\delta}{\sqrt{m}} \sum_{j=1}^m \mathbf{1}\{\text{sign}(\theta_j) \neq v_j\}. \end{aligned}$$

We use Cauchy-Schwarz inequality in the first line and the fact that if the sign of θ_j is different from v_j , then θ_j and $[\theta_v]_j$ must be at least δ apart. Then applying Assouad's Lemma (Yu, 1997), the minimax risk is bounded by

$$\mathcal{M}_n(\theta(\mathcal{P}), L2) = \inf_{\hat{\theta}} \sup_{P \in \mathcal{P}} \mathbb{E}_P[\|\hat{\theta}(X_1, \dots, X_n) - \theta(P)\|_2] \geq \frac{\delta}{2\sqrt{m}} \sum_{j=1}^m 1 - \|P_{+j}^n - P_{-j}^n\|_{TV}.$$

$\hat{\theta}(X_1, \dots, X_n)$ is an estimate of θ based on the n observable data points, while $\theta(P)$ is the canonical parameters of a distribution P . $P_{\pm j}^n = \frac{1}{2^{m-1}} \sum_v P_{v, \pm j}^n$, where $P_{v, \pm j}^n$ is the product of n distributions parametrized by θ_v with $v_j = \pm 1$. We use the convexity of total variation distance, Pinsker's inequality, and decoupling of KL-divergence to get

$$\|P_{+j}^n - P_{-j}^n\|_{TV}^2 \leq \max_{d_{ham}(v, v') \leq 1} \|P_v^n - P_{v'}^n\|_{TV}^2 \leq \frac{1}{2} \max_{d_{ham}(v, v') \leq 1} KL(P_v^n \| P_{v'}^n) = \frac{n}{2} \max_{d_{ham}(v, v') \leq 1} KL(P_v \| P_{v'}).$$

v and v' above only differ in one term. Then our lower bound becomes

$$\mathcal{M}_n(\theta(\mathcal{P}), L2) \geq \frac{\delta}{2\sqrt{m}} \sum_{j=1}^m 1 - \sqrt{\frac{n}{2} \max_{d_{ham}(v, v') \leq 1} KL(P_v \| P_{v'})} = \frac{\delta\sqrt{m}}{2} \left(1 - \sqrt{\frac{n}{2} \max_{d_{ham}(v, v') \leq 1} KL(P_v \| P_{v'})} \right). \quad (15)$$

We must bound the KL-divergence between P_v and $P_{v'}$. Suppose WLOG that v and v' differ at the i th index with $v_i = 1, v'_i = -1$, and let z_v and $z_{v'}$ be the respective terms used to normalize the distributions. Then the KL divergence is

$$KL(P_v \| P_{v'}) = \mathbb{E}_v[\langle \theta_v - \theta_{v'}, \lambda Y \rangle] + \ln \frac{z_{v'}}{z_v} = 2\delta \mathbb{E}_v[\lambda_i Y] + \ln \frac{z_{v'}}{z_v}. \quad (16)$$

We can write an expression for $\mathbb{E}_v[\lambda_i Y]$:

$$\begin{aligned} \mathbb{E}_v[\lambda_i Y] &= 2(P_v(\lambda_i = 1, Y = 1) + P_v(\lambda_i = -1, Y = -1)) - 1 \\ &= \frac{2}{z_v} \left(\sum_{\lambda_{-i}} \exp(\theta_Y + \delta + \sum_{j \neq i} (\delta v_j) \lambda_j) + \exp(-\theta_Y + \delta - \sum_{j \neq i} (\delta v_j) \lambda_j) \right) - 1 \\ &= \frac{2}{z_v} \exp(\delta) \sum_{\lambda_{-i}} 2 \cosh(\theta_Y + \sum_{j \neq i} (\delta v_j) \lambda_j) - 1. \end{aligned} \quad (17)$$

Similarly, z_v and $z_{v'}$ can be written as

$$\begin{aligned} z_v &= \exp(\delta) \sum_{\lambda_{-i}} 2 \cosh(\theta_Y + \sum_{j \neq i} (\delta v_j) \lambda_j) + \sum_{\lambda_{-i}} \exp(\theta_Y - \delta + \sum_{j \neq i} (\delta v_j) \lambda_j) + \sum_{\lambda_{-i}} \exp(-\theta_Y - \delta - \sum_{j \neq i} (\delta v_j) \lambda_j) \\ &= (\exp(\delta) + \exp(-\delta)) \sum_{\lambda_{-i}} 2 \cosh(\theta_Y + \sum_{j \neq i} (\delta v_j) \lambda_j) = 4 \cosh(\delta) \sum_{\lambda_{-i}} \cosh(\theta_Y + \sum_{j \neq i} (\delta v_j) \lambda_j) \\ z_{v'} &= 4 \cosh(\delta) \sum_{\lambda_{-i}} \cosh(\theta_Y + \sum_{j \neq i} (\delta v'_j) \lambda_j) \end{aligned}$$

Plugging z_v back into (17), we get:

$$\mathbb{E}_v [\lambda_i Y] = 4 \cdot \frac{\exp(\delta) \sum_{\lambda_{-i}} \cosh(\theta_Y + \sum_{j \neq i}^m (\delta v_j) \lambda_j)}{4 \cosh(\delta) \sum_{\lambda_{-i}} \cosh(\theta_Y + \sum_{j \neq i}^m (\delta v_j) \lambda_j)} - 1 = \frac{\exp(\delta)}{\cosh(\delta)} - 1.$$

Also note that $\frac{z_{v'}}{z_v} = 1$ since $v'_j = v_j$ for all $j \neq i$. The KL-divergence expression (16) now becomes

$$KL(P_v \| P_{v'}) = 2\delta \left(\frac{\exp(\delta)}{\cosh(\delta)} - 1 \right) + \ln(1) = 2\delta \left(\frac{\exp(\delta)}{\cosh(\delta)} - 1 \right).$$

We finally show that this expression is less than $2\delta^2$. Note that for positive δ , $f(\delta) = \frac{\exp(\delta)}{\cosh(\delta)} - 1 < \delta$, because $f(\delta)$ is concave and $f'(0) = 1$. Then we clearly have that $KL(P_v \| P_{v'}) \leq 2\delta^2$. Putting this back into our expression for the minimax risk, (15) becomes

$$\mathcal{M}_n(\theta(\mathcal{P}), L2) \geq \frac{\delta \sqrt{m}}{2} (1 - \sqrt{n\delta^2}).$$

Then if we set $\delta = \frac{1}{2\sqrt{n}}$, we get that

$$\mathcal{M}_n(\theta(\mathcal{P}), L2) \geq \frac{\sqrt{m}}{8\sqrt{n}}.$$

Lastly, to convert to a bound over the mean parameters, we use Lemma 8 to conclude that

$$\inf_{\hat{\mu}} \sup_{P \in \mathcal{P}} \mathbb{E}_P [\|\hat{\mu}(X_1, \dots, X_n) - \mu(P)\|_2] \geq \frac{e_{min}}{8} \sqrt{\frac{m}{n}}.$$

From this, we can conclude that the estimation error on the label model parameters $\|\hat{\mu} - \mu\|_2$ is also at least $\frac{e_{min}}{8} \sqrt{\frac{m}{n}}$.

D.3. Proof of Theorem 3 (Generalization Error)

We base our proof off of Theorem 1 of Ratner et al. (2019) with modifications to account for model misspecification. To learn the parametrization of our end model f_w , we want to minimize a loss function $L(w, \mathbf{X}, \mathbf{Y}) \in [0, 1]$. The expected loss we would normally minimize using some $w^* = \operatorname{argmax}_w L(w)$ is

$$L(w) = \mathbb{E}_{(\mathbf{X}, \mathbf{Y}) \sim \mathcal{D}} [L(w, \mathbf{X}, \mathbf{Y})].$$

However, since we do not have access to the true labels \mathbf{Y} , we instead minimize the expected noise-aware loss. Recall that μ is the parametrization of the label model we would learn with population-level statistics, and $\hat{\mu}$ is the parametrization we learn with the empirical estimates from our data. Denote P_μ and $P_{\hat{\mu}}$ as the respective distributions. If we were to have a population-level estimate of μ , the loss to minimize would be

$$L_\mu(w) = \mathbb{E}_{(\mathbf{X}, \mathbf{Y}) \sim \mathcal{D}} \left[\mathbb{E}_{\tilde{\mathbf{Y}} \sim P_\mu(\cdot | \lambda(\mathbf{X}))} [L(w, \mathbf{X}, \tilde{\mathbf{Y}})] \right].$$

However, because we must estimate $\hat{\mu}$ and further are minimizing loss over n samples, we want to estimate a \hat{w} that minimizes the empirical loss,

$$\hat{L}_{\hat{\mu}}(w) = \frac{1}{n} \sum_{i=1}^n \mathbb{E}_{\tilde{\mathbf{Y}} \sim P_{\hat{\mu}}(\cdot | \lambda(\mathbf{X}_i))} [L(w, \mathbf{X}_i, \tilde{\mathbf{Y}})].$$

We first write $L(w)$ in terms of $L_\mu(w)$.

$$\begin{aligned}
 L(w) &= \mathbb{E}_{(\mathbf{X}, \mathbf{Y}) \sim \mathcal{D}} [L(w, \mathbf{X}, \mathbf{Y})] = \mathbb{E}_{(\mathbf{X}', \mathbf{Y}') \sim \mathcal{D}} [\mathbb{E}_{(\mathbf{X}, \mathbf{Y}) \sim \mathcal{D}} [L(w, \mathbf{X}', \mathbf{Y}) | \mathbf{X} = \mathbf{X}']] \\
 &= \mathbb{E}_{(\mathbf{X}', \mathbf{Y}') \sim \mathcal{D}} [\mathbb{E}_{(\mathbf{X}, \tilde{\mathbf{Y}}) \sim P_\mu} [L(w, \mathbf{X}', \mathbf{Y}) | \mathbf{X} = \mathbf{X}']] + \mathbb{E}_{(\mathbf{X}, \mathbf{Y}) \sim \mathcal{D}} [L(w, \mathbf{X}', \mathbf{Y}) | \mathbf{X} = \mathbf{X}']] \\
 &\quad - \mathbb{E}_{(\mathbf{X}, \tilde{\mathbf{Y}}) \sim P_\mu} [L(w, \mathbf{X}', \mathbf{Y}) | \mathbf{X} = \mathbf{X}']] \\
 &\leq \mathbb{E}_{(\mathbf{X}', \mathbf{Y}') \sim \mathcal{D}} [\mathbb{E}_{(\lambda, \tilde{\mathbf{Y}}) \sim P_\mu} [L(w, \mathbf{X}', \mathbf{Y}) | \lambda = \lambda']] \\
 &\quad + \mathbb{E}_{(\mathbf{X}', \mathbf{Y}') \sim \mathcal{D}} \left[\left| \sum_{x, y} L(w, \mathbf{X}', y) (\mathcal{D}(\mathbf{X} = x, \mathbf{Y} = y | \mathbf{X} = \mathbf{X}') - P_\mu(\mathbf{X} = x, \mathbf{Y} = y | \mathbf{X} = \mathbf{X}')) \right| \right] \\
 &\leq L_\mu(w) + \mathbb{E}_{(\mathbf{X}', \mathbf{Y}') \sim \mathcal{D}} \left[\sum_{x, y} L(w, \mathbf{X}', y) \cdot |\mathcal{D}(\mathbf{X} = x, \mathbf{Y} = y | \mathbf{X} = \mathbf{X}') - P_\mu(\mathbf{X} = x, \mathbf{Y} = y | \mathbf{X} = \mathbf{X}')| \right] \\
 &\leq L_\mu(w) + \mathbb{E}_{(\mathbf{X}', \mathbf{Y}') \sim \mathcal{D}} \left[\sum_{x, y} |\mathcal{D}(\mathbf{X} = x, \mathbf{Y} = y | \mathbf{X} = \mathbf{X}') - P_\mu(\mathbf{X} = x, \mathbf{Y} = y | \mathbf{X} = \mathbf{X}')| \right]
 \end{aligned}$$

Here we have used the fact that $L(w, \mathbf{X}', y) \leq 1$. Note that $\mathcal{D}(\mathbf{X} = x, \mathbf{Y} = y | \mathbf{X} = \mathbf{X}') = \mathcal{D}(\mathbf{Y} = y | \mathbf{X} = \mathbf{X}')$ only when $\mathbf{X}' = x$, and is 0 otherwise. The same holds for P_μ , so

$$L(w) \leq L_\mu(w) + \mathbb{E}_{(\mathbf{X}', \mathbf{Y}') \sim \mathcal{D}} \left[\sum_y |\mathcal{D}(\mathbf{Y} = y | \mathbf{X} = \mathbf{X}') - P_\mu(\mathbf{Y} = y | \mathbf{X} = \mathbf{X}')| \right].$$

Note that the expression $\sum_y |\mathcal{D}(\mathbf{Y} = y | \mathbf{X} = \mathbf{X}') - P_\mu(\mathbf{Y} = y | \mathbf{X} = \mathbf{X}')|$ is just half the total variation distance between $\mathcal{D}(\mathbf{Y} | \mathbf{X}')$ and $P_\mu(\mathbf{Y} | \mathbf{X}')$. Then, using Pinsker's inequality, we bound $L(w)$ in terms of the conditional KL divergence between \mathcal{D} and P_μ :

$$\begin{aligned}
 L(w) &\leq L_\mu(w) + \mathbb{E}_{\mathbf{X}' \sim \mathcal{D}} [2 \cdot TV(\mathcal{D}(\mathbf{Y} | \mathbf{X}'), P_\mu(\mathbf{Y} | \mathbf{X}'))] \\
 &\leq L_\mu(w) + 2 \cdot \mathbb{E}_{\mathbf{X} \sim \mathcal{D}} \left[\sqrt{(1/2) KL(\mathcal{D}(\mathbf{Y} | \mathbf{X}) \| P_\mu(\mathbf{Y} | \mathbf{X}))} \right] \\
 &\leq L_\mu(w) + \sqrt{2 \cdot KL(\mathcal{D}(\mathbf{Y} | \mathbf{X}) \| P_\mu(\mathbf{Y} | \mathbf{X}))}.
 \end{aligned}$$

There is a similar lower bound on $L(w)$ if we perform the same steps as above on the inequality $L(w) \geq L_\mu(w) - \mathbb{E}_{(\mathbf{X}', \mathbf{Y}') \sim \mathcal{D}} \left[\left| \mathbb{E}_{(\mathbf{X}, \mathbf{Y}) \sim \mathcal{D}} [L(w, \mathbf{X}', \mathbf{Y}) | \mathbf{X} = \mathbf{X}'] - \mathbb{E}_{(\mathbf{X}, \tilde{\mathbf{Y}}) \sim P_\mu} [L(w, \mathbf{X}', \mathbf{Y}) | \mathbf{X} = \mathbf{X}'] \right| \right]$. This yields

$$L(w) \geq L_\mu(w) - \sqrt{2 \cdot KL(\mathcal{D}(\mathbf{Y} | \mathbf{X}) \| P_\mu(\mathbf{Y} | \mathbf{X}))}.$$

Therefore,

$$L(\hat{w}) - L(w^*) \leq L_\mu(\hat{w}) - L_\mu(w^*) + 2\sqrt{2 \cdot KL(\mathcal{D}(\mathbf{Y} | \mathbf{X}) \| P_\mu(\mathbf{Y} | \mathbf{X}))}.$$

We finish the proof of the generalization bound with the procedure from [Ratner et al. \(2019\)](#) but also use the conversion from canonical parameters to mean parameters as stated in [Lemma 8](#), and note that the estimation error of the mean parameters is always less than the estimation error of the label model parameters. Then our final generalization result is

$$L(\hat{w}) - L(w^*) \leq \gamma(n) + \frac{8|\mathcal{Y}|}{e_{min}} \|\hat{\boldsymbol{\mu}} - \boldsymbol{\mu}\|_2 + \delta(\mathcal{D}, P_\mu),$$

where $\delta(\mathcal{D}, P_\mu) = 2\sqrt{2 \cdot KL(\mathcal{D}(\mathbf{Y} | \mathbf{X}) \| P_\mu(\mathbf{Y} | \mathbf{X}))}$, e_{min} is the minimum eigenvalue of $\mathbf{Cov}[\boldsymbol{\lambda}, \mathbf{Y}]$ over the construction of the binary Ising model, and $\gamma(n)$ bounds the empirical risk minimization error.

E. Extended Experimental Details

We describe additional details about the tasks, including details about data sources, supervision sources, and end models. We also report details about our ablation studies. All timing measurements were taken on a machine with an Intel Xeon E5-2690 v4 CPU and Tesla P100-PCIE-16GB GPU. Details about the sizes of the train/dev/test splits and end models are shown in Table 4.

E.1. Dataset Details

Dataset	End Model	N_{train}	N_{dev}	N_{test}
Spouse	LSTM	22,254	2,811	2,701
Spam	Logistic Regression	1,586	120	250
Weather	Logistic Regression	187	50	50
Commercial	ResNet-50	64,130	9,479	7,496
Interview	ResNet-50	6,835	3,026	3,563
Tennis Rally	ResNet-50	6,959	746	1,098
Basketball	ResNet-18	3,594	212	244

Table 4. We report the train/dev/test split of each dataset. The dev and test set have ground truth labels, and we assign labels to the training set using our method or one of the baseline methods.

Spouse, Weather We use the datasets from Ratner et al. (2018) and the train/dev/test splits from that work (**Weather** is called **Crowd** in that work).

Spam We use the dataset as provided by Snorkel² and those train/dev/test splits.

Interview, Basketball We use the datasets from Sala et al. (2019) and the train/dev/test splits from that work.

Commercial We use the dataset from Fu et al. (2019) and the train/dev/test splits from that work.

Tennis Rally We obtained broadcast footage from four professional tennis matches, and annotated segments when the two players are in a rally. We temporally downsampled the images at 1 FPS. We split into dev/test by taking segments from each match (using contiguous segments for dev and test, respectively) to ensure that dev and test come from the same distribution.

E.2. Task-Specific End Models

For the datasets we draw from previous work (each dataset except for **Tennis Rally**), we use the previously published end model architectures (LSTM (Hochreiter & Schmidhuber, 1997) for **Spouse**, logistic regression over bag of n-grams for **Spam** and over Bert features for **Weather** (Devlin et al., 2018), ResNet pre-trained on ImageNet for the video tasks). For **Tennis Rally**, we use ResNet-50 pre-trained on ImageNet to classify individual frames. We do not claim that these end models achieve the best possible performance for each task; our goal is to compare the relative improvements that our weak supervision models provide compared to other baselines through label quality, which is orthogonal to achieving state-of-the-art performance for these specific tasks.

For end models that come from previous works, we use the hyperparameters from those works. For the label model baselines, we use the hyperparameters from previous works as well. For our label model, we use class balance from the dev set, or tune the class balance ourselves with a grid search. We also tune which triplets we use for parameter recovery on the dev set. For our end model parameters, we either use the hyperparameters from previous works, or run a simple grid search over learning rate and momentum.

²<https://www.snorkel.org/use-cases/01-spam-tutorial>

	Spouse	Spam	Weather
Random abstains	20.9	64.1	69.1
FLYINGSQUID	49.6	92.3	88.9
Single Triplet Worst	4.5	67.0	0.0
Single Triplet Best	51.2	83.6	77.6
Single Triplet Average	37.9	73.4	31.0
FLYINGSQUIDLabel Model	47.0	89.1	77.6

Table 5. End model performance in terms of F1 score with random votes replacing abstentions (first row), compared to FLYINGSQUID, for the benchmark applications.

E.3. Supervision Sources

Supervision sources are expressed as short Python functions. Each source relied on different information to assign noisy labels:

Spouse, Weather, Spam For these tasks, we used the same supervision sources as used in previous work (Ratner et al., 2018). These are all text classification tasks, so they rely on text-based heuristics such as the presence or absence of certain words, or particular regex patterns.

Interview, Basketball Again, we use sources from previous work (Sala et al., 2019). For **Interview**, these sources rely on the presence of certain faces in the frame, as determined by an identity classifier, or certain text in the transcript. For **Basketball**, these sources rely on an off-the-shelf object detector to detect balls or people, and use heuristics based on the average pixel of the detected ball or distance between the ball and person to determine whether the sport being played is basketball or not.

Commercial In this dataset, there is a strong signal for the presence or absence of commercials in pixel histograms and the text; in particular, commercials are book-ended on either side by sequences of black frames, and commercial segments tend to have mixed-case or missing transcripts (whereas news segments are in all caps). We use these signals to build the weak supervision sources.

Tennis Rally This dataset uses an off-the-shelf pose detector to provide primitives for the weak supervision sources. The supervision sources are heuristics based on the number of people on court and their positions. Additional supervision sources use color histograms of the frames (i.e., how green the frame is, or whether there are enough white pixels for the court markings to be shown).

E.4. Ablation Studies

We report the results of two ablation studies on the benchmark applications. In the first study, we examine the effect of randomly replacing abstains with votes, instead of augmenting G_{dep} . In the second study, we examine the effect of using a single random selection of triplets instead of taking the mean or median over all triplet assignments.

Table 5 (top) shows end model performance for the three benchmark tasks when replacing abstains with random votes (top row), compared to FLYINGSQUID end model performance. Replacing abstentions with random votes results in a major degradation in performance.

Table 5 (bottom) shows label model performance when using a single random assignment of triplets, compared to the FLYINGSQUID label model, which takes the median or mean of all possible triplets. There is large variance when taking a single random assignment of triplets, whereas using an aggregation is more stable. In particular, while selecting a good seed can result in performance that matches (**Weather**) or exceeds (**Spouse**) FLYINGSQUID label model performance, selecting a *bad* seed result in much worse performance (including catastrophically bad predictors). As a result, FLYINGSQUID outperforms random assignments on average.

As a final note, we comment on using means vs. medians for aggregating accuracy scores. For all tasks except for **Weather**, there is no difference in label model performance. For **Weather**, using medians is more accurate, since the supervision sources have a large abstention rate. As a result, many triplets result in accuracy scores of zero (hence the 0 F1 score in Table 5). This throws off the median aggregation, since the median accuracy score becomes zero for many sources. However, mean aggregation is more robust to these zero's, since the positive accuracy scores from the triplets can correct for the accuracy.